Effects of inhibition of bone resorption and cyclooxygenase on bone and tendon-to-bone healing

Experimental studies of fracture and tendon-to-bone healing in the rat

Thesis by

Geir Aasmund Hjorthaug

UiO : Faculty of Medicine
University of Oslo

2019

Institute of Clinical Medicine, Faculty of Medicine, University of Oslo, Norway.

Division of Orthopedic Surgery, Oslo University Hospital (OUS), Oslo, Norway.

Experimental orthopedic research, Institute for Surgical Research, OUS, Oslo, Norway.

Department of Orthopedic Surgery, Martina Hansen's Hospital, Sandvika, Norway.

Series of dissertations submitted to the
Faculty of Medicine, University of Oslo

ISBN 978-82-8377-634-8

Cover: Hanne Baadsgaard Utigard.
Print production: Reprosentralen, University of Oslo.

Populærvitenskapelig norsk sammendrag

Bruddtilheling og tilheling av sene mot ben ved leddbåndsrekonstruksjon

Pasienter med brudd har behov for smertelindring, men de effektive medisinene av typen smertestillende/betennelsesdempende (NSAIDs) kan virke negativt på tilhelingen av selve bruddskaden.

I sin avhandling "*Effects of inhibition of bone resorption and cyclooxygenase on bone and tendon-to-bone healing; Experimental studies of fracture and tendon-to-bone healing in the rat"* har Geir Aasmund Hjorthaug og medarbeidere brukt eksperimentelle dyremodeller for å studere tilhelingsprosesser ved leggbrudd og ved sene til bentunnel.

De fant at tre dagers behandling med et NSAID (parecoxib) etter skade eller bruddoperasjon ikke hadde noen negativ virkning på bruddtilhelingen når dette ble evaluert etter fire uker. Denne kunnskapen kan komme pasienter med bruddsmerter til gode.

Ved leddbåndsrekonstruksjon må den myke senen gro fast i det harde benet, og gruppen bekrefter gjennom sine studier at dette er en relativt langsom prosess med risiko for dårlig vevsforankring, spesielt i tidlige faser etter operasjon. Den etablerte forbindelsen mellom senen og benet lignet arrvev, og manglet den strukturelle lagdelingen som gir styrke til et uskadet og nativt senefeste. Tilleggsbehandling med medisin mot benskjørhet (zoledronsyre) førte ikke til bedret tilheling, tvert imot ga dette dårligere styrke av sene-ben-reparasjonen etter tre og seks ukers tilheling.

Contents

Acknowledgements

The work resulting in this thesis was started at Oslo Univerity Hospital in 2011. The University of Oslo later provided me a position as a clinical research fellow until 2013. I was privileged to continue both my research and my clinical residency at Ullevål, Department of Orthopedic surgery, and later at Martina Hansens Hospital from who I was provided time and financial support from internal research fund. The work was also supported by grants from Smith&Nephew Research Fund and Norwegian Orthopaedic Association. The *in vivo* experiments and *ex vivo* lab analyses were conducted at Rikshospitalet in excellent facilities at the Department of Comparative Medicine and Institute for Surgical Research, respectively.

First and foremost, I would like to express my sincere gratitude to my main supervisor, senior consultant orthopedic surgeon and PhD *Sigbjørn Dimmen* at Lovisenberg Diaconal Hospital for sharing his knowledge on experimental research, for his dedication and persistence throughout my PhD-period, and for excellent supervision. I am especially thankful for his hands-on supervision style, our friendship, and the way he shared his first-class surgical skills in the lab at late hours during the most critical phases of our experiments.

Secondly, I wish to express my gratitude to my co-supervisors, Professor *Lars Nordsletten* and Professor *Jan Erik Madsen* at Oslo University Hospital. I am deeply thankful and greatly inspired by their remarkable knowledge of orthopedic surgery and science. Throughout the years, they consistently supported me, gave valuable advice and criticism in all phases that resulted in this thesis. Lars Nordsletten is acknowledged for the primary initiative of the project. Jan Erik Madsen contributed pricelessly in the lab with his excellent surgical skills, pragmatic approach and effortless collaboration style.

Furthermore, I wish to thank my co-authors and collaborators, as they all played unique parts in my PhD-puzzle: Orthopedic surgeon *Endre Søreide* was one of several fellow students in the PhD-community at Oslo University Hospital that always was there to support me. Endre Søreide helped me faithfully in the lab and donated many and late hours of data analysis. I am especially thankful for his always encouraging academic support, personal support, and friendship. Orthopedic surgeon *Lene Solberg* is acknowledged for her important encouraging contribution and inspiration at the beginning of the project. I would like to thank Professor *Harald Steen* and Senior Engineer *Sanyalak Niratisairak (Pop)* at the Biomechanics lab for teaching me the basics of biomechanical testing and for essential contributions in biomechanical analysis. I also wish to thank Professor *Finn P. Reinholt* at the Department of

Pathology for sharing of his great knowledge in bone tissue and analysis, and Senior Engineer *Linda Trobe Dorg* for excellent help with the histological work.

The personnel at the Department of Comparative Medicine have all been very sincere and professional in their care of the animals. I am very thankful for all I have learned from them regarding the respectful handling of research animals and assessment of animal behavior. Vets *Gro Furset Flatekval* and *Henrik Rasmussen* provided valuable input in the planning phases of the animal studies. Moreover, I am especially thankful for the help with the multiple injections in the last study from vet.technicians *Christine Sandsnes Olsen* and *Vibeke Stensrud Krohn*.

The completion of this work would not have been possible without the support, flexibility, and research enthusiasm from all my colleagues at the Orthopedic Department at Martina Hansens Hospital and its head *Kjetil Nerhus*. A special thanks to my hardworking and dear colleagues at the Section of Foot, Ankle and Rheumasurgery for continuous reality-checking and an inspiring working environment.

I wish to thank my friends, parents, and family for all the good times outside of work. Last but not least, thanks for support from my very best friends in life; my love and wife *Marit* and our kids *Brage* and *Selma*. Thanks for making my life complete and filled with play, snow, music, dance, art, books, curiosity, and devotion. And true love.

List of studies

The thesis constitutes of the following studies:

I. **Hjorthaug GA, Madsen JE, Nordsletten L, Reinholt FP, Steen H, Dimmen S.** Tendon to bone tunnel healing-a study on the time-dependent changes in biomechanics, bone remodeling, and histology in a rat model. *Journal of Orthopaedic Research* 2015;33:216-23.

doi:10.1002/jor.22756

II. **Hjorthaug GA, Søreide E, Nordsletten L, Madsen JE, Reinholt FP, Niratisairak S, Dimmen S.** Negative effect of zoledronic acid on tendon to bone healing - In vivo study of biomechanics and bone remodeling in a rat model. *Acta Orthopaedica* 2018; 1-7.

doi:10.1080/17453674.2018.1440189

III. **Hjorthaug GA, Søreide E, Nordsletten L, Madsen JE, Reinholt FP, Niratisairak S, Dimmen S.** Short-term perioperative parecoxib is not detrimental to shaft fracture healing in a rat model. *Bone & Joint Research* 2019;8:472-80.

doi: 10.1302/2046-3758.810.BJR-2018-0341.R1

Abbreviations and context

Short term	Long term	Context
ABG	autologous bone graft	surgery
ACL	anterior crucial ligament	anatomy
ACLR	anterior crucial ligament reconstruction	surgery
AFF	atypical femoral fracture	pathology
ANOVA	analysis of variances (test)	statistics
BMC	bone mineral content	radiology
BMD	bone mineral density	radiology
BMP	bone morphogenetic protein	molecular biology
BP	bisphosphonate	pharmacology
BPTB	bone-patellar tendon-bone (autograft)	surgery
BRI	bone resorption inhibitor	pharmacology
BS	bone surface	histology
CABG	coronary artery bypass graft	surgery
COX	cyclooxygenase	molecular biology/pharmacology
DEXA	dual-energy X-ray absorptiometry	radiology
ECM	extracellular matrix	molecular biology
H+E	hematoxylin-eosin (stain)	histology
HA	hydroxyapatite	molecular biology
HT	hamstrings tendon (autograft)	surgery
IL	interleukin	molecular biology
IM	intramuscular	pharmacology (administration)
IP	intraperitoneal	pharmacology (administration)
IV	intravenous	pharmacology (administration)
KW	Kruskal-Wallis (test)	statistics
LD	load-displacement	mechanics

MGT	Masson-Goldner´s trichrome (stain)	histology
MMP	matrix metalloproteinase	molecular biology
MRI	magnetic resonance imaging	radiology
MSC	mesenchymal stem cell	cell biology
NSAID	non-steroid anti-inflammatory drug	pharmacology
ONJ	osteonecrosis of the jaw	pathology
OPG	osteoprotegerin	molecular biology
OS	osteoid surface	histology
PG	prostaglandin	molecular biology
pQCT	peripheral quantitative computed tomography	radiology
RCT	randomized controlled trial	research
ROI	region of interest	histology/radiology
RPM	rounds per minute	surgery
SC	subcutaneous	pharmacology (administration)
TGF	transforming growth factor	molecular biology
TNFα	tumor necrosis factor alpha	molecular biology
TRAP	tartrate-resistant acid phosphatase	molecular biology/histology
Wnt	wingless-type MMTV integration site family(1)	molecular biology
ZA	zoledronic acid	pharmacology
µCT	micro-computed tomography	radiology

1. Introduction

The outcome after musculoskeletal injuries and reconstructions depend on trauma energy, location of fractures, adjacent soft tissue injury, concomitant injuries to other organ systems, and patient-specific factors like age, comorbidity, nutrition status, smoking status, genetics, and medication. Orthopedic treatment and timing also greatly influence the outcome. Surgical technique and access, fixation, and rehabilitation are essential issues. Interventions to augment tissue healing may have an important role to play and might be pivotal for the clinical outcome(2-4). The overall factors that are of importance in tissue healing response may be summed up as mechanics and biology.

Tendon grafting into a bone tunnel is a commonly used technique in ligament reconstructions. Rupture of the reconstructed ligament or increased laxity by repeated loading constitutes significant problems. Stability is achieved only by firm tendon to bone healing(5, 6). The potential conflict between loading, the need for early active rehabilitation, and sound tissue healing is a clinical challenge. The goal is always to facilitate the best possible functional outcome(7). The healing of tendon to bone is slow, and it would be desirable to be able to speed up these healing processes and reduce failure rates after procedures like anterior cruciate ligament reconstruction (ACLR), repair of the rotator cuff and in tendon reinsertion and transfers. These clinical scenarios are associated with decreased loading that might lead to impaired quality of both bone and tendon tissue(8). Local and regional bone loss, both before and after surgical repair of the tendon-bone interface, are potential targets for adjuvant treatment to improve healing and outcome. Bone resorption inhibitors (BRIs) are developed to prevent fractures in patients with osteoporosis but are also being hypothesized to prevent local bone loss associated with impaired tendon-to-bone healing(9). The knowledge of the effects of BRIs in tendon-to-bone healing is sparse.

In fracture treatment, healing is often delayed or lacking, and as for tendon-to-bone healing, many pharmaceuticals are tested and may positively affect healing. However, it is also essential to identify factors that may affect tissue healing negatively. Inhibitors of cyclooxygenase (COX) are effective against pain in orthopedic trauma. Nevertheless, there are concerns about COX-inhibitors concerning musculoskeletal healing, especially in fractures and bone healing(10-13). A common clinical question regarding the use of COX-inhibitors and fracture healing is whether it is safe to administer these drugs in only a short period following injury or surgery, or if it is safer to delay the administration for a few days.

Studies designed to investigate these effects in clinically relevant doses regimen and timing are few. There is still an active discussion about the matters of several positive and negative factors and adjuncts in musculoskeletal tissue healing, in particular on COX-inhibitors(14).

This thesis contributes to the knowledge of the effects of inhibition of bone resorption and cyclooxygenase on fracture and tendon-to-bone healing. To explain the purpose of the current studies, relevant basic knowledge of bone, tendon, tendon insertions, and tissue healing are summarized below.

1.1 Bone tissue

Bone (l. *os*) and tendon (ml. *tendo*, infl. by l. *tendere*, to stretch) are highly organized, dynamic, and living tissue. Cells, blood supply, and nerves are essential tissue components in both development, maintenance, and tissue healing. The muscle develops tendon tension, and together with bones, they form functional units that are essential for movement and life.

Bone cells are involved in the formation and mineralization of the extracellular matrix (ECM). The bone matrix consists of an organic component, mostly collagen, and an interspersed inorganic component of bone mineral, mostly hydroxyapatite (HA), $Ca_{10}(PO_4)_6(OH)_2$. Collagen is organized as a fibrilous web, and the HA is distributed among the fibrils, forming larger structures. This composite material makes the bone lightweight, but still provides strength, rigidity and energy storing properties. Bones usually consist of both cancellous and cortical bone. Cancellous (spongy or trabecular) bone is distributed inside bones (Figure 1). Multiple trabeculae form a porous network with large internal surfaces and proximity to abundant circulation and the bone marrow. The trabeculae are aligned along internal mechanical load axes and are typically found inside the vertebra, proximal to joints at the ends of long bones.

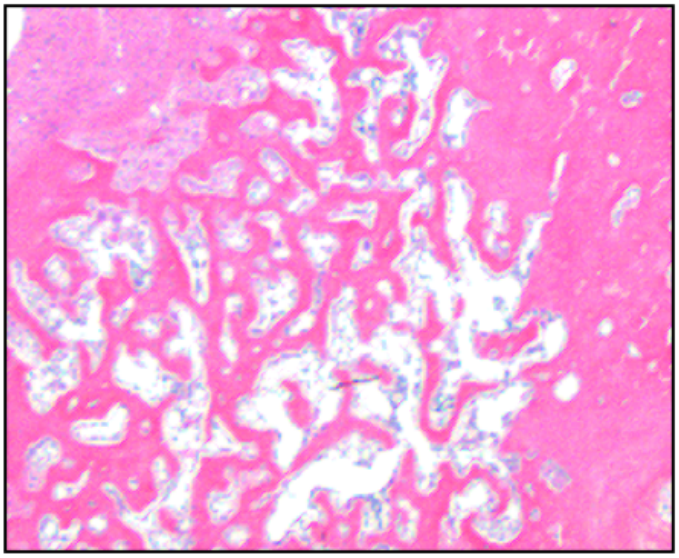

Figure 1. Cancellous bone. Distal metaphyseal rat tibia. *Photo: Obtained from AnalySIS V, Geir Aasmund Hjorthaug*

Cortical (compact) bone form the exterior (cortex) of bones (Figure 2). It consists of thick bone lamellae surrounding a central longitudinal canal containing blood vessels that supply the bone tissue. These pillars of bone are the morphological and functional units of compact bone and are called osteons (Haversian systems). The periosteum coats the exterior and the endosteum coats the interior. The periosteum is a membrane of connective tissue and contains multiple cells, including nerves, nociceptors, and vessels that descend into transverse canals (Volkmann´s canals) perforating the osteons. Collagen fibers attach the periosteum to the cortical bone surface, and the periosteum also contributes to the attachment of muscles and tendons.

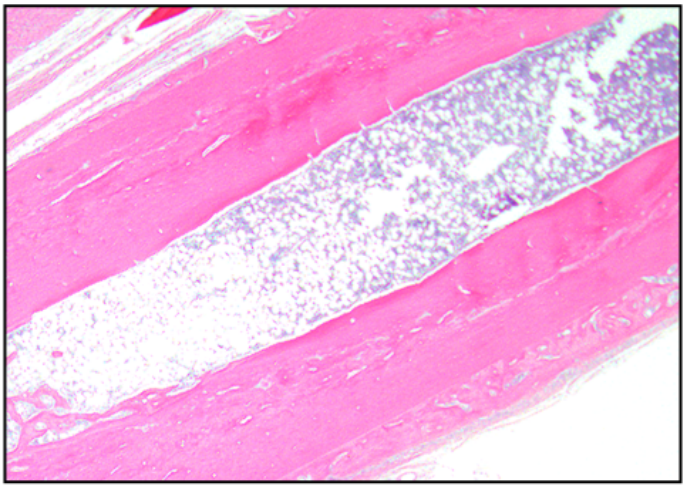

Figure 2. Cortical bone. Diaphyseal rat tibia. *Photo: Obtained from AnalySIS V, Geir Aasmund Hjorthaug.*

Osteoblasts (gr. *osteon*: bone and *blastanō*: sprout) are single nucleated differentiated mesenchymal stem cells (MSC) that produce osteoid, the organic nonmineralized first stage of ECM. The osteoid consists mainly of collagen type I, and the rest is ground substance with osteocalcin and chondroitin sulfate. The mineralization of osteoid with formation of HA binding to the proteins and ground substance is dependent on several factors, including availability of vitamin D and calcium. Groups of osteoblasts with its osteoid and mineralized bone matrix form osteons in cortical bone in an anabolic process called ossification or new bone formation.

Osteoclasts (gr. *klastos*: broken) are large multinucleated cells from monocyte-macrophage lines that resorb bone tissue. The cytoplasm of osteoclasts is filled with lysosomes containing enzymes. These enzymes, mainly acid phosphatase and proteases, permits the identification of osteoclasts by staining for tartrate-resistant acid phosphatase (TRAP or TRAPase) or the protease cathepsin K. The osteoclast seals its border zones by adhesion structures (podosomes), and form bone resorption pits. The active osteoclast releases its enzymes and a large amount of H^+-ions from a villous surface (ruffled border) into the closed pit. The local pH acidic environment facilitates organic (collagenolysis by proteases) and inorganic (dissolution of mineralized bone matrix) catabolism resulting in bone resorption. Fragments of collagen and small mineral molecules and ions are released to the circulation.

The osteocytes are former osteoblasts that are trapped inside the bone matrix made by themselves. They communicate with each other and with active osteoblasts on bone surfaces via gap junctions through thin channels in the bone matrix (canaliculi), and via complex

endocrine and paracrine signaling pathways. The continuous process of bone formation by osteoblasts and resorption by osteoclasts is called bone remodeling. The osteocytes are load sensors that control bone remodeling. Bone remodeling serves several purposes including the shaping of bones during growth, calcium homeostasis, repair of microdamage in bone from physiological stress. This remodeling with the ordered coupling of osteoblasts and osteoclasts is different from the repair processes following fracture or bone surgery where osteoblasts can form bone independently(15) .

1.2 Tendon tissue

The tendon cells are mainly tenocytes that are elongated former fibroblasts (Figure 3). The tenocytes are connected to the tendon ECM. Tenocytes also communicate via gap junctions and can detect mechanical changes in the ECM environment. The response to increased mechanical load would be recruitment of MSCs, differentiation to fibroblasts/tenocytes, and an increase in the production of ECM. The tendon ECM consists of large molecules of collagen and proteoglycans. Proteoglycans retain water inside the tendon and assist the process of collagen arrangement in large crosslinked fibrils. The fibrils are arranged parallel in larger and strong fibers separated by layers of connective tissue, the endotenon, that provide the tendon with blood vessels and nerves. At rest, the tendon fibers are arranged in a crimp pattern that store energy. The tendon buckles with compression; it behaves like a rope. When loaded, the fibers are stretched out, and further energy is transferred to the tendon-bone insertion. These elastic properties of tendons are limited, and if it exceeds the capacity, micro ruptures or even total tendon rupture may occur(16).

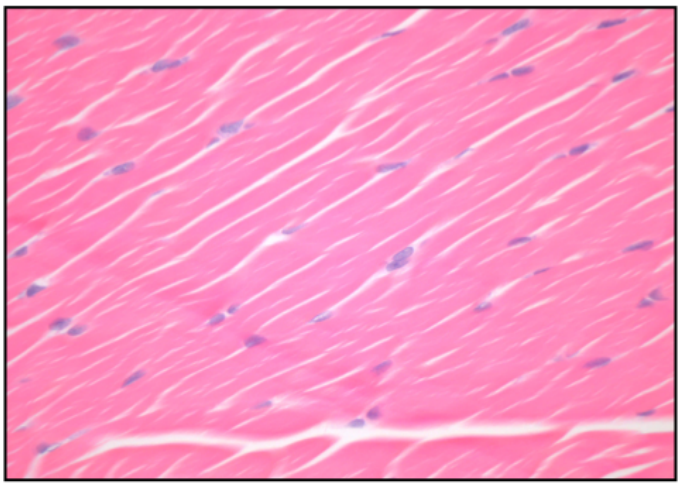

Figure 3. Tendon tissue with parallel collagen fibrils and interspaced tenocytes. Flexor digitorum longus in rat ankle. *Photo: Obtained from AnalySIS V, Geir Aasmund Hjorthaug*

1.3 Tendon enthesis

Tendons and ligaments attach to bone through a transitional tissue called the enthesis. The function of the tendon enthesis is to transfer load from tendon to the bone, necessary to create movement. Similarly, the function of the ligament enthesis is to transfer load between bones, necessary for joint stability. Nevertheless, the enthesis has to withstand tremendous forces concentrated in a minimal area. More correct, it is a continuous graded *volume* specialized to effectively distribute force from a flexible (tendon) to a rigid (bone) material. The native enthesis has a complex structure, composition, and mechanical behavior(17). Collagen fibers crossing the tendon-bone interface are anchoring the soft tendon to the relative hard bone surface within a distance of 1 mm.

Different terminologies were discussed by Benjamin et al., who proposed the terms *fibrocartilaginous* and *fibrous* entheses for the two main types described(18). They reserved the terms *direct* and *indirect* entheses for fibrous enthesis *sub*groups they also called *bony* or *periosteal*. The terms direct and indirect have been used differently by Woo et al.(19). They describe fibrocartilaginous as direct and fibrous as indirect entheses. It is required to acknowledge the great variety of how tendons, ligaments, and muscles attach to bone in respect to different sizes, shapes, profiles, angles, regions, and tendon lengths. More recent studies also indicate variations between individuals, as well as variations within one enthesis itself. An enthesis may be partially fibrocartilaginous *and* fibrous, and the amount of cartilage is region-dependent within the volume borders of the enthesis organ(20). In this

thesis we prefere to use the terminology described by Benjamin et al., and try to avoid the use of direct or indirect entheses in our terminology.

A four-layer pattern characterizes the fibrocartilaginous enthesis type, separating the bone and tendon by a thin tidemark (watershed line). Crossing collagen fibers perforates the interface between the tendon tissue and *non*mineralized fibrocartilage on one side and into mineralized fibrocartilage and bone tissue on the other side of the tidemark.

The first zone consists of tendon tissue with the same properties of that of the mid substance tendon, collagen type I and the proteoglycan decorin. The second zone with fibrocartilage is composed of collagen type II and III, with small amounts of type I, IX and X, and small amounts of proteoglycans like decorin and aggrecan. The mineralized fibrocartilage found in the third zone is surrounded mostly of collagen type II and X, that fit with the proximity of the bony environment. The fourth zone consists of bone with mainly collagen type I and high mineral content(17).

The fibrocartilaginous entheses are typically found close to joints and are called epi- or metaphyseal entheses. Examples of direct insertions are rotator cuff insertion in the proximal humerus, the anterior cruciate ligament (ACL) insertions in femur and tibia, and the Achilles insertion onto the dorsal calcaneus (Figure 4).

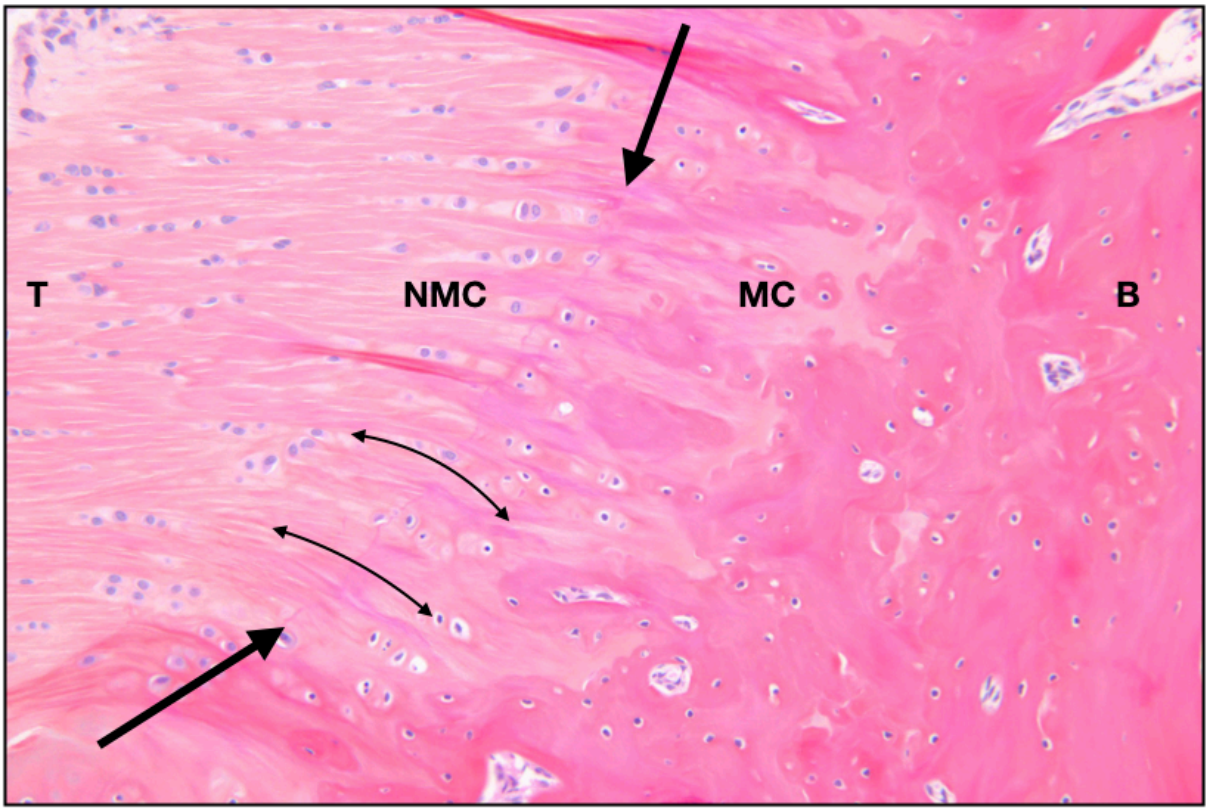

Figure 4. Four-layered fibrocartilaginous tendon enthesis; the Achilles insertion into rat calcaneus. Tendon **(T)** and non-mineralized fibrocartilage **(NMC)** are separated from the zones of mineralized fibrocartilage **(MC)** and bone **(B)** by a thin watershed line/tidemark (Large arrows). Small arrows indicate bending collagen fibers crossing the watershed line. *Photo: Obtained from AnalySIS V, Geir Aasmund Hjorthaug.*

The other main type is the fibrous enthesis. Histologically, the fibrous type lacks the four-layer cartilaginous architecture. Collagen fibers from ligament/tendon may insert directly to the bone and indirectly via the periosteum. Again, these subgroups of fibrous entheses can be referred to as bony or periosteal. Fibrous entheses are typically located in diaphyseal bone regions, along bone ridges, and the tendons or ligaments are relatively short or partially lacking. Examples of fibrous insertions are the tibial insertion of the knee medial collateral ligament (MCL) and the deltoid tendon insertions in the humerus.

1.4 Bone healing

Bone healing is a complex process that results in regeneration and functional restoration of bones. It is a highly regulated physiological process that takes place in time and space. The time of injury represents the starting shot. After a fracture, the local biomechanical environment has suddenly changed dramatically. The external soft tissue, periosteum, bone

marrow, and cortex are all tissues (spaces) that simultaneously host the bone healing processes, often extended far from the bony fracture itself. Following specific time sequences, the bone fragments gradually unite as new bone is formed as a result of highly orchestrated signaling cascades where multiple genes are turned on or off. Knowledge of these complex processes is increasing; however, still limited(21, 22).

In contrast to other tissue, bone has the unique ability to heal without scarring. The bone of a fully remodeled united fracture does not differ from the original bone. Though the process of bone healing often starts with an injury with a fractured bone, bone healing is also clinically relevant in the context of osteointegration of implants and in elective bone surgery like osteotomy and joint fusion (arthrodesis). Bone healing processes are also inevitable interleaved with tendon-to-bone healing in ligament reconstructions, tendon transfers, and reinsertions. Understanding and interpreting bone healing depends on your perspective.

1.4.1 Patient´s perspective

A patient suffering from an acute fracture may describe the process in overlapping phases, starting with an accident with immediate severe pain, grinding noise, swelling, bruising, deformity, and loss of function. The instinctive auto-treatment starts with unloading and self-protection of the fractured region. Regardless of any treatment, most of the fracture symptoms will last for several days or weeks while slowly improving. Gradually there will be less pain and swelling, and as time goes by, function can more or less slowly recover. Even some untreated deformities may straighten out within months or years. Patients with access to modern healthcare, including radiologic diagnostics and proper conservative or surgical treatment will often benefit in all phases of the fracture healing process. Early stabilization, pain control, guided mobilization, and rehabilitation are prerequisites for a favorable outcome. Most fracture patients can expect a full recovery without any or minimal sequelae. However, in some cases, the patient may report persistent pain and impaired function because of soft tissue -or joint injuries, fracture malunion, fracture non-union, or other complications.

1.4.2 Surgeon´s perspective – primary and secondary bone healing

The orthopedic surgeon is aware of the fact that time and course of fracture healing may vary significantly, depending on location (diaphyseal vs. metaphyseal) and “personality” of the fracture including blood supply, multiple patient-related factors and the treatment to be chosen. The surgeon is probably also concerned of two possible fracture healing patterns:

primary bone healing and secondary bone healing. Primary (direct) bone healing without callus formation is relatively rare but desired in (peri)articular fractures or certain simple shaft fractures. General principles to achieve primary bone healing are anatomical fracture reduction, absolute stability, and compression to reduce fracture gap, preferably < 0.01 mm. Secondary (indirect or natural) bone healing with callus formation is the more common healing pattern of long bones and is seen in most conservatively treated fractures or in fractures treated with semi-rigid osteosyntheses. The surgeon will often follow the patient and healing process until adequate recovery from functional impairment and pain. Correspondingly, X-rays may show increasing callus formation and eventually complete bridging solid bone formation over the fracture site along with disappearance of the initial fracture gap.

1.4.3 The 4-stage model

The traditional model of bone healing describes histologically and radiographically that is seen in secondary fracture healing:

1) Fracture hematoma and inflammation	(days)
2) Soft callus formation	(days/weeks)
3) Hard callus formation	(weeks/months)
4) Remodeling	(months/years)

Stage 1: A fracture is said to be considered a soft tissue injury with an adjacent broken bone. Disruption of vessels from the injured soft tissue, periosteum, and bonemarrow leads to bleeding. A fracture hematoma is rapidly formed. The fracture hematoma with early coagulation also hosts the inflammatory and cellular environment necessary for starting the later stages of bone healing(23). Activated thrombocytes, macrophages, granulocytes, lymphocytes, and monocytes infiltrate the hematoma and start an immune response of non-specific phagocytosis, signaling that leads to increase of local prostaglandin (PG) synthesis by the endothelium (pain, vasodilation) and large signal cascades by cytokines and growth factors. Essential cytokines for fracture healing are interleukin 1 (IL-1) and IL-6 in addition to tumor necrosis factor alpha (TNFα) that rapidly increase the first day after fracture and rapidly falls during the first three days after fracture(24). IL-1 and TNFα are produced by macrophages and lead to the recruitment of further inflammatory cells and promote angiogenesis. These cytokines, in turn, stimulates the production of IL-6 in osteoblasts and

are one of several vital signals for the first cartilaginous callus production. Later, MSCs are recruited from the local bone marrow, periosteum, circulation, and overlying muscle, probably induced by growth factors like bone morphogenetic proteins (BMP)(25).

Stage 2: After a few days, capillaries invade the fracture hematoma, and a granulation tissue is formed. The MSCs differentiate to chondrocytes that produce matrix, and together with fibroblasts and their contribution with unspecific fibrous tissue, the fracture gap and surrounding is filled. Osteoblasts form woven bone and, gradually, the cartilaginous matrix is mineralized, slowly increasing the stability of the fracture and the bone mineral may be visible as early (soft) callus formation upon X-rays. The callus formation process in secondary bone healing usually consists of *endochondral ossification* (cartilage > mineralized cartilage > bone). This process is the same that is seen in fetal skeletal development and growth. *Intramembranous ossification* (from the periosteal layer, without cartilage) is the other crucial developmental bone process and is also seen together with endochondral ossification in early fracture healing(26).

Stage 3: In areas of stability within the increasing callus, osteoblasts under the influence of transforming growth factors (TGFs) (most important: BMPs) secrete several specific proteins that form layers of extracellular osteoid on internal and external bone surfaces. Simultaneously, extensive angiogenesis and the mineralization of the osteoid result in the formation of lamellar bone. Further lamellar bone formation by numerous osteoblasts arranged in a trabecular pattern increases the stability of the hard callus, and if stability is kept adequate, the hard callus bridge the fracture and functional healing has occurred.

Stage 4: The remodeling of hard callus refers to a specific process where the trabecular bone is replaced by compact bone. The remodeling phase may start as early as 3-4 weeks after fracture and may continue for several years. In contrast to remodeling of the soft callus (stage 2 and 3), remodeling of hard callus (in stage 4) is primary driven by and dependent on osteoclasts, secondary the coupling mechanism to osteoblasts(27). Osteocytes percept the mechanical load environment and regulate the recruitment of osteoclasts to areas of trabecular bone. Later, the osteoblasts fill the empty resorption pits. The two cell types form remodeling units that slowly shape the bone according to the mechanical environment. Even healed angulated or overlapping fractures may remodel into well functional bones.

One problem with the 4-stage model is that it gives the false impression of transitory and independent phases. This model is not sufficiently comprehensive. Newer schemas have attempted to describe the underlying cellular and molecular mechanisms. Cellular activity like migration, proliferation, differentiation, and cell death (apoptosis or necrosis) are time and space-dependent overlapping processes. Moreover, signaling cascades regulating cellular activity involve growth factors, hormones, PGs, cytokines, and genes. Furthermore, they are dependent on local factors like oxygen, pressure, pH, and temperature(26). Although defined stages of fracture healing still are recognized, the complexity of the several simultaneous processes is striking and far from elucidated.

1.4.4 Anabolic-catabolic model

Based on the traditional stages of fracture healing, also interpreting cells and molecules, two polarized forces are present: anabolism (bone formation) and catabolism (bone resorption) (Figure 5). The waves of anabolism and catabolism in the first stages of fracture healing, when fibrocartilage of the soft callus is formed and removed, resembles healing response in other tissue. Hence, the term non-specific anabolism and non-specific catabolism are proposed(28).

The formation and remodeling of the hard callus are thought to be bone-tissue specific processes, and the metabolic waves during these later stages can be called specific anabolism/catabolism. Contribution of the osteoclasts during specific catabolism is probably crucial. In contrast, during non-specific catabolism in earlier stages, other cells and pathways are more important. The non-specific catabolism that results in removal of the soft callus is poorly understood, but several studies report significantly increased levels of matrix metalloproteinases (MMPs) during this stage of the healing process(29). MMPs are a group of enzymes with multiple effects, but important ones are, firstly degradation of ECM, secondly promotion of angiogenesis. MMPs are produced by pre-osteoblasts, mature osteoblasts, hypertrophic chondroblasts, inflammatory cells, by endothelial and other vascular cells, and by osteoclasts. In early hypertrophic stages, the soft callus is mainly avascular, but the invasion of new vessels into the callus is thought to be the most critical step for further healing to occur. The role of the osteoclast at this stage of non-specific catabolism does not seem prominent, but this is still not clear.

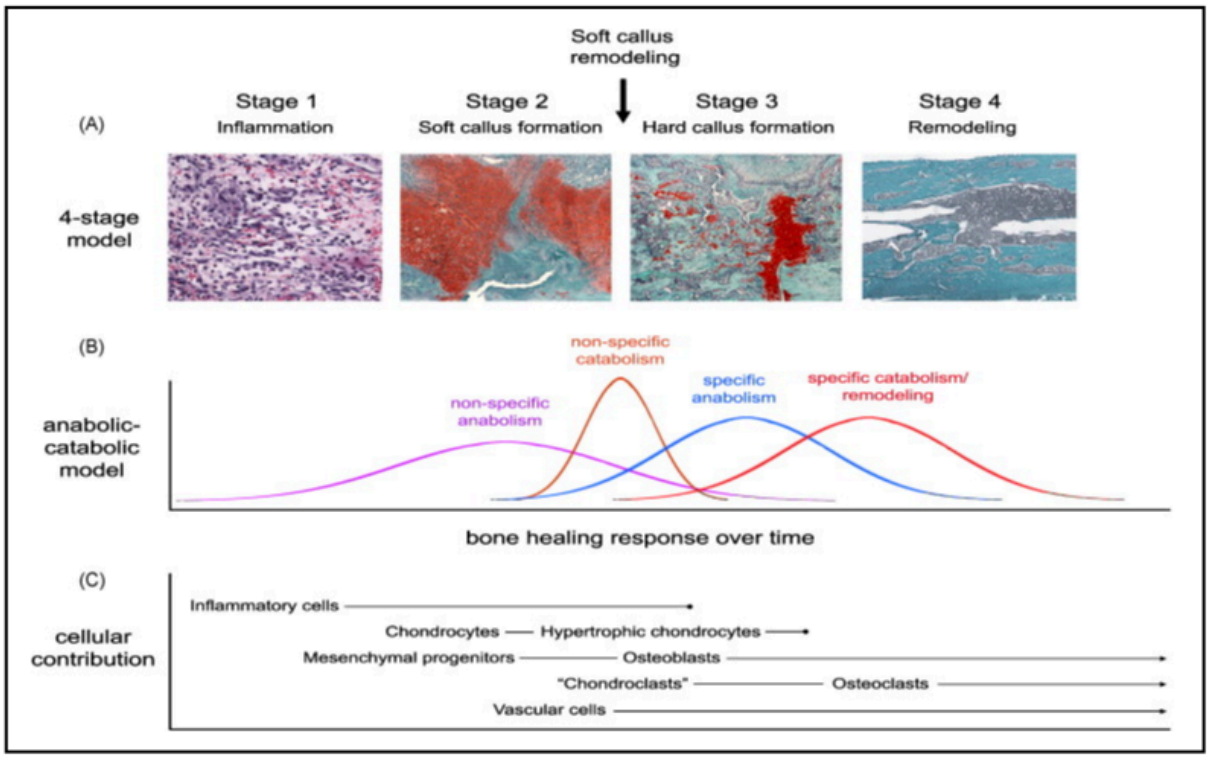

Figure 5. Models of fracture repair and cellular participants. **(A)** The four-stage model of fracture healing. Between stages 2 and 3, the soft callus is systematically remodeled. **(B)** The anabolic/catabolic model **(C)** Cellular contributors. *Reprinted from(28), with permission from Elsevier, License number: 4672530746260.*

If we apply the anabolic-catabolic model on top of the recent discoveries of molecular and cellular contributions, this may provide a useful alternative understanding of fracture healing. With this concept, the outcome of fracture healing depends on a delicate balance between the anabolic and catabolic responses. It is crucial to determine which stages, phases, or processes of bone healing that are of importance for healing outcome, regardless of a strict timeline or what is seen microscopically. Schindeler et al. have made speculations in this regard: If the speed of fracture healing is dependent of non-specific anabolism and/or catabolism and the strength of fracture healing is dependent of specific anabolism and/or catabolism, adjuvant treatment to promote fracture healing or avoidance of risk factors for delayed or non-union may be targeted(28). So far, this hypothesis has not been confirmed.

1.4.5 The diamond model

All fractures do not heal. The risk of developing a non-union following a fracture is 2-5% with significant variations between fracture type and trauma energy(30). Moreover, the etiology of non-unions can be classified by patient-related factors, biological factors, and mechanical factors(31). Often, the most prominent cause can predict the type of non-union

observed and also how to treat it: Hypertrophic non-unions (excessive callus formation) are often treated with revision surgery to increase stability. Atrophic non-unions (paucity of callus formation) require restoration of the fracture biology, traditionally by an autologous bone graft (ABG). The ABGs contain *MSCs*, *growth factors*, and bone that serves as a *scaffold* for new bone formation. Respectively, the three ingredients of ABG have osteogenetic, osteoinductive, and osteoconductive features. Together with the fourth element *optimal mechanical environment*, these factors of interaction have been defined as prerequisites for bone healing to occur in "the diamond concept"(32) (Figure 6).

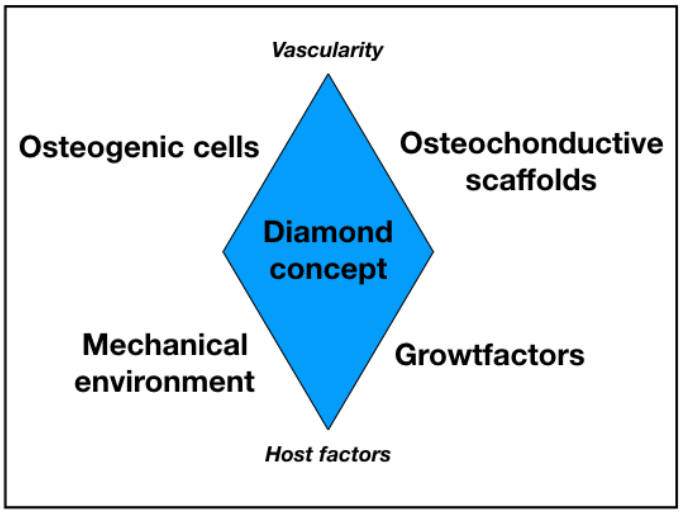

Figure 6. The diamond model, adapted from Andrzejowski and Giannoudis 2019(33), CC-link: http://creativecommons.org/licenses/by/4.0/.

One problem with ABG, in addition to donor site morbidity, is the relatively low levels of MSCs, especially in the elderly patient. MSC-augmentation is possible from bone marrow aspirate concentrate. BMP-2 and BMP-7 are commercially available, and osteoconductive scaffolds are numerous and still evolving. The diamond concept has been further explored and its principles used to treat non-unions, and it seems like "polytherapy" with optimization of all four walls of the diamond also including blood supply and host factors, may produce the best results(33). However, future studies on the topic are needed.

1.4.6 Metaphyseal vs. diaphyseal fracture healing

The knowledge of fracture healing, as summarized above, is dependent mainly on animal models utilizing diaphyseal (cortical) fractures. The majority of clinical fractures occur in metaphyseal (corticocancellous/trabecular) bone regions. There is an increased awareness that these two fracture locations are different in terms of healing mechanisms, stages, healing potential, and sensitivity to external positive and negative healing factors. Compared to cortical fractures, cancellous fractures are generally more stable, heal more often, heal faster, and usually without callus formation. Cancellous bone is more vascularized, and MSCs are already at the site of injury and start osteogenesis in just a week or two. In metaphyseal fractures, the MSCs that differentiate into osteoblast precursors arrive just as fast as the inflammatory cells(34). Though initial inflammation is present(35), the unspecific bone remodeling is skipped for the benefit of direct woven bone formation and specific bone remodeling, first between and later connecting to the old bone trabeculae(36).

In diaphyseal fractures, large macro segments of cortical bone respond and contribute to healing also of bony defects, by extensive endochondral ossification in the fracture center and eccentric (periosteal) intramembranous ossification. In contrast, the healing response in cancellous bone resembles intramembranous ossification and occurs in the very local area of bone damage. Moreover, the membranous ossification seen in cancellous fracture healing is probably not identical to intramembranous ossification in cortical fractures. Sandberg and Aspenberg have proposed the term "inter-trabecular ossification" and argue that osteocytes form osteoid that becomes mineralized woven bone *between* the old trabeculae, not on old trabecular surfaces(37). Osteoid-formation in inter-trabecular ossification coincide throughout the entire injured volume and explains the rapid healing response compared to classical (cortical) healing responses.

1.5 Tendon-to-bone healing

Tendon-bone interfaces heal slowly and inferiorly compared to bone-bone interfaces(38). The result of tendon-to-bone healing will result in a functional, poor functional, or not functional fibrovascular scar tissue. Preclinical studies of tendon-bone repair show a lack of the four-layer architecture with a transitional zone between tendon and bone, lack of collagen integration, and local bone loss (8, 39, 40). In contrast to fracture healing, the ruptured enthesis tissue probably does not regenerate into its original form, but a fibrous scar tissue

develops. Nevertheless, that does not mean the healed tendon-bone interface cannot be functional.

In the case of enthesiolysis (by injury or surgery), a gap without biomechanical stimulus will usually prevent a functional tendon-bone interface. Surgery must aim to close the gap, firmly attaching the tendon to the bone. Techniques include tendon fixation in mono or bicortical bone tunnels, bone grooves, or directly to bone/periosteal surfaces. Fixation can be achieved by interferences screws, post screws, suture anchors, suture endo-button, or sutures through drill holes. The tendon can also be looped through a bicortical bone tunnel and sutured to itself, in which case a combination of tendon-bone and tendon-tendon healing may occur.

In anterior crucial ligament reconstruction (ACLR), popular free tendon grafts include the bone-patellar tendon-bone (BPTB) autograft or hamstrings tendon (HT) autograft. One advantage of the BPTB-graft is the preservation of the strong native patellar tendon entheses with bone blocks on both sides of the graft. After graft fixation in the femur and tibia bone tunnels, a combination of bone-bone healing and tendon-bone healing occurs. The use of the HT-graft features tendon-bone healing only. Regardless of technique, the grafted tendon is slowly transformed into a ligament. A study of human biopsies showed that remodeling of the grafts was not complete up to two years after ACLR(41). However, the biopsies did not include the tendon-bone interface, which makes the study less valid to evaluate the actual tendon-bone healing response.

Stable fixation remains vital for a functional outcome of the tendon-bone interface. However, without biologic tendo-osseointegration (tendon-bone *healing*), the interface will often fail in the long term(5, 6). Compared to bone healing, the biomechanical process of tendon-to-bone healing remains far less investigated. Tendon-to-bone healing consists of a combination of tendon healing and bone healing processes; both tissues seem to contribute.

As in other tissues, tendon to bone healing is commonly described by overlapping phases:

1) Inflammation	(days/weeks)
2) Proliferation	(weeks/months)
3) Repair/remodeling	(months/years)

Inflammation starts the healing response as described in bone healing. Both inflammatory cells and cells derived from the tendon release factors (cytokines and growth

factors), which promote repair processes. There is increasing neovascularization, proliferation, and chemotaxis of fibroblasts and collagen and extracellular matrix deposition(42). Loose granulation tissue is formed. In bone tunnels, the tendon graft is early surrounded by a fibrous tissue separating the tendon graft from bone containing poorly oriented collagen fibers. Simultaneously, bone healing processes can be observed. Bone healing response in the repair phase may consist of both endochondral ossification and intramembranous ossification, depending on the location of the site of surgery and the technique used. Eventually, new woven bone ingrowth may be observed both inside the tunnel, the adjacent bone marrow, around the outer/periosteal/cortical area around the tendon ostium, and the callus may partially fill the tunnel at the expense of the tendon graft tissue. The neovascularization is seen both in the tendon and new bone.

After the proliferative phase, remodeling starts and results in a decrease of vascularity and cellularity of the tissue. The collagen fibers are gradually more organized. Actual tendon-bone healing occurs through a process of progressive re-establishment of an oriented and integrated bridge of collagen from the callus that protrudes through the fibrous tissue and into the tendon(43). Crossing collagen fibers correlate with healing in terms of (sub)normal mechanical tendon-bone interface strength, and are observed after 6 weeks of healing in rats(44) and shown to progressively increase, changing from tendon-bone failure to tendon-clamp failure at 12 weeks in dogs(39). A degloving mechanism of failure between the outer and inner parts of the tendon graft has been observed(45). Remodeling after the first repair phase may take even a longer time. After 2 years, the fibers crossing the tendon-bone interface was still disorganized, and the tissue remained hypercellular compared to native entheses in a study of patellar tenotomy and repair in sheep(40).

1.5.1 Factors of importance in tendon-to-bone healing

Several local factors of importance for healing have been described and include both bony and tendinous elements. It seems that factors from both bone and tendon are necessary for solid tendon-to-bone healing. Large callus formation at the tendon-bone repair site was found and depended on the presence of tendon in the bone tunnel, according to a tibia bone tunnel study in rats(44). The tendon graft fixed to the bone may release factors necessary for osteogenesis and healing of the tendon-bone interface. In this study, the control group was tibia bone tunnel only (without tendon graft), and the callus formation after 6 weeks in this group was minimal. Other factors that influenced callus formation in this study were tendon graft viability, intact periosteum, and mechanical load. Callus formation is probably an

essential factor, but the role of callus in tendon-bone healing, especially in restoration of mechanical healing strength, is still unclear. The amount, duration of callus, but also its quality, seems fundamental. Late callus is remodeled by osteoclastic activity, and in the long term, the tendon graft must heal firm to bone surfaces to be able to transfer high and repetitive loads for years. The ingrowth of bone into the tendon-bone interface is described as a crucial factor for solid healing of this tissue and was studied by Rodeo et.al(3, 39, 46).
In a clinical situation, mechanical factors of importance in tendon-bone healing include graft type (bony vs. soft tissue graft, allo vs. autograft), size, tunnel placement, graft tensioning, angle, bundle numbers, fixation, share forces, and load/rehabilitation. Biological factors include immunological (graft immune response), inflammatory, vascular, synovial pressure, and specific tendon-bone healing mechanisms(47).

Tunnel widening is another obvious concern following primary ACLR and a significant challenge in revision surgery. The etiology of tunnel widening remains unclear, but both mechanical and biological factors are probably involved(48, 49). The correlation between tunnel widening and outcome in primary ACLR surgery is, however, not documented(50, 51).

1.6 Bone resorption inhibitors

Bone resorption inhibitors are mainly used to prevent fractures in patients with osteoporosis. By blocking the action of osteoclasts, bone resorption is inhibited, and a net gain of bone mineralization and formation is achieved. The result is increased BMD and a decreased risk of fractures. Subgroups of BRIs are small molecules, hormones, and biological drugs, all acting as antiresorptive agents, but by different mechanisms and stages in bone remodeling.

1.6.1 Bisphosphonates

BRIs in the drug class “small molecules” have a narrow mechanism of action. The most important small molecular group is the bisphosphonates (BPs) (Figure 7).

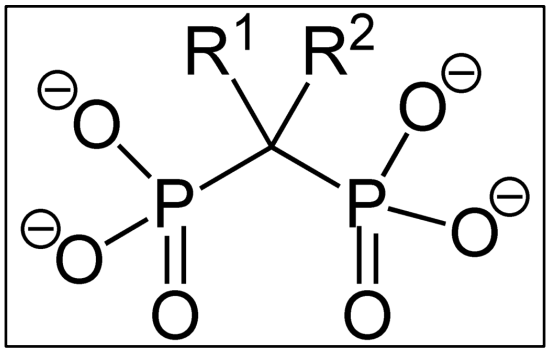

Figure 7. BPs are pyrophosphate derivates, containing one carbon atom instead of an oxygen atom between the phosphonate (PO_3)-groups. Bis (two) refers to the number of phosphonate groups. Two side-chains (R1 and R2) are also attached to the carbon atom, and the structure of these chains determines the biological activity of the BP. The side-chains determine the antiresorptive potential, the affinity to bone matrix, and the pharmacokinetics. Nitrogen-containing BPs (e.g., alendronate, ibandronate, risedronate, zoledronate) have both higher antiresorptive and greater bone affinity compared to non-nitrogen containing BPs (e.g., etidronate, clodronate)(52). *Image from Wikimedia Commons, the free media repository; https://commons.wikimedia.org/wiki/File:Biphosphonate_Structural_Formulae.png*

The intestinal absorption of oral BPs is deficient (<1%). Depending on the affinity, 20% (etidronate) or 80% (alendronate) of the absorbed BP rapidly bind onto the bone surface, the rest is excreted unchanged by the kidneys. The half-life of the portion BP incorporated in the bone may exceed 10 years. Once resided in bone, BP is ingested by osteoclasts where they block the enzyme farnesyl diphosphate synthase in the HMG-CoA reductase pathway. This enzyme-blocking leads to disruption of synthesis of several proteins inside the osteoclast and results in reduced cytoskeletal properties affecting the ruffled border and reduced cell survival. This anti-osteoclastic effect results in decreased bone resorption that can be measured by serum bone markers after a few weeks. Osteoblasts fill the empty resorption pits, and increased BMD can be measured after a few months(53).

Main indications for BPs are adult men and postmenopausal women with osteoporosis and increased risk of fractures and glucocorticoid-induced osteoporosis. Also, the BP zoledronic acid (ZA) is indicated in Paget's disease and for the prevention of skeletal-related events in adult patients with cancer involving the skeleton or with tumor-induced hypercalcemia.

In addition to the clinical effect of reduced risk of fractures, several other biologic effects of BPs have been reported *in vitro* and *in vivo*: Direct stimulation of osteoblasts, direct chondroprotective effects, anti-angiogenic and anti-inflammatory effects(54-57). BPs are

therefore being tested for off-label indications with or without bone marrow lesions in the contexts of several conditions like osteoarthritis, avascular necrosis, augmentation of implant fixation, regional transient osteoporosis, complex regional pain syndrome, and bone healing(15, 58-62).

1.6.2 Bisphosphonates and effects on bone and tendon-to-bone healing

The way BPs inhibit bone resorption in an ongoing (patho)physiologic state as in osteoporosis, is relatively predictable and well documented(52, 63). Bone resorption in phases of fracture healing, both the remodeling of initial callus and later the remodeling of hard callus, is necessary to restore the healthy bone tissue and strength. As inhibitors of bone remodeling, one might expect BPs to impair fracture healing. However, experimental studies of simulated fracture repair have demonstrated that BP treatment does not interfere(64) or even may enhance bone healing by stabilizing the fracture callus(65). BPs are extensively examined in secondary bone healing. Analyses that include radiography, QCT, microCT, biomechanical testing, and histology show that BPs consistently decrease the remodeling of fracture callus with a concomitant increase in fracture bridging and retained cancellous bone structures within the callus(61, 66-69). Utilization of these effects can be important in scenarios at risk of non-union like high energy trauma, diaphyseal fractures, instability, and critical size defects, but may not be relevant in metaphyseal fractures or when primary fracture healing can be expected. Human studies of BPs and effects on bone healing are few, but a meta-analysis of 8 randomized controlled trials (RCTs) conclude BPs does not cause a clinically detectable delay to indirect bone healing. In lumbar fusions, positive effects were noted(70).

The rationale for the investigation of BRIs in tendon to bone healing is that these drugs may reduce the local bone loss that can be observed around grafted tendons/reconstructed ligaments. If we can prevent the local bone loss before or after repair, the result may be an increased healing response. Apart from two animal studies of the BP alendronate(9, 71) and one animal study of osteoprotegerin (OPG)(72), the effect of BRIs on tendon-to-bone healing has not been much investigated. These studies are further discussed below, in light of the results from our study of ZA and the effect of tendon-to-bone tunnel healing (*section 6.2*). To our knowledge, no clinical studies on the effect of BRIs in tendon-bone healing exist.

1.6.3 Zoledronic acid

Zoledronic acid (also called zoledronate) (Figure 8) is to date the most potent BP available. Compared to etidronate, ZA is 5-10 000 times more potent. Compared to alendronate, ZA is 10-20 times more potent (73), and is administered by intravenous infusion.

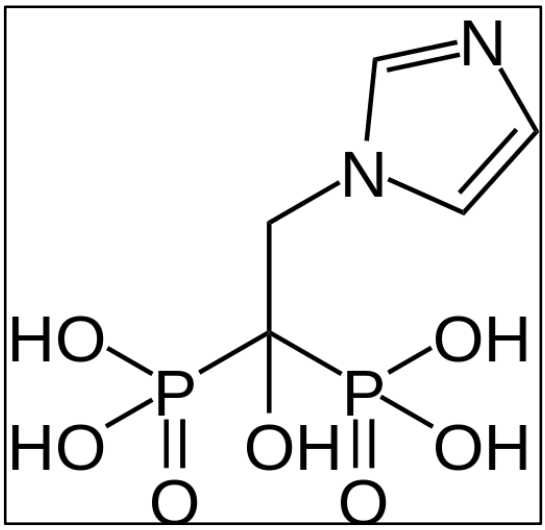

Figure 8. Chemical structure of zoledronic acid. The nitrogen-containing R1-group has an exceptionally high affinity for bone HA. *Image from Wikimedia Commons, the free media repository; https://commons.wikimedia.org/wiki/File:Zoledronate.svg*

1.6.4 Zoledronic acid and clinical effects on osteoporosis

In postmenopausal osteoporosis, annual infusions of 5 mg ZA were introduced shortly after the millennium, following studies showing both effects on bone resorption markers, effects on BMD(53), and, most important, effects by reduction low energy fractures(74). A reduction of subsequent fracture was reported in a study of ZA administered within 90 days after surgical repair of a hip fracture(75). Moreover, ZA reduced all-cause mortality, and subgroup analyses showed that these effects were apparent when the first ZA-infusion was given in the interval 2-12 weeks after surgical fracture repair(76). Hip fracture healing was not disturbed(77). The two phase-III clinical trials reported relative risk reductions that ranged from 25% to 27% for nonvertebral fractures, 30% to 41% for hip fractures, and 46% to 77% for vertebral fractures

after 3 and 1.9 years(74, 75). In an RCT in men with osteoporosis, ZA reduced the relative vertebral fracture rate by 67% after 2 years(78).

1.6.5 Safety of zoledronic acid

Safety of high doses ZA have been studied in male and female rats(79), and no physiological, hematological or biochemical adverse events or increased mortality was noted after doses as high as 2 mg/kg, which is 20 times the dose we used in our study (Study II). ZA-infusions in patients with severe renal impairment (creatinine clearance < 35 ml/min) is contraindicated due to an increased risk of renal failure. Following the first infusion of ZA, 40% of patients suffer from post-infusion syndrome with mild to moderate acute phase response with fever, musculoskeletal pain/stiffness, or gastrointestinal adverse events, starting day 1 and with a mean duration of 3 days(80). Post infusion syndrome is a benign and self-limiting condition and rarely result in discontinuity of the drug, also since only <2% of patients report adverse reactions on subsequent infusions.

Several issues are debated regarding paradoxical adverse skeletal events of BRIs. BRIs arrest the natural bone remodeling, and accumulation of unrepaired microdamage in the bone matrix may lead to fatigue fractures or other skeletal impairment. Severe adverse events like osteonecrosis of the jaw (ONJ) and atypical femoral fractures (AFF) have been reported for zoledronate, alendronate, and other BRIs like denosumab(81). The risk of ONJ and AFF is low (1/10000 to 1/100000) and associated with long-term use of BRIs and cancer(82-85). Also, these risk numbers are only slightly higher than that seen in the general population. When it comes to BRIs in the treatment of osteoporosis, it seems clear that the benefit of these drugs exceeds the risk of rare adverse events. However, the disruption of the cupelling mechanism between osteoclasts and osteoblasts that may lead to an unfavorable outcome should also be a concern when testing BRIs on off-label indications in research.

1.6.6 Other small molecules

Strontium ranelate is a small molecule that also incorporates into the bone matrix and acts both as a BRI and a stimulator of bone formation, but was never clinically approved because of increased risk of thromboembolism.

Cathepsin K inhibitors such as *odanacatib* had the potential as a highly selective and potent BRI acting by inhibiting the last step in bone resorption process; the release of protease from the osteoclastic surfaces into the resorption pits. By inhibiting the osteoclastic proteases

only, the decreased bone formation seen as a result of BPs or RANKL-inhibitors (that have more upstream effects) could be avoided. The phase III clinical trial of odanacatib in postmenopausal women showed that BMD increased and fractures were reduced(86). Later, a significantly increased risk of atrial fibrillation and stroke was revealed, leading to a discontinue of the drug development(87).

1.6.7 Hormones

The hormones, especially *estrogen,* have broad biological effects and are mediated through intranuclear estrogen receptors that are present in all bone cells. The result of estrogen withdrawal will lead to a rapid decrease in BMD and is the most important cause of postmenopausal osteoporosis. The molecular and cellular mechanisms are not fully understood. All three bone cell types express estrogen receptors. The main effect seems to be that estrogen promotes survival of osteoblasts and inhibits genes necessary for differentiation, survival, and activation of osteoclasts, both by direct effects of osteoclasts and indirectly through the osteocyte modulated coupling mechanism between these two cell types(88). Treatment with estrogen was not considered as the first-line treatment for osteoporosis based on the safety concerns(89, 90), but in postmenopausal women younger than 60 years or within 10 years after menopause, the consensus is now that estrogen replacement, after all, may be appropriate(91).

The use of other hormones that have antiresorptive effects has also been associated with adverse events. Selective estrogen receptor modulators (SERMs) such as *raloxifene* increases BMD, decreases the risk of vertebral fractures, decreases the risk of breast cancer, but increases the risk of venous thromboembolism(92). *Tibolone* and *calcitonin* are less effective in fracture prevention compared to other BRIs, and both are associated with an increased risk of cancer(93, 94).

1.6.8 Biologic drugs

In recent years, biological drugs have become an available BRI subgroup. *Denosumab* is a human monoclonal antibody for subcutaneous administration. The antibody binds to and inhibits receptor activator of nuclear factor kappa-B ligand **(**RANK-L) that is produced by osteoblasts. RANK-L is necessary for the activation of RANK that is found on the surfaces of pre-osteoclasts and mature osteoclasts. OPG produced by osteoblasts normally regulates RANK-L levels. OPG binds to RANK-L and inhibits this system in a negative-feedback

manner. Denosumab 60 mg subcutaneously will fulfill the action of OPG and completely block RANK-L. Without RANK- activation, both osteoclast recruitment, function, and survival will be reduced, resulting in a rapid decrease in bone resorption and increased BMD. This effect is more substantial compared to the similar effect of the BP alendronate(95), and also on par with or more substantial than ZA(96).

Clinically, treatment with denosumab reduces fracture risk in postmenopausal osteoporosis(97) and increases BMD in osteoporotic men(98, 99). Theoretically, in the context of enhancement of bone healing or implant fixation, denosumab should perform better than BPs. Denosumab prevents the recruitment of osteoclasts to the fracture site, but with BPs, the osteoclasts first have to ingest some bone to get poisoned by the BP. Unfortunately, denosumab does not recognize rodent RANK-L and therefore, does not suppress bone resorption in normal mice or rats. Thus, in experimental animal studies, we are left with the more sophisticated alternatives recombinant rodent OPG as a surrogate RANK-L-inhibitor, or denosumab treatment using human RANKL knock-in animals (100, 101).

1.7 COX inhibitors

COX-inhibitors are also called non-steroid anti-inflammatory drugs (NSAIDs). These drugs are mainly used because of their analgesic, antipyretic, and anti-inflammatory effects, both in acute(102) and chronic(103) conditions. COX-inhibitors are effective and well documented as fundamental parts in modern multimodal analgesia regimens in both elective and trauma orthopedic surgery (104, 105). An often-highlighted advantage of COX-inhibitors is their opioid-sparing potential. The risk of opioid-related adverse events like respiratory depression, nausea, vomiting, fatigue, and addiction can be reduced with multimodal analgesia that includes COX-inhibitors. Therefore, the use of COX-inhibitors fits well with healthcare system's focus on early discharge and outpatient surgery, but also for clinician´s focus on early active rehabilitation that may improve patient outcomes.

COX-enzymes are necessary for the arachidonic acid pathway for the production of PGs (106). PGs needed for basic cell survival are produced by the enzyme isoform COX-1 in blood platelets, gastrointestinal lining, kidney, and in smooth muscle in vessels and airways. The much higher PG production of the isoform COX-2 is turned on when excess PGs are desired as following trauma and surgery or other causes of acute inflammation(107, 108). Conventional COX-inhibitors (e.g., ibuprofen, naproxen, diclofenac, indomethacin, ketorolac, piroxicam) target both COX-isoforms. It has been demonstrated that the analgesic and anti-

inflammatory effects of the non-selective COX-inhibitors are attributed to the inhibition of COX-2 (109). The selective COX-2-inhibitors (e.g., etoricoxib, parecoxib, celecoxib) are believed to have the same desired effects but are designed to avoid potential adverse effects by maintaining COX-1 function (108). The main advantage of COX-2-inhibitors compared to non-selective COX-inhibitors are their reduced risk of surgical and gastrointestinal bleeding.

1.7.1 COX inhibitors effects on bone and tendon-to-bone healing

The effects of COX-inhibitors on bone metabolism and related tissue healing have still not been adequately elucidated. It has been shown that COX-2 is required for endochondral and intramembranous bone formation(110). Moreover, COX-2 function is imperative for fracture healing (111). Furthermore, stimulation of the PG-E2 receptor specifically promoted fracture healing in a rat study(112).

Experimental studies since mid-1970 have reported that COX-inhibitors delay healing of long bones(113-115), and concerns have been raised if this effect may increase the risk of delayed healing, non-union, and impaired outcome for orthopedic patients(10). After several decades of scientific debate, several controversies still exist on the translational potential from animal studies to the clinical situation on this topic, mainly due to the lack of high-quality RCTs.

The apparent reasons why COX-inhibitors may impair bone healing are these drugs´ inhibitory effects on necessary steps of healing; inflammation(116) and angiogenesis(117). Several other mechanisms are also involved. COX-2-inhibitors might inhibit genes produced by the Wnt signaling pathway, which inhibits osteoclastogenesis and promote differentiation and proliferation of immature osteoblasts(118).

The effect of COX-inhibitors is probably different in diaphyseal and metaphyseal bone healing. Therefore, it is imperative to be careful not to refer results from experimental fracture studies as being relevant for bone healing in general(119). Experimental data of diaphyseal fracture healing indicate uniformly adverse effects, but the data of metaphyseal fractures are indifferent. Parecoxib has been tested in a metaphyseal rat model, and transient impairment of bone healing was reported in female but not in male rats(120).

Though less studied, the adversarial effect of COX-inhibitors is also reported in experimental studies in early phases of tendon healing(121, 122). COX-inhibitors also seems to impair tendon-to-bone healing in models of rotator cuff repair(123) and Achilles tendon in tibia bone tunnel(124). Recently, similar effects were reported by Sauerschnig et al. in a rabbit ACLR-model(45). In this study, treatment with celecoxib for the 3 first weeks

suppressed levels of PG-E2 in the synovial fluid at 3 weeks, and a compensatory increase in PG-E2 concentration was seen at 6 weeks. Still, COX-inhibition resulted in a decrease of BMD and new bone formation [peripheral quantitative computed tomography (pQCT)] and decreased graft stability as measured by biomechanical tests at 6 weeks.

Human studies of COX-inhibitors and tendon-bone healing are very few. To our knowledge, we have published the largest registry study on this topic, with 7822 included patients with primary ACLR(125). Surgeon-reported use of COX-inhibitors (mean duration of 6.7 days, range 1-14 days) did not negatively affect the risk of revision or patient-reported knee function at 2 years. Together, the current experimental and clinical evidence is inconclusive regarding the use of COX-inhibitors and tendon-bone healing(126, 127).

1.7.2 Parecoxib

Parecoxib (Figure 9) is a prodrug of the COX-2-inhibitor valdecoxib for parenteral use. In humans, the recommended starting dose is 40 mg, followed by 20 mg or 40 mg every 6th and 12th hour as required. Max daily dose of parecoxib is 80 mg (about 1 mg/kg). There is limited clinical experience with parecoxib treatment beyond three days in humans. While still approved in Europe, a non-approval for parecoxib was issued in the USA in 2005. These concerns were raised because of studies that reported an increased risk of cardiovascular adverse events following coronary artery bypass graft surgery (CABG) when treated with parecoxib compared to placebo(128). CABG surgery is now a contraindication to all NSAIDs.

In over 80 countries, including most of Europe, parecoxib is commonly used for trauma and perioperative pain management due to its analgesic and anti-inflammatory effects with reduced risk of gastrointestinal or surgical bleeding compared to nonspecific COX-inhibitors(129). A recent meta-analysis of 28 RCTs and a review of 10 years of post-authorization data concluded that serious adverse events associated with parecoxib are rare when adherence to prescribing guidelines are followed(130).

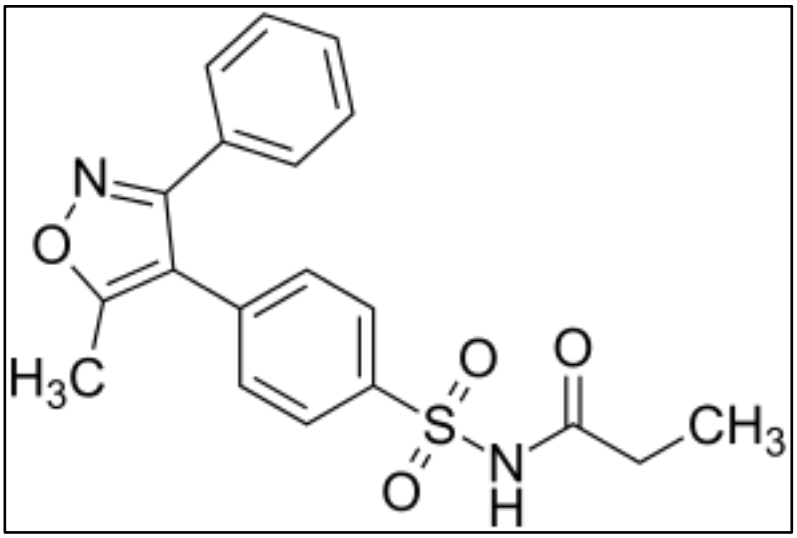

Figure 9. Chemical structure of parecoxib. *Image from Wikimedia Commons, the free media repository; https://commons.wikimedia.org/wiki/File:Parecoxib_200.svg*

2. Aims

Knowledge of the healing process of a tendon in a bone tunnel is limited. We intended to characterize the mechanical and histological properties of a healing tendon graft subjected to physiological load. We also wanted to improve and validate the tendon-to-bone model before assessing the effect of bone resorption inhibition. There are concerns attached to the use of COX-inhibitors in pain management following trauma and orthopedic surgery. We wanted to investigate the effect of clinically relevant immediate and delayed short time COX-inhibition on diaphyseal fracture healing. The following questions were particularly emphasized:

- What are the mechanical, bone mineral, and histological characteristics at 2, 3, 4, and 12 weeks of tendon-to-bone tunnel healing?

- What is the effect of a 1 week delayed single intravenous (IV) dose of the bisphosphonate zoledronic acid at 3 and 6 weeks of tendon-to-bone tunnel healing?

- What is the effect of immediate 3 days administration of the COX-2-inhibitor parecoxib on diaphyseal fracture healing?

- What is the effect of 3 days delayed administration of the COX-2-inhibitor parecoxib on diaphyseal fracture healing?

3. Summary of the papers

3.1 Paper I

Hjorthaug GA, Madsen JE, Nordsletten L, Reinholt FP, Steen H, Dimmen S. Tendon to bone tunnel healing-a study on the time-dependent changes in biomechanics, bone remodeling, and histology in a rat model. *J Orthop Res* 2015; 33:216-23.

Biomechanical tests, local BMD, BMC, and histology were studied in a tendon-to-bone tunnel rat model at 2, 3, 4, and 12 weeks of healing. Aims of the study were to elucidate early phases of tendon-to-bone healing and to validate the model. Rats (n=61) were operated by proximal release of the Achilles tendon and transfer to a 1.8 mm bone tunnel in the distal tibia. We found a slow increase in pull-out force and other biomechanical variables during the first 4 weeks of healing. After 12 weeks, there was a five times stronger tendon-bone interface compared to the earliest time point. Bone minerals did not increase during the first 4 weeks, but after 12 weeks, a significant increase in peri tunnel BMD and BMC were seen. Evaluation of hematoxylin-eosin (H+E)-stained cross-sections of the bone tunnel and tendon graft at all time points showed chronologically maturation of the tendon-bone interface and collagen fibers crossing the interface at 12 weeks. A significant number of *in model* variations were discovered.

3.2 Paper II

Hjorthaug GA, Søreide E, Nordsletten L, Madsen JE, Reinholt FP, Niratisairak S, Dimmen S. Negative effect of zoledronic acid on tendon to bone healing - In vivo study of biomechanics and bone remodeling in a rat model. *Acta Orthop* 2018; 1-7.

Biomechanical tests, local BMD, BMC, and histology were studied in a refined version of the tendon-to-bone tunnel rat model at 3 and 6 weeks of healing. The aim of the study was to assess the effect of the bisphosphonate zoledronic acid on tendon-to-bone healing. Rats (n=92) were operated by proximal release of the Achilles tendon and transfer to a 1.5 mm bone tunnel in the distal tibia. After 1 week, rats were infused IV with a single dose of zoledronic acid or placebo. Treatment of zoledronic acid resulted in reduced pull-out strength and stiffness of the tendon-bone interface. We found no differences between the study groups

by evaluation of bone mineral, qualitative H+E-sections in light microscopy, histomorphometry, or osteoclast counting after TRAP-staining.

3.3 Paper III

Hjorthaug GA, Søreide E, Nordsletten L, Madsen JE, Reinholt FP, Niratisairak S, Dimmen S. Short-term perioperative parecoxib is not detrimental to shaft fracture healing in a rat model. *Bone Joint Res* 2019; 8:472-80.

Biomechanical tests, local BMD, BMC, and histology were studied after 4 weeks of healing in an established shaft fracture model in rats. The aim of the study was to assess the effect of immediate and delayed 3 days administration of the COX-2-inhibitor parecoxib on diaphyseal fracture healing. Rats (n=66) were operated by reaming of the tibia medullary canal, a closed midshaft fracture was induced, reduced, and fixed with a nail. Parecoxib was administrated as intramuscular (IM) injections during the first 3 days or by delaying the dose until days 3-5 postoperatively. Controls received IM-injections with saline. We found no differences between the study groups in biomechanical variables, bone mineral, qualitative light microscopy of Masson-Goldner´s trichrome (MGT)-stained sections, or in histomorphometric evaluation of osteoid/bone ratio and callus area.

4. Methodological considerations

4.1 Experimental animals and drug administration

Laboratory rats (l. *Rattus norvegicus*) are the most used animal for experimental scientific research ever since the late 18th and early 19th century because of their usefulness as models of *in vivo* mammalian systems. In 1906, the Wistar Institute (Philadelphia, US) developed and bred the albino Wistar rat, the first standardized laboratory animal model from which more than half of all laboratory rats today are descended.

Rat´s body temperature is 37°C, respiratory rate 75-115/min, heart rate 260-400/min, and birth weight is around 5 g. They reach weaning age at 3 weeks, sexual maturity at 7 weeks, and mate at the age of 10-12 weeks (females, 180-225 g). Adult weight for males and females is 450-550 g and 250-300 g, respectively. Females reach menopause at 15-18 months age, and rats of both genders have a life span of 2,5 -3.5 years. In average, 16.4 rat days correlate to 1 human year, but these calculations largely depend on and vary with life phases(131). Strength and stiffness of femoral cortical bone have been tested in healthy rats aged 3-36 weeks(132). At 14 weeks of age (mean weight 341 g, male rats), a plateau in the mechanical parameters was found, which might be indicative of skeletal maturity in Wistar rats.

In the current models, we have used the rat tibia, which is approximately 42 mm long(133). Compared to humans, rat tibias are around ten times shorter. Another difference is that the rat fibula does not extend to the ankle joint, but is attached to tibia´s distal third diaphysis posterolaterally via a rigid tibiofibular synostosis. This means that the rat fibula is not weight-bearing, in contrast to human fibulas that account for around 20% of the load of the leg(134). The rat tibia is significantly curved anteriorly in the sagittal plane. Furthermore, the distal metaphyseal part of the rat tibia is characterized by several deep, almost invaginated, longitudinal grooves (sulci) wherein the long tendons passing the ankle joint can be found. In two dimensional sections (microscopy or CT), these sulci must not be confused with cortical fractures.

Several nonmammalian species lack typical Haversian systems(135). Rat bone tissue does have a similar organization of bone tissue as humans, but the Haversian systems seem to be few and small(136). The process of continuous bone remodeling follow the same stages in rats and humans, but at a ten-fold increased speed(137). Phases of fracture healing also are similar, but probably faster in rats, but not at all as fast as their homeostatic bone remodeling.

The expected time to union of simple fractures is 4-6 weeks in rats(138). At 8 and 13 weeks, fractured rat femurs regained bending strength and torsional strength, respectively, as reported in Ekeland´s study(139). Similar biomechanical *in vivo* studies in humans do not exist, for obvious reasons.

Even though similarities are striking when comparing rats and humans, care should be taken when interpreting results from experimental animal studies. A lot of discovered and undiscovered differences in physiology and anatomy do exist. Nevertheless, the rat model in bone research is widely used, and findings have contributed significantly to skeletal knowledge in humans.

We used rats of the Wistar strain in all three studies. Because of different drug metabolism between rat genders, in particular for COX-inhibitors(140, 141), only female rats were used. We also wanted to compare the results with our previous studies utilizing the same models in female rats(124, 142). The rats used in Study I and II (tendon-bone-model) had a mean weight of 251 g (SD 10) and 238 g (SD 9), respectively. They were 10-14 weeks of age, which means they were young and recently sexually and soon/recently skeletally mature. In Study III (fracture model), we intentionally wanted slightly larger rats because we learned from the cadaveric pilot study that fracture induction and fixation was technically easier on larger specimens. Mean weight of the rats in Study III was 288 g (SD 14). Still, they were skeletally mature and relatively young.

As thoroughly reported in all papers, the animals were housed in a modern animal facility with educated personnel or research personnel supervising daily. Rats were always kept in pairs in wire-topped plastic cages with controlled temperature, humidity, ventilation, and light/dark cycles. They were allowed water and standard laboratory rodent nutrition *ad libidum*. Acclimatization was done before any intervention in all studies. Subcutaneous (SC), intraperitoneal (IP), and IM injections were performed with carpet immobilization. IV infusions, surgical procedures, and radiologic measurements were performed in general anesthesia. Because rat eyes remain open under anesthesia, protection from cornea drying and ulcers was used (Viscotears gel). During recovery, wrapping in fleece blankets and controlled electric heating pads was used to prevent hypothermia. Opioid analgesics (buprenorphine) was scheduled twice a day postoperatively the first 48 hours. A standardized system of labeling of ears for animal identification was used. Parameters like animal behavior, look, movement, body weight, and wound status was registered throughout the study periods in predefined forms with scores, defining thresholds for humane endpoints and additional administration of analgesics if required. The scheduled killing of animals was initiated by

deep general anesthesia followed by either IP-pentobarbital overdose or by *in vivo* vascular transcardial perfusion fixation after thoracolaparatomy.

In previous studies, and including the current Study I, we have had good experience using an anesthesia protocol with Hypnorm (fluanisone and fentanyl) and Dormicum (midazolam) (H/D) for SC-injections. Due to temporarily unavailability of H/D, a new anesthesia protocol was introduced at our institution before Study II. In Study II we used Zoletil Mix (ZRF cocktail). The cocktail consisted of Zoletil Forte Vet.(zolazepam and tiletamine), Rompun Vet. (xylazine), Fentanyl (fentanyl), and 0.9% NaCl (Appendix 1). IP-injections was used to minimize skin rash, which is a known adverse event of Zoletil Mix if given SC. Unexpected, we experienced a substantial loss of animals suspected due to anesthesia-related complications. Animals that died after IP-injections of Zoletil Mix were autopsied to rule out internal bleeding. In total, we found an unacceptable rate of anesthesia-related deaths at 22/105 (21%) in Study II when using Zoletil Mix (Table 1). This adverse event was unfortunate; firstly concerning the warranted reduction of animals used in experimental research; secondly it might have made the study prone to type II experimental errors. On the other hand, only 2 animals were excluded *after* randomization by 1 week (wound complications). Hence, we consider the loss of animals to represent only a minor bias to the experimental results.

In Study III, H/D anesthesia for surgery was reintroduced, and we used inhalation anesthesia (isoflurane) for dual-energy X-ray absorptiometry (DEXA) measurements. Reintroduction of H/D anesthesia resulted in an acceptable anesthesia-related loss of animals of 2/66 (3%).

Table 1. Overview of the number of animals and losses in Study II.

Event pr. time point	Running number of animals	Loss of animals
In animal facility	105	
Anesthesia-related deaths before surgery		13
Surgeries performed	92	

Anesthesia-related deaths during/after surgery, (<24h)		7
Humane endpoint, (wound complications during the 1st week)		2
Randomized and infused IV (at 1 week)	83	
Anesthesia-related deaths during infusion (at 1 week)		2
Total number for further analyses	**81**	**24 (total loss)**

4.2 Administration of study drugs

4.2.1 Zoledronic acid

BPs are well established in experimental animal research. They are absorbed and incorporated in rat bone in the same manner as in humans(143). In Study II we tested the effect of bone resorption inhibition with BP on tendon-to-bone tunnel healing by the administration of a single dose ZA (Aclasta, Novartis, UK) 0.1 mg/kg IV (or control, saline) in the tail vein 1 week postoperatively. The dose was similar to that of ordinary human doses(53). The IV route is technically demanding. Due to this, trained personnel did the infusions, and the volume (0.5 ml) was infused, only following positive aspiration of blood from the tail vein. A small butterfly peripheral venous catheter was used (BD Valu Set 25G, 0.5 x 19 mm) and flushed with saline after infusion before removal. The dose, route, and 1-week delay were chosen based on a rat fracture study(66). By delaying the dose 1 or 2 weeks, the binding of ZA to the forming callus was significantly increased and also resulted in increased mechanical strength compared both to the administration of ZA at the time of fracture and to control (saline).

4.2.2 Parecoxib

In earlier studies, we demonstrated that the COX-2-inhibitor parecoxib given perioperatively for 1 week, in doses analogous to those used in humans, reduced the biomechanical strength and local bone mineral density (BMD) in early tibia shaft fracture healing in rats (142). The dose used in this study may be inadequate due to the fast metabolism of COX-2-inhibitors in rats (122, 144). We still found significant differences in the mechanical properties of the healing fractures. With higher and more adequate doses of parecoxib, the adverse effects may

be even more pronounced. In the current Study III, we tested the effect of inhibition of COX once again with parecoxib using the same model of tibia shaft fracture healing. However, instead of 7 days treatment, we used only 3 days of treatment with a high dose parecoxib, and also added a 3 days delayed group. The daily dose of parecoxib (Dynastat, Pfizer, GB) was 6.4 mg/kg body weight, using allometric scaling based on the basic caloric demand, which is increased by a factor of 4 in rats compared to humans (144-146). We consider the use of this higher dose a significant refinement in regards to clinically relevant doses of parecoxib in rat studies. Rats in all study groups received IM injections in the center of the right gluteus maximus muscle to avoid damage to the sciatic nerve. The injections contained parecoxib or saline with a volume of 0.04 ml twice a day for 6 days. Plasma concentration of parecoxib was not measured but has been done previously at our institution in male rats(147).

4.3 Tibia fracture model

We used a closed tibia diaphyseal (shaft) fracture model, as opposed to open osteotomy models also used by others (147, 148). Closed fractures and open osteotomies heal differently, as reported in a tibia diaphysis rat study(149). The main difference found in this study was that healing of the open osteotomies was slower. Reasons for this might be the increased periosteal damage and reduced fracture hematoma formation in the open vs. closed model. The investigator´s choice of model and the reader´s interpretation of the results should consider such differences. If the focus is trauma, osteotomy models should be used and read with caution; closed induced fracture models are considered more valid(138).

The closed tibia shaft fracture model is well established at our group(142, 150, 151). The medullary canal was reamed with a nail consisting of a stylet and two cannulas. The cannulas were retracted to the proximal part, and with the stylet remaining inside all the way into the distal tibia metaphysis, middle shaft fracture was induced by 3-point bending by using a manual fracture forceps with an adjustable plate(139). The two outer cannulas were then advanced over the stylet/mandarin, which resulted in reduction and press-fit fixation of the fracture. The nail was cut flush with the tibia plateau. Following fracture and nail fixation, most animals limped for a few days, then normal behavior, movement, and gait would be expected.

Refinements in Study III included the development of a new a fracture inducing forceps that was tested in a pilot study on cadaveric tibia rat bones with and without soft tissue. The forceps produced closed standardized midshaft fractures with minimal soft tissue damage. In most cases, a simple transverse or short oblique fracture was seen, sometimes also with a small wedge fragment. Complex fractures were not observed. Concomitant fibula fractures were common. Locking of the nail was not performed, and even though we did not observe nonunions in the current study after 4 weeks of healing, malunions with some degrees of external rotation was noted. Probably, the presence of the fibula fracture also contributes to the rotational instability observed, and the tibia fracture is to be considered semi-stable. Nevertheless, we consider the current tibia shaft fracture rat model as highly relevant to human diaphyseal fractures or when secondary bone healing is anticipated.

The pilot study also allowed us to choose optimal nail diameters that best fitted the size of the rats (mean weight 288 g). Components of the nail used in Study III are shown in Figure 10.

Figure 10. Components of the nail as tested in the cadaveric pilot study. **a)** Outer cannula: 23G 0.6x60 mm Sterican, Braun, Germany. **b)** Middle cannula: 19G 1.1x40 mm Microlance3, BD, Spain. **c)** Inner mandrin: Spinal needle, the stylet only. 22G 0.7x90 mm Yale Spinal, BD, Spain. *Photo: Geir Aasmund Hjorthaug*

Further surgical refinements in Study III was the placement of the 3 mm skin incision 15 mm more proximal than previously. This refinement was done to prevent the nail from

penetrating the wound in case of proximal nail migration. The pronounced laxity of the rat skin made sufficient skin retraction possible, and still nailing was quick and easy.

4.4 Tendon-to-bone model

The tendon-to-bone model has been developed using pilot studies and then established by our group by testing the effect of COX-inhibitors on tendon-bone healing by 2 weeks(124). In Study I, we used an unchanged surgical method and evaluated healing by 2, 3, 4 and 12 weeks. Briefly, the proximal Achilles tendon was cut from the calf muscle using a 10 mm skin incision dorsally and medially. The Achilles-calcaneal enthesis was preserved. The dorsal tibia metaphysis was exposed, and a bone tunnel with a diameter of 1.8 mm was drilled at high speed [(12000 rounds per minute (RPM)] and aimed 3 mm proximal to the ankle joint. With the ankle in neutral position, the tendon was passed through the tunnel and fixated anteriorly to the periosteum using a resorbable suture (Polysorb 4-0, Covidien, Dublin, Ireland). Even though this tendon transfer will decrease or remove the rat´s ankle plantarflexion, the tendon graft is to some extent loaded during mobilization.

Because loading is a crucial factor for tendon-bone healing, this model provides relevance also to human tendon-bone tunnel healing. The bone tunnel is localized in an extra-articular environment as opposed to the intra-articular environments of ACLR or rotator cuff repairs. Though still in metaphyseal bone, mechanisms of tunnel widening under the influence of synovial pressure may be different. Another limitation of the current model is undoubtedly the point of fixation. The single half Kessler suture that grasped the tendon was securely sutured to the ventral soft tissue. Fixation was evaluated peroperatively, but we did not evaluate if fixation failure occurred at any time postoperatively *in vivo*. This method of fixation would seldom be used for tendon-bone tunnel fixation in humans without an implant, looping graft, or at least osteosutures.

In Study I, healing was evaluated not by biomechanical testing only, but for the first time, we also added DEXA-measurements and histology. Light microscopy of the tendon-bone interface showed a significant number of surgical complications that may cause internal variation and decrease both the reliability and validity of the tendon-bone model. The main issues discovered by microscopy was:

1) Heat necrosis in peri tunnel bone (excessive).

2) Misplacement of bone tunnels (partially intraarticular or *ad latus* with cortical cut-out).
3) Foreign body reactions (excessive lymphocyte infiltration around polyfilament suture material or bone fragments).
4) Bicortical complete tibia fractures (with or without cortical healing).
5) Bone tunnels without tendon tissue (suggestive of fixation failure).

Some of these complications can be explained by the challenging small dimensions of the rat tibia, making precise and less invasive surgery difficult. Even with perfect placement of a 1.8 mm bone tunnel in the rat distal tibia metaphysis, the medial and lateral cortex remaining will measure only around 0.6 mm, as the total width of the current part of the tibia is around 3.0 mm.

Because of the internal model variations revealed by microscopy in Study I, we tested several surgical modifications in a pilot study in rat cadavers before adapting refinements in Study II. Initial surgical access remained the same, but by incising the superior and inferior peroneal retinaculum and holding the lateral and medial long ankle tendons anteriorly by using one or two needles, the dorsal distal tibia exposure was improved and standardized. The plantaris tendon was excised. We used precise instruments (Colibri and Compact Hand, DePuy Synthes, Oberdorf, Switzerland) and predrilled the tunnel with a 1.0 mm drill bit and over-drilled with a 1.5 mm drill bit at medium speed (3200 RPM) (Figure 11). Saline was used for tunnel lavage to remove small bone fragments. The surfaces of the tendon were trimmed to match the diameter of the tunnel. The tendon was grasped by a half Kessler two-string monofilament nonabsorbable suture with two needles (Prolene 5-0, Ethicon, Somerville, New Jersey, USA). By using a cannula through the tunnel from anterior to posterior, the two needles were passed through the tunnel from posterior to anterior, the tendon was gently pulled through the tunnel, and sutured to the anterior soft tissue. The incision was closed using resorbable sutures (Polysorb 4-0, Covidien, Dublin, Ireland) and sealed with spray dressing (Opsite, Smith & Nephew, Hull, UK).

The most important refinement was probably the reduction of bone tunnel diameter from 1.8 (r=0.9) mm to 1.5 mm (r = 0.75). Since the length (h) of the tunnel was 3 mm, the calculated cylinder volume ($\pi r^2 h$) of bone loss from the drilling of the tunnel was at least 30% reduced. Microscopy in Study II showed that the refinements were effective in preventing fractures, heat necrosis, misplacement of bone tunnels, and foreign body reactions compared to Study I.

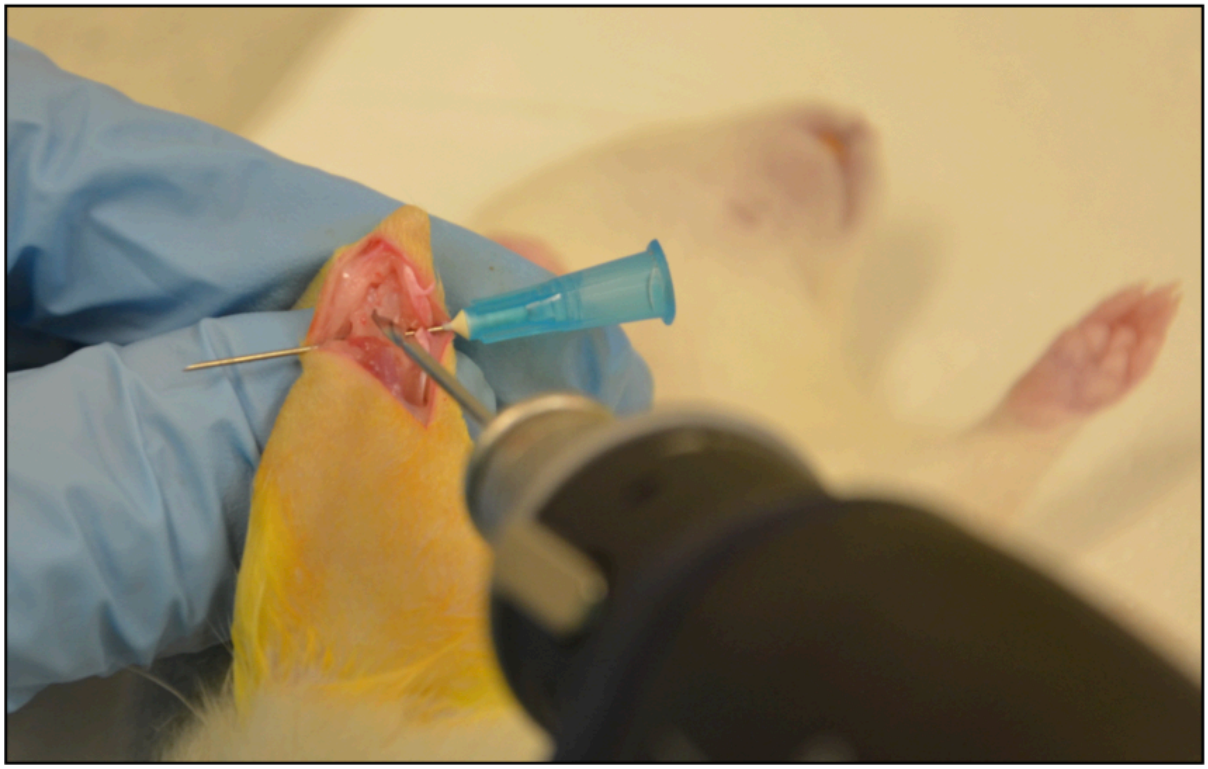

Figure 11. Peroperative image showing dorsal distal tibia exposure, Achilles tendon graft, and predrilling of the bone tunnel. *Photo: Geir Aasmund Hjorthaug.*

4.5 Biomechanical bone testing and analyses

For biomechanical testing of the tibia fractures and contralateral non-fractured tibias in Study III, we used a standardized three-point bending test(142, 151, 152). Frozen tibias were thawed, rinsed of all soft tissues, and kept moist during testing. The nail was removed. Callus diameter was measured with a sliding caliper. In the jig, the distal tibia was fixed, a fulcrum was placed over the center of the fracture, and a wedge of a clam wheel applied force to the proximal tibia (Figure 12).

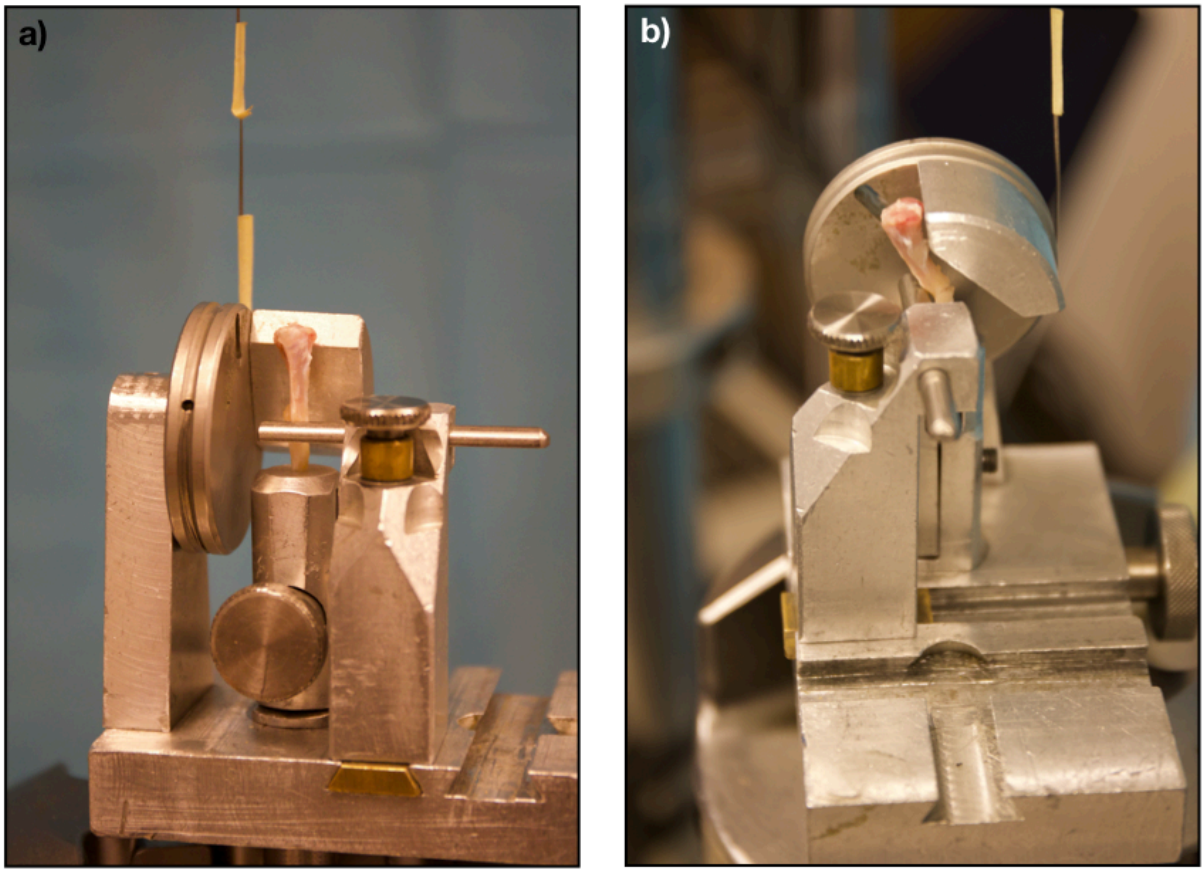

Figure 12. **a)** Mounting and preloading of tibia in the three-point cantilever bending test jig. Anterior view. **b)** Lateral view, captured at the moment of fracture when the force of the clam wheel overcomes the ultimate bending capacity of the tibia. *Photo: Endre Søreide.*

The force was registered by a hydraulic material testing machine (Model 858 Mini Bionix with MTS FlexTest digital controller, MTS Systems Corporation Eden Prairie, Minnesota, USA). The machine and a 250N load cell were calibrated by the manufacturer before testing. We used a preload of 0.5 N (outside the test), speed 2.67 mm/s, tibia bending rate 7.2°/s, and sampling frequency of 20Hz. Data was exported to Origin (Origin v. 8.6 for Windows, OriginLab Corporation, Northampton, MA, USA) for analysis of classical load-displacement (LD) curves (Figure 13).

Ultimate load (N) was defined as the maximum bending load the tibia could withstand before failure (=fracture or refracture). On the LD-curve, this was the highest value on the Y-axis (highest peak). Deflection (mm) was the maximum deformation before failure and was read from the peak´s corresponding X-value (stroke). Stiffness (N/mm) was the ratio of the applied force on the corresponding deformation in the straight, elastic part of the curve. Total energy (Nmm) was the energy absorbed by the tibia before failure as calculated from the area

under the curve. Following initial data collection, ratios between fractured and non-fractured corresponding tibias were used in the statistical analyses. In Study II and III, all biomechanical analyses were performed by two independent observers, and the mean values were reported. LD-curve analyses were performed in the same manner for both fracture bending tests and tendon-bone pull-out tests, as specified in Figure 15.

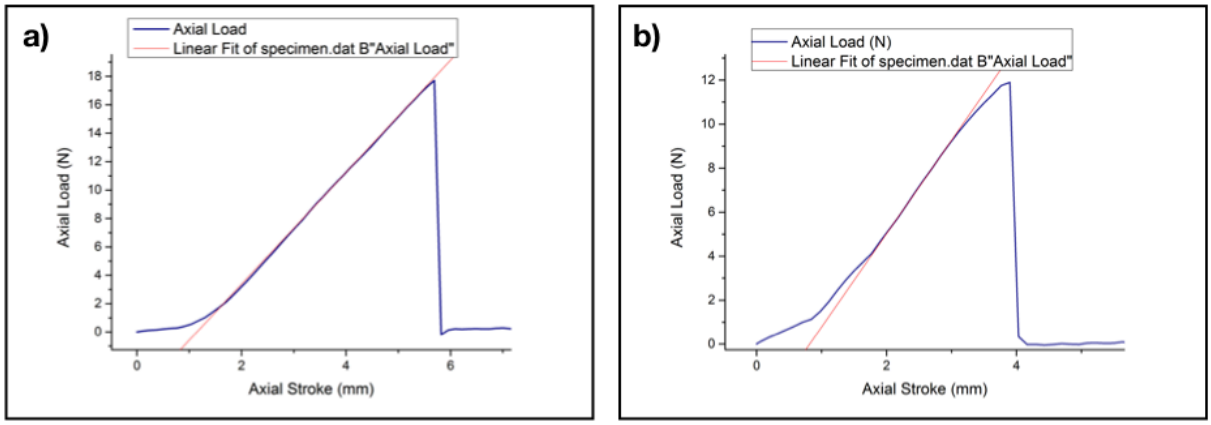

Figure 13. Representative LD-curves from three-point bending tests in Study III. LD-curves in the fracture model were relatively easy to analyze because, in most specimens, one defined peak (moment of failure) was observed. **a)** Left non-fractured tibia. **b)** Right tibia with fracture after 4 weeks of healing from the same specimen (parecoxib immediate group). The ultimate bending moment ratio between fractured and non-fractured tibia of this specific specimen was (11.8 N / 17.4 N) = 0.7.

4.6 Biomechanical tendon-bone testing and analyses

For biomechanical testing of the healed tendon-bone interface in Study I and II, we used a pull-out test described previously(124). Dissection of the specimens included removal of all soft tissue except the grafted tendon. A refinement was that we preserved the fibrous and callus tissue surrounding the tendon graft. Fibula, talus, and ankle capsule were removed. The suture was also removed before biomechanical testing, to ensure that we assessed the healing and not the contribution of fixation. The dissection allowed mounting of the calcaneus with an intact Achilles enthesis to be secured in a claw. The graft was pulled by the testing machine perpendicularly to the longitudinal axis of the tibia with a constant speed, while the tibia was secured horizontally in a clamp. Preload was not used due to the relatively small forces. Specimens always ruptured in the tendon-bone interface.

We used definitions of the four biomechanical variables pull-out strength (N), elongation (mm), stiffness (N/mm), and energy (Nmm) that was similar to the ones described

for fracture testing above. Furthermore, the definitions in the tendon-bone model are clearly stated in Paper I. Ratios were not obtained.

In contrast to bone testing, the LD-curves from tendon-bone-interfaces often had multiple peaks (Figure 14). This phenomenon reflected the different material properties of hard bone tissue *versus* the healing tendon-bone interface where at least two different and partially disorganized biomaterials unite. In cases of multiple peaks, the highest was chosen as the point of failure. Generally, the force before failure of the tendon-bone interface, compared to the forces in fracture testing at the same timepoints was approximately half. When comparing Study I and control specimens in Study II at one common timepoint of healing (3 weeks), forces in Study II were around 3 times higher before tendon-bone failure. The reason for this was probably the refinements made from Study I into Study II that promoted healing. Similar forces were recently confirmed in a study using the same refined version of the tendon-bone model(153).

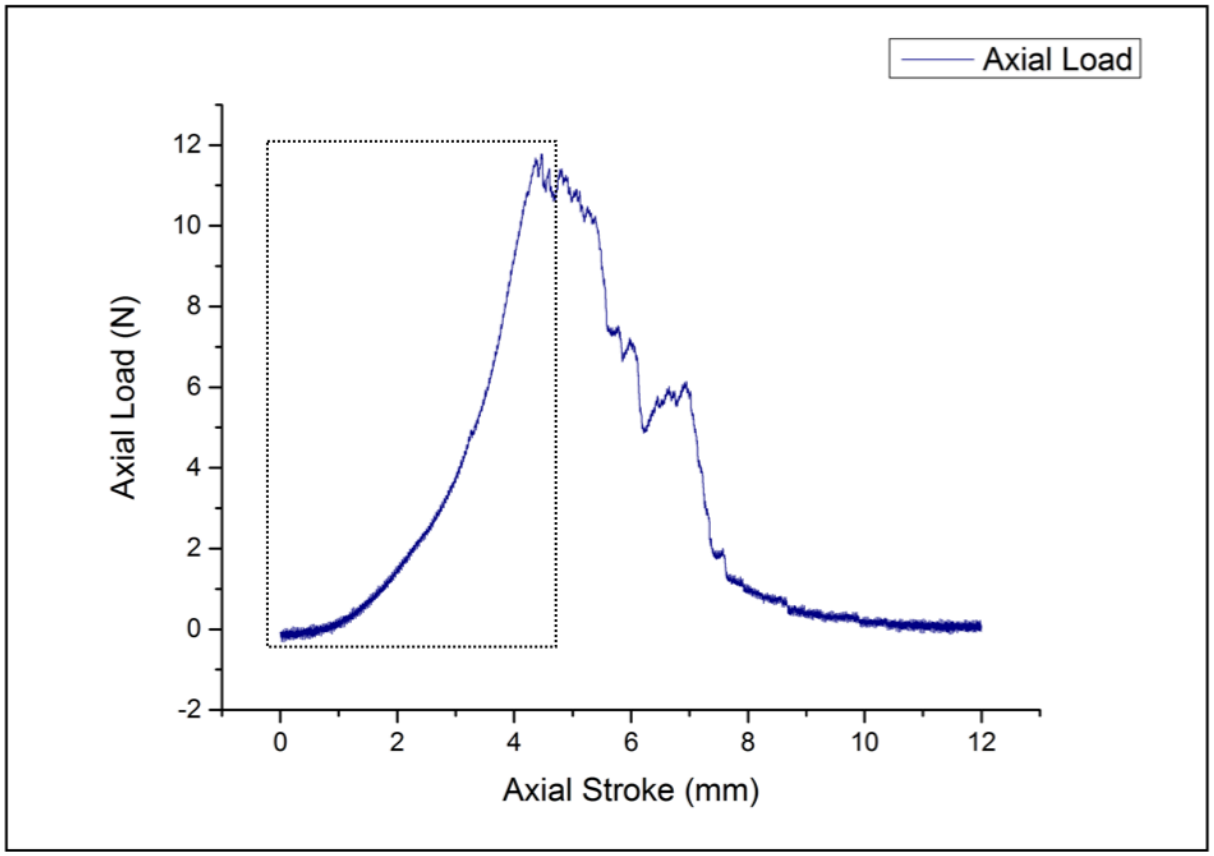

Figure 14. Representative LD-curve for tendon-bone pull-out test in Studies I-II. In this figure, all test data (120s, speed 0,1 mm/s = 12 mm) is shown (specimen from Study II, control 6 weeks). The pattern with multiple peaks after the first elastic part of the curve was typical. For further analyses, the highest peak was included (rectangle, the same data displayed in Figure 15). The remaining data were excluded.

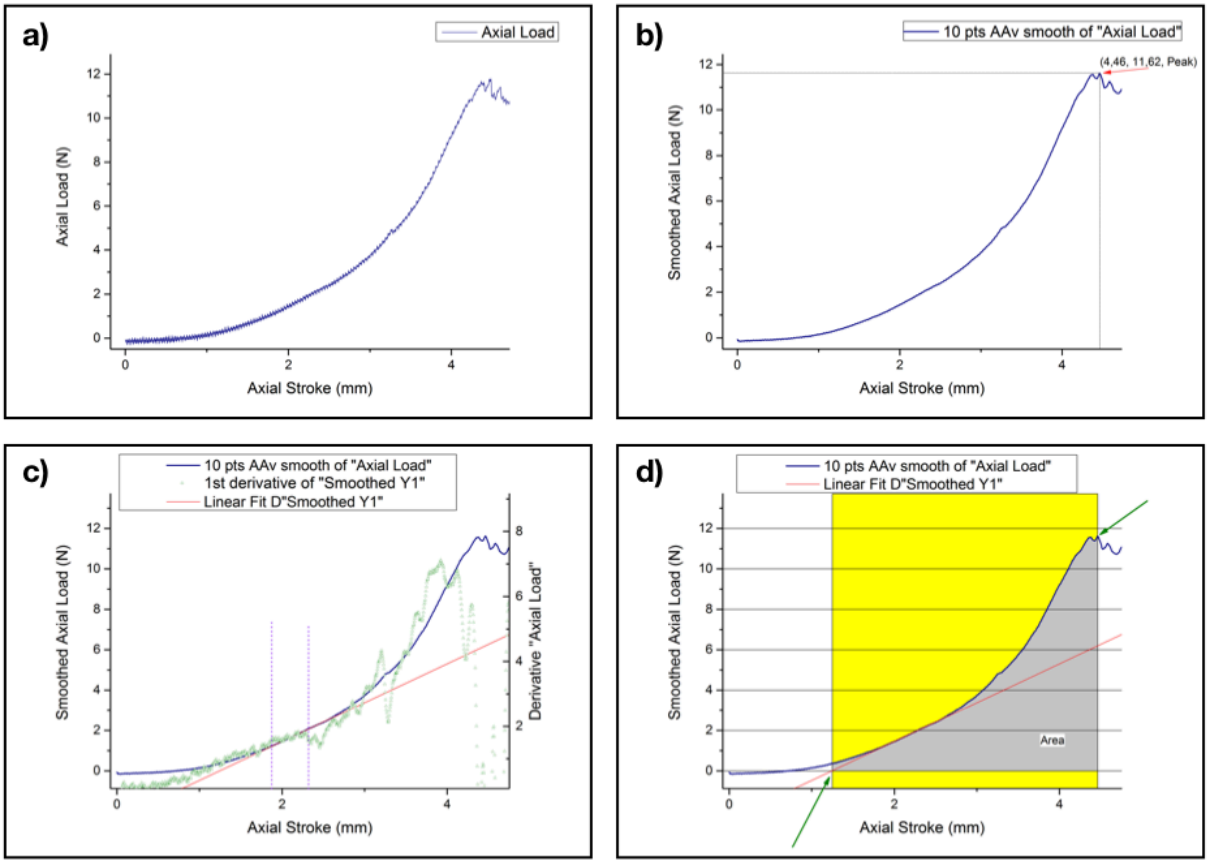

Figure 15. LD-curves from the same specimen displayed in Figure 14 (rectangle). The data analysis followed a strict sequence: **a)** ROI after exclusion of data. **b)** We used smoothing of the data by averaging 10 adjacent data points to reduce "noise." Highest peak was determined. Ultimate load/pull-out force and deflection/elongation were read from the Y and X-axis, respectively. **c)** The plot for the 1st derivative of the axial load was drawn (green plot), and its flattest region was identified (between the purple dotted vertical lines). This range was selected for the linear fit (red line) from which the slope represented the stiffness of the biomaterial. **d)** The energy was calculated by area under the curve, and the range for this integration ($f(x)$) was between intercept of the stiffness-line and peak (green arrows).

4.7 Bone mineral measurements and analyses

The PIXImus DEXA-machine (Lunar PIXImus, Lunar, Madison, WI) is designed to obtain accurate bone mineral and total body composition results in smaller animals, like mice. However, it is possible to use it for local bone mineral data from the extremities of larger animals. In all of our rat studies, we used the PIXImus to measure *in vivo* local BMD (gcm^2) and bone mineral content (BMC) (g) at predefined regions of interest (ROI). Daily calibration and quality control were performed. Imaging takes about 5 minutes, and the animal must be adequately sedated as movement will impair image and data quality. In Study II and III we

used isoflurane inhalation on a mask during DEXA-measurements. ROI of the tendon-bone interface was a square of 4x4 mm aligned along the axis of the bone tunnel and flush with the anterior bone cortex. In Study II, we also wanted to assess any systemic bone mineral effects and included a secondary ROI that was a rectangle of 4 x 7 mm that fitted the 3rd tail vertebra. ROI in Study III was a square of 3 x 3 mm that was aligned to the tibia over the fracture, including the anterior cortical bone, the callus, and the nail. The nail was measured independently, and its constant value was subtracted from the *in vivo* measurements. This method was validated previously(154). In addition to BMD and BMC, the PIXImus provided low-resolution X-ray images, and we used these to assess the postoperative quality of bone tunnel placements, fractures, and nails. In Study II and III, all DEXA analyses were performed by two independent observers, and the mean values were reported.

The main limitation by the use of a conventional densitometer is that the DEXA measurements give 2D (area) only, admittedly superimposed areas with high accuracy. However, it is a crude modality compared to micro-computed tomography (μCT) or pQCT, which would be the preferred method to detect smaller changes of mineralized bone formation in 2D and 3D (volume). μCT/pQCT provides multiple opportunities to also study bone mineral in several subROIs within the main ROI as well as 2D sections and 3D-reconstructions to assess any differences in bone microarchitecture. After the completion of the current studies, μCT has replaced conventional DEXA in the tendon-bone model, clearly being the superior modality(153). Also, in the evaluation of fracture healing, μCT have been widely used and was highlighted in a review of small animal bone healing models(155).

4.8 Histology

As a refinement to the tendon-bone model that was proposed earlier(124), the current studies included histological analyses to evaluate healing of the tendon-bone interface and fractures. Both biomechanical and histological analyses are recommended to obtain valid information on the process of bone healing in experimental studies(155). However, it is not possible to perform destructive biomechanical tests in the same animals subjected to histology without disrupting the pathoanatomy of interest. Therefore, a larger number of animals in each experiment is needed.

In all studies, tissues of animals subjected to histological analyses were fixed by *in vivo* transcardial vascular perfusion of 0.1 M phosphate-buffered 2% paraformaldehyde to obtain optimal histological quality. In Study I and II, the skin was removed, and the tibias

were further fixated by immersion before decalcified in 7% EDTA with buffer. Sections of 5 µm thickness were obtained in the coronal plane of the tibia, embedded in paraffin, and stained by H+E.

In study 1, H+E-sections were qualitatively evaluated by light microscopy. The most important finding was recognition of *in model* complications, as described earlier (*section 4.4*). Secondly, because the study was longitudinal with four different time points, we were able to describe phases of tissue healing with early inflammation, callus formation and remodeling, tendon neovascularization, and eventually collagen fiber crossing from tendon into bone.

In Study II, H+E-stained sections of the distal tibia containing the bone tunnel and tendon graft were also subjected to evaluation by light microscopy. Due to the model modifications, surgical adverse events were not apparent. In addition to the qualitative analyses, we also performed semiquantitative measurements (histomorphometry) by using a circular grid superimposed to the bone tunnel to be able to measure the amount of mineralized bone tissue inside the tunnel. Furthermore, we wanted to count osteoclasts. On paraffin sections, a standard protocol for the osteoclast marker TRAP was used (histochemistry). ROIs were the bone tunnel, the ipsilateral calcaneus, and the 3rd tail vertebra. Osteoclasts were defined as TRAP-positive cells containing more than 1 nucleus.

In Study III, preparation of the tibia included removal of the nail, fibula and soft tissues. The middle 15 mm of the tibia diaphysis contained the fracture with callus. These segments were immersed in fixative and dehydrated. Without decalcification, the segments were embedded in plastic before sectioning in the coronal plane with a thickness of 5 µm. (Figure 16). Sections were stained by the Masson-Goldner´s trichrome method. One section from the middle coronal plane of each specimen was subjected to light microscopy, and images were obtained by a digital camera. The presence of cartilage within the callus was noted. Then we applied histomorphometry by using a software (AnalySIS V, Olympus Soft Imaging Solutions GmbH, Germany) to obtain total callus area (Cal Ar; mm^2) and the ratio of osteoid surfaces vs. bone surfaces (OS/BS;%) (Figure 17). OS/BS-ratio was considered an indirect measure of bone formation(156).

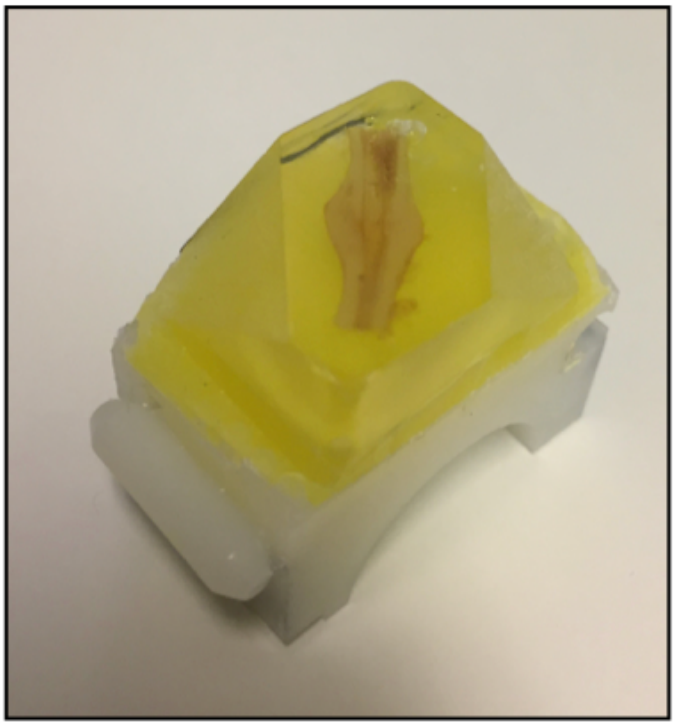

Figure 16. Plastic embedding and sectioning block from the middle tibia containing the callus/fracture. *Photo: Geir Aasmund Hjorthaug.*

There were several limitations of our evaluation of tendon-to-bone and fracture healing by using histology. Firstly, the total number of specimens was low in all studies because we had to include specimens to represent multiple time points and study groups (intervention or control) (Table 2). Secondly, the number of section ROIs were low, though our coverage of the chosen ROI was good (>95%). In Study I and II, we chose one representative section from the mid coronal plane of the bone tunnel and have therefore analyzed 2D cross-section regions only. Moreover, the inner and outer apertures of the tendon-bone interfaces were not investigated. In Study III, the fracture was histologically evaluated also in one plane and the mid-region only.

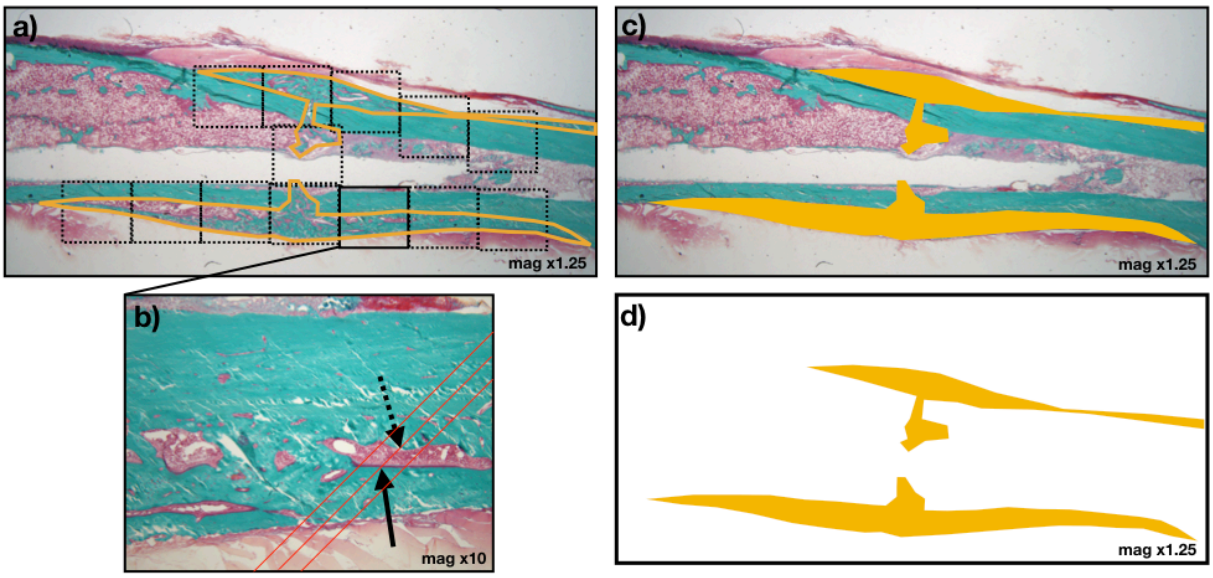

Figure 17. The Masson-Goldner´s trichrome stain provided excellent visualization of mineralized bone matrix (green color) and bone marrow (red color). At medium and high magnification, it was easy to determine whether bone surfaces were uncovered or covered by newly formed non-mineralized bone; the osteoid (deep purple). ROI was the total callus area, and this was defined by outlining the callus´ perimeter, including cortical fracture surfaces, but excluding the original bone, bone marrow, and periosteum [**a)** x1.25 magnification, yellow line]. The callus was extrapolated and calculated by using the software, as illustrated in **c)** and **d)**. Next, medium resolution images (x10 magnification) were obtained to cover > 95% of the ROI [**a)** dotted rectangles]. In the medium resolution images [**b)**], a virtual line grid spaced 100 µm with random angles was superimposed to the sections. For illustrative simplicity, only three lines are shown. Where lines crossed a bone surface, the presence of osteoid (**solid arrow**) or bare bone surfaces (**dotted arrow**) was noted. *Photos: Obtained from AnalySIS V, Geir Aasmund Hjorthaug.*

Table 2. Number and distribution of animals subjected to histological evaluation in the studies.

	Time points	Study groups	Animals pr. point or group	Total animals
Study I	4	1	5 or 6	21
Study II	2	2	5	20
Study III	1	3	6 or 7	20

4.9 Statistics

A priori power calculations were not performed in the studies, but the number of animals for each evaluation form, time point, and study groups were empirically determined from our previous studies utilizing the same models. Histograms were used to evaluate distributions of normality. Leven´s test or non-parametric Leven´s test was used to evaluate variances of the primary outcome. If heterogeneity of variances was found, comparisons were run on log-transformed data. Non-parametric tests were used in cases of smaller sample sizes. Alpha level was set to 0.05. In Study I, we compared the groups by Kruskal-Wallis (KW) test followed by *post hoc* KW-tests when significance was found. In Study II, we compared the groups and time points by 2-way Analysis of Variances (2-way ANOVA) with time and treatment as fixed factors. Main effects for both factors were analyzed, and pairwise comparisons were run. P-values were Bonferroni adjusted due to multiple comparisons. Mann–Whitney test for independent samples, without correction of the p-value, was used for the data from histomorphometry. In Study III, we used KW-test on biomechanical and histomorphometric data and 1-way ANOVA on the DEXA-data.

5. Ethical considerations

All studies included in this thesis were experimental studies in rats. The studies were approved by the Norwegian National Animal Research Authority (NARA, no. *Mattilsynet*), after applications using «Forsøksdyrforvaltningens tilsyns- og søknadssystem» (FOTS). The studies were conducted according to guidelines provided by Norecopa and respected the welfare of the animals according to The World Medical Association´s (WMA) Declaration of Helsinki, §21.

Study I: FOTS ID 3779. Approval date 30.01.2011
Study II: FOTS ID 5839. Approval date 01.02.2014
Study III: FOTS ID 8155. Approval date 18.12.2015

The use of animals in experimental studies is likely to cause pain and distress, and generates some ethical issues. Anticipated pain in the current studies was graded as moderate. All surgeons were accredited FELASA researchers(157) and surgeons in clinical orthopedic practice. In the animal facility, especially educated personnel supervised the animals daily. Analgesics were given postoperatively. A custom-made form to evaluate animal pain and defining humane endpoints were developed and used (Appendix 2). Details of animal handling pre, per and postoperatively for all experiments are discussed earlier (*section 4.1*).

The Papers all adhered to the guidelines from The National Centre for the Replacement, Refinement & Reduction of Animals in Research; "Animal Research: Reporting of *In Vivo* Experiments" (ARRIVE-guidelines). When reporting, the ARRIVE Checklist (Appendix 3) was filled out and uploaded to the respective journals along with the manuscripts. The three experiments were all evaluated in the light of the three R´s of Animal research:

Replacement: No *in vitro* or humane models exist to study biomechanical and histological properties of tendon-to-bone healing or shaft fracture healing. Thus, there are no relevant alternatives to animal studies.

Refinement: The rat models are well established in our group. Refinements in Study I was adding DEXA-measurements and histology to the tendon-to-bone model. The latter was

important as it revealed potential experimental bias such as unintended fractures, pronounced heat necrosis, misplacement of bone tunnels, and foreign body reactions from suture material. The tendon-to-bone model was further refined between Study I and Study II by pilot studies aiming to avoid these potential adverse events. In Study II and III, we also implemented a series of surgical, drug administrative, and evaluative refinements to both models. Two independent observers analyzed all biomechanical and bone mineral data in Study II and II. Refinements are further discussed elsewhere (*sections 4.2.2, 4.3, 4.4, 4.6 and 4.8*)

Reduction: Pilot studies were performed on cadaveric animals before all three studies to reduce the risk of losing animals due to technical errors and for surgical practice. *A priori* power calculations were not performed, but the number of animals was based on our previous studies and estimated based on the primary outcomes and groups.

We believe the experiments have a high probability of meeting the stated objectives through high scientific quality, and that the objectives have a reasonable chance of contributing to human welfare. Therefore, we find the animal experiments to be justified. The work of this thesis was supported by minor grants from Smith&Nephew Research Fund (2012) and the Norwegian Orthopedic Association (2016).

6. Discussion

In this thesis, we have studied early healing processes in orthopedic surgically relevant tissues. We have studied tissue healing effects of two drugs commonly used by orthopedic patients. Both common ("on-label") indication and explorative novel indication ("off-label") were studied for parecoxib and zoledronic acid, respectively. We improved the tendon-bone model and further adapted refinements from Study I to Study II. The studies confirmed that healing is a slow process and that a native interface may not be recreated in tendon-bone-tunnel healing. The BP zoledronic acid had a negative effect on tendon-bone healing. Short term treatment with the COX-inhibitor parecoxib did not affect shaft fracture healing. It is, however, essential to recognize that our findings from animal experiments cannot be directly extrapolated to human patients. In the following, the results from the three papers will be discussed in details.

6.1 Tendon-to-bone healing

In Study I, we explored the time-dependent healing process of tendon graft to bone tunnel at three relatively early time points (2, 3, and 4 weeks) and one mid-term time point (12 weeks). Due to limited resources, we did not include additional time points. Both 6, 8, and >24 weeks would be of interest, but these time points have also been covered by others(39). Our findings in Study I of weak and slow initial tendon-to-bone tunnel healing corresponds to the literature(38, 39, 158-160). At 2, 3, and 4 weeks, the biomechanical properties were generally weak. Median pull-out strength at these early time points was < 5 N and distributed with relatively narrow ranges. When comparing to our previous study with the same model at 2 weeks(124), we reproduced similar forces in the current study. After 12 weeks of healing, the median pull-out force was 11.2 N, but the medians were widely distributed with an IQR of 11.4. Similar patterns of all time points were found in biomechanical tests of stiffness and energy absorption, but elongation was not time dependent in our study. All specimens tested biomechanically ruptured by pull-out of the tendon from the bone tunnel. It means that all native Achilles-calcaneus insertions remained intact, tibias were not fractured during testing, and the specimens were stable in the testing jig. However, we did not investigate if a degloving mechanism was present. To do that, sections for histology from biomechanically tested bone tunnels could be analyzed to evaluate if the tunnel walls contained a (partially) healed graft tissue envelope.

It is necessary to recognize that in contrast to the clinical scenario after ligament reconstruction or tendon transfer to bone tunnels, we have not studied the contribution of fixation. The total strength of the repaired tendon-bone interface is considered the product of fixation and healing. Initially, fixation is the most critical factor. However, fixation may fail over time unless adequate healing of tissue occurs. This mechanism is well known for surgically treated fractures, but less is known of the topic in the repaired tendon-bone interface.

Previously, we had not used DEXA to evaluate healing in the tendon-bone model. We found an increased BMD over the bone tunnels when comparing the 12 weeks time point to both 2, 3, and 4 weeks of healing. This finding supported the biomechanical findings. In contrast to the variable pull-out force, we did not find differences among the early time points. Data from BMC measurements in the same ROIs were very similar to BMD and did not provide additional useful information. If DEXA-measurements (at all) should be used to evaluate healing in the same model in the future (*discussed in section 4.7*), BMD and BMC-measurements will produce identical results. Therefore, one of these variables may be skipped.

By studying the morphology of the tendon-bone tunnel interface in light microscopy, we confirmed what others have reported. There were initial inflammation and persistent hypercellularity, early endochondral bone formation within the tunnel, and around the tibia and late remodeling of callus into lamellar bone. Further, the neovascularization of the tendon graft was striking after 12 weeks, and we also observed remodeling of collagen tendon graft fibers that eventually crossed perpendicularly into the bone. At 12 weeks, most of the cartilage was remodeled into lamellar bone. Fibrous rather than fibrocartilaginous interfaces were found. Our finding of fibrovascular scar tissue is consistent with most experimental literature, and this has been reviewed by Bunker et al.(161).

The human tendon-bone-tunnel interface has been evaluated by histology in one case study. This rare opportunity was possible at 4 months after ACLR due to a necessary knee resection because of osteosarcoma(162). Presence of bony invasion with subsequent reorientation and reintegration of collagen fibers was found, as reported in animal studies. The four-layer fibrocartilaginous pattern of native ACL-enthesis was not found. Furthermore, a better fibrous and bony healing response was found on the tibia side (interference-screw) compared to the femoral side (endo-button).

It is not quite clear whether the result of tendon-bone healing always results in a fibrous tissue. Augmentation of healing of the HT-graft with a periosteal flap has been

advocated, as this technique may reduce the tunnel outlet diameter and widening(163, 164). To our knowledge, histological studies on periosteal augmented tendon-bone-tunnel grafts do not exist. In a rabbit ACL-study by Takigami et al., HT-grafts were injected by BMP-2(165). After 8 and 12 weeks, the BMP-2 grafts were replaced by new bone inside the tunnel, and morphology resembled native fibrocartilaginous entheses. This finding is remarkable, especially since a bone tunnel technique was used. Notable, BMP-2 was necessary to achieve this effect. ACL-surgeons like to refer placements of their grafts as "anatomic" by aiming the intraarticular bone tunnel entry-point to the anatomic footprint of the ACL to be reconstructed. If the term "anatomic reconstruction" is to be used strictly correct, two requirements must be fulfilled: Firstly, complete bone healing of the relatively long (centimeters) bone tunnels must have taken place. Secondly, healing must also result in a short (millimeters) healed four-layer fibrocartilaginous and fibrous ligament/tendon-bone intraarticular interface.

Anatomic reconstruction by these terms may never be achieved with pure tendon grafts like HT, but the use of BPTB-grafts may more closely mirror an anatomic structure. It seems almost like BMP-2 in Takigami´s study was able to transform HT-grafts into something similar to what is seen in healing of BPTB-grafts. Interestingly they conclude that BPs should be added to the tendon-bone-tunnel model along with BMP-2 in future studies. That brings us to Study II.

6.2 Effect of inhibition of bone resorption on tendon-to-bone healing

In Study II, we assessed the effect of a single dose with the BP ZA administered 1 week after surgery with tendon graft in a bone tunnel at 3 and 6 weeks. The hypothesis was that administration of a potent anti-osteoclastic agent could promote tendon to bone healing by reducing peritunnel bone loss. We found the opposite. ZA-treatment had a negative effect on tendon-bone tunnel healing. Postoperative peritunnel bone loss was not present.

Firstly, local BMD-measurements over the bone tunnels showed an increase from baseline (immediate postoperatively) to 3 weeks and density was further increased at 6 weeks. This result was consistent with the findings in Study I. However, postoperative peritunnel bone loss as judged from DEXA-analyses was not observed, regardless of study groups. Neither was peritunnel bone loss evident as evaluated by histological analyses. Admittedly, we did not include baseline specimens for histology.

Secondly, ZA-treatment resulted in inferior pull-out force and stiffness compared to controls. No differences between the ZA-group and controls were found in energy or elongation. Furthermore, bone ingrowth into tunnels and around the distal tibias increased from 3 to 6 weeks. However, no differences between ZA-treatment and control were found by histomorphometric analysis of the area of new bone formation in the coronal plane of the middle of the bone tunnels. At last, counting of TRAP-stained osteoclasts did not reveal differences between the study groups.

We did not assess whether the BP was absorbed by the peritunnel bone, or that osteoclasts were inhibited and resulted in systemic reduced bone turnover. We did measure BMD at the 3rd tail vertebra at both baseline, 3 and 6 weeks, but no differences were observed. Future possibilities for internal controls on these matters could be to include the use of radio-labeled BP(66, 143). In Amanat´s study, $Carbon^{14}$-labeled ZA was used, and on autoradiographic analyses, binding of ZA to the bone that was present at the time of administration could be visualized. The use of bone resorption serum markers is also a possibility to control that systemic bone resorption is inhibited when administering BRIs in animal studies(101).

Muscular atrophy and fatty infiltration are well known negative predictors of rotator cuff healing (166), and this is routinely assessed by clinicians on magnetic resonance imaging (MRI) scans. As in bone healing, the quality of the local bone is also an essential factor for tendon-bone healing. Local and regional bone loss in the humeral head has been well documented following rotator cuff rupture in the shoulder (167, 168). This bone loss, *before repair*, is driven by osteoclast-mediated bone resorption accelerated by the decreased loading from the missing/ruptured tendon, and the local bone loss will be more pronounced by inactivity or by delaying the repair (8, 72). In degenerative rotator cuff repairs, the patients have often tried conservative treatment for several months or years before surgery.

Bone loss *after repair* of entheses or after ligament reconstruction may also negatively affect healing. Transient bone loss lasting for 5 months in the knee region was reported in an RCT of patients operated with ACLR using three different bone tunnel grafts(169). In an experimental study by Silva et al., dogs underwent injury and bone tunnel repair of the flexor digitorum profundus (FDP) of the distal phalanx(158). Even with this distal surgical location, peri-tunnel bone loss after 3 and 6 weeks was found and correlated with decreased strength of the tendon-bone interface, demonstrating a need for new treatment strategies to improve tendon-to-bone healing. By using the FTP model, they later tested the effect of the BP alendronate and found that both daily PO systemic administration and systemic + local

administration of alendronate prevented local bone loss and resulted in improved strength of the tendon-bone interface(71). Notably, the FTP was cut proximally to remove all load during healing in this model. In a rat ACL study, weekly SC injections with low, medium, and high dose of alendronate resulted in reduced peritunnel bone loss, increased bone formation inside tunnels, and increased biomechanical strength at 6 weeks(9). Similar results for treatment with the RANK-L inhibitor OPG were reported in a rabbit ACL-study(72).

We could not confirm the positive BRI effects on tendon-to-bone tunnel healing from the literature in our study of ZA. Reasons for the divergent findings may be related to dose, timing, or the chosen bone region. There may also be bias within the study model or analyses that we are not aware of. Any bone loss *after repair* was the concern in Study II. We used non-osteoporotic rats, did not delay the tendon transfer, did not restrict postoperative loading, and trusted the Achilles tendon-bone tunnel model in distal rat tibia. The rationale for the use of BRIs (including ZA) as adjuvant treatment in tendon-bone healing remains plausible. There is a need for further experimental studies on the topic before clinical trials should be considered. Especially interesting studies would be ZA in animal ACL-models. In our tendon-bone tunnel model, adding unloading and osteoporosis as study factors are possible by the use of IM botulinum toxin injections to the operated limb(170) and the use of the vitamin-D depleted ovariectomized rat model(150), respectively.

In animal diaphyseal fracture studies, treatment with BPs seems to delay the osteoclast-dependent remodeling of the hard callus in lamellar bone. This seems to result in a larger bridging callus and increased biomechanical strength and stiffness at early time points of healing (*section 1.6*). As discussed earlier (*section 1.4*), the remodeling of soft callus is probably not dependent on the osteoclast. Therefore, the timing and duration of BP-treatment in different phases of healing may significantly affect the outcome. In early fracture healing, this effect of BPs remains unclear. The anatomical space for callus volume formation within bone tunnels that also contains the tendon graft is limited. In Study II, we observed that the bone ingrowth sometimes partially replaced the tendon graft, which we interpreted as indicative of a robust healing response. The bone ingrowth was equally distributed among the study groups. It is important to recall that the BP did incorporate into the bone that was present at the time of administration. In our experiment, this was mainly the peritunnel bone; not the callus formed later than 1 week of healing. It is possible that these mechanisms can explain the adverse effects of ZA we found in our study.

6.3 Effect of inhibition of cyclooxygenase on diaphyseal fracture healing

In Study III, we did not find any effect of COX-2-inhibition with parecoxib on diaphyseal fracture healing after 2 or 4 weeks. The paper was a follow-up study on our previous studies with COX-inhibitors and shaft fracture healing(142, 154). Previously, the inflammation phase was inhibited by parecoxib for 7 days, starting at the time of fracture. In those studies, we found a negative effect at 2 weeks and 3 weeks, but not after 6 weeks of healing.

In the recent study, we used a higher parecoxib dose that was administered for 3 days only. One group started treatment immediately at the time of fracture, and a delayed group started their treatment 3 days post-fracture. Healing was similarly evaluated in previous and current studies. In the current study, DEXA analyses showed an overall increase in BMD at the fracture site of 50% at 2 weeks and 75% at 4 weeks compared to the time of fracture (baseline). However, no differences between the parecoxib groups or controls were found at any time point. For maximum bending moment, the overall ratio between fractured and non-fractured tibia was 54% by 4 weeks and no non-unions were found. Again, no differences were found among the study groups. Previously, we found a negative effect of parecoxib on maximum bending moment at 3 weeks, but not at 6 weeks.

As judged by histology at 4 weeks in our recent study, all fractures were healed with callus bridging the fracture gap, endochondral ossification was ongoing in some specimens, and in others, the cartilage/soft callus was remodeled into more mature woven bone. The distribution of maturity was equal among the study groups. The ratios between osteoid and non-osteoid shrouded bone surfaces within the calluses did not reveal differences between parecoxib groups or control.

Data from a large number of animal studies indicate that COX-inhibitors, both nonselective and selective COX-2-inhibitors, does have adverse effects on bone healing(115, 171-173). In Simon and O´Connor´s study, only 5 days of treatment post-fracture with celecoxib was sufficient to observe impaired healing of closed femoral fractures in rats. Delayed administration (14 days delay), did not impair fracture healing, suggesting that PG-synthesis during the early inflammatory phase of healing is critical. However, the negative effect of COX-inhibition (duration 7 days and 21 days) might be reversible, according to Gerstenfeld et al. who evaluated femoral fracture healing in rats after 3 weeks and 5 weeks(174).

There are also animal studies that do not find negative effects of COX-inhibitors on bone healing(147, 175). *In model* variations like fracture type, stability, animal gender differences in drug metabolism, different doses, timing, route, and COX-inhibitor type may

explain the conflicting findings in the experimental literature. An advantage in our subsequent studies is that we used the same model, female rats, higher parecoxib dose, and therefore investigated the effect of *duration*. In total, our animal studies of shaft fracture healing suggest that 7 days of COX-2-inhibition with parecoxib is long enough to observe a negative, yet transitory, effect, but 3 days treatment seems safe without the risk of delayed fracture healing.

The results from animal studies, including our findings, may not be directly applied to humans. Retrospective studies in humans report inconsistently on the effect of COX-inhibitors on fracture healing(176). An RCT with COX-inhibitors in trauma patients with high energy fractures showed that acetabulum-fractures (metaphyseal) healed, but concomitant femoral fractures (diaphyseal) yielded a significantly increased risk of non-union in the same patients(177). Treatment with COX-inhibitors in this study was indomethacin 25 mg three times daily for 6 weeks. Similar results were reported in an RCT by Sagi et al.(178); 6 weeks of indomethacin treatment resulted in 2-3 times increased the risk of non-union by surgically treated acetabular fractures (mostly posterior wall non-union), but 1 week or 3 days of indomethacin treatment did not increase the risk of non-union. In both of these studies, COX-inhibition with indomethacin was mainly used to assess the effect on HO; the effect on union rates was secondary outcomes.

Recently, effects of ibuprofen were studied in an RCT of 95 patients with surgically treated distal radius low energy fractures (metaphyseal bone)(179). Study groups were ibuprofen 3 days, ibuprofen 7 days, and placebo, both treatment groups with clinically relevant duration and indication (against pain). In this study, there was no effect of ibuprofen-treatment on radiological migration of fracture fragments after 6 weeks, and no effect on wrist motion or DASH-score after one year. Patients treated with 7 days of ibuprofen reported more often gastrointestinal adverse events compared to the other study groups. Union rate or measures of any delayed healing was not reported directly, and illustrates one of the problems in human studies of fracture healing; how to measure bone healing.

Caution should be undertaken when reporting effects on “bone healing” when only indirect measures have been used. A few other human studies on the effect of COX-inhibitors and bone healing exist. A recent study included 16 prospective or retrospective clinical trials with long bone fractures, osteotomies, spine, and joint fusions that reported on union rates for groups treated with COX-inhibitors or controls(180). In this meta-analysis, the use of COX-inhibitors indicated an overall negative effect on bone healing, but no effect was observed in the pediatric populations.

In conclusion, it is likely that the negative effects reported in animal studies of COX-inhibitors on bone healing are proportional with dose, timing, and duration, and also highly dependent on patient-specific factors like age, comorbidity, habits as well as fracture/bone-specific factors like region and stability. Our studies have contributed to the knowledge of early diaphyseal fracture healing in young, healthy individuals under treatment with COX-inhibitors and the impact of treatment duration and timing.

6.4 Generalizability and implications for future research

Understanding tissue healing processes is highly relevant to clinicians. It is imperative when consulting the individual patient, choosing treatment for the condition, choosing between specific techniques, and choosing safe and effective analgesia. Generally, our knowledge of bone healing is increasing with a better understanding of the cellular, molecular, and genetic contributions that mutually influence each other in overlapping phases of healing. More models describing bone healing will develop in the future. Often, the principles from bone healing will also apply to descriptions of tendon-to-bone healing processes. As an example, the diamond model of bone healing (MSCs, growth factors, scaffolds, and mechanical environment, *section 1.4.5*) has already been reviewed on tendon-bone healing in an ACLR-context(181).

When facing a clinical problem of failed healing, it is mandatory to take all factors affecting healing into consideration. Delayed fracture union is undoubtedly a clinical problem; more importantly, nonunion will significantly impair the outcome after a fracture. On the effect of COX-inhibitors and if the use of these drugs is associated with nonunion, the animal data is relatively clear; in contrast, the human data is not(182). Recommendations often emphasize that prolonged COX-inhibitor treatment (> 14 days) may result in nonunion and should be avoided(177). Short treatment (5-7 days) might delay union(115, 117, 174), and the presence of other risk factors for impaired fracture healing should be carefully assessed before considering the use of COX-inhibitors(183). The results from our current study support the use of 3 days duration of treatment the first week after fracture, regardless of starting COX-inhibition on day 0 or day 3 post-fracture.

A 3 days COX-inhibitor limit seems reasonable in the light of the existing experimental literature, but there is an overdue need for randomized, parallel, double-blinded, and placebo-controlled human studies of both diaphyseal and metaphyseal fractures,

diaphyseal and metaphyseal osteotomies, joint fusions and arthroplasties/implant fixations, ligament reconstructions, tendon repairs - and transfers.

In contrast to the warranted clinical studies of COX-inhibitors and tissue healing, targeted adjuvant treatment strategies to augment musculoskeletal healing remains more immature, and more experimental animal studies *and* clinical trials are needed. Studies of augmentation of bone and tendon-bone healing might focus on two main strategies; bone/tendon resorption inhibition (inhibit catabolism) and bone/tendon formation stimulation (induce anabolism).

Firstly, experimental research so far has focused the most on bone healing issues, and the use of BRIs to augment both bone and related soft tissue healing remains controversial. Interesting studies would be to assess the effect of continuous BP-administration during all phases of healing (e.g., by daily administration of alendronate). A better strategy might be to induce a complete blocking of osteoclast recruitment and activity during healing by the administration of RANK-L inhibitors (OPG or denosumab in genetically modified rodents). This strategy may suppress bone resorption in all phases of bone healing response, also the newly formed bone in the callus itself. Our observation of ZA´s possible negative effect on tendon-bone healing needs to be confirmed in similar animal models, and optimal timing of ZA-infusion(66) in both fracture and tendon-bone models needs further to be explored. It would also be of interest to repeat the tendon-bone study by adding a group with a bone formation stimulator like BMP-2(165). Anabolic agents like parathyroid hormone, drugs modulating the Wnt-pathway (e.g., anti-sclerostin), members of the TGF superfamily (other than BMP-2), cell therapy and epigenetic drugs also holds the potential in augmentation of bone tissue repair(184, 185).

Secondly, when designing clinical studies aiming to assess positive and negative drug effects on healing of musculoskeletal tissue, guidelines are developed and should be used. Agents type and doses regimen must be clinically relevant and any adverse events recorded. Study objectives should include evaluation of bone union, acceleration of return to normal function, and any reduction of healing complications like nonunion, re-rupture, or revision must be reported(186). There are several challenges regarding human studies and tissue healing response. Hard outcomes like surgically treated non-unions require a large number of enrolled patients with similar risk factor profiles to detect differences among study groups. Measures of union are often restricted to radiographic (subjective) evaluation using vague definitions and does not necessarily correlate with outcome, especially when assessing

delayed union. Therefore, clinical studies of tissue healing augmentation or negative factors should always aim for patient-orientated outcomes.

The total amount of literature on experimental and clinical research to understand the complexity of bone and tendon tissue healing and agents that might augment tissue healing increases exponentially. It is not apparent that a single drug ever will effectively ensure rapid and reliable healing. By targeting multiple anabolic and/or catabolic pathways involved in the healing processes at the right time, in the right doses, to the right indication for the right patient, it may be possible to discover novel multi-specific therapeutic strategies that can support and speed up the tissue´s natural healing processes and improve outcome.

6.5 Conclusions

- Tendon-to-bone tunnel healing is a slow process.

- A native four-layered tendon-bone interface does not recreate at early or medium timepoints of tendon-to-bone tunnel healing.

- Crossing collagen fibers can be anticipated and is associated with an increase of biomechanical strength and bone mineral density between 4 and 12 weeks of tendon-to-bone tunnel healing.

- There may be a negative effect of a single dose of the BP zoledronic acid on tendon-to-bone tunnel healing at early time points.

- There is no negative effect of three days of immediate treatment with the COX-2-inhibitor parecoxib on early diaphyseal fracture healing.

- There is no negative effect of three days of treatment delayed for three days with the COX-2-inhibitor parecoxib on early diaphyseal fracture healing.

7. References

1. Nusse R, Brown A, Papkoff J, Scambler P, Shackleford G, McMahon A, et al. A new nomenclature for int-1 and related genes: the Wnt gene family. Cell. 1991;64(2):231.
2. Virk MS, Lieberman JR. Biologic adjuvants for fracture healing. Arthritis Res Ther. 2012;14(6):225.
3. Rodeo SA, Potter HG, Kawamura S, Turner AS, Kim HJ, Atkinson BL. Biologic augmentation of rotator cuff tendon-healing with use of a mixture of osteoinductive growth factors. J Bone Joint Surg Am. 2007;89(11):2485-97.
4. Gulotta LV, Hidaka C, Maher SA, Cunningham ME, Rodeo SA. What's new in orthopaedic research. J Bone Joint Surg Am. 2007;89(9):2092-101.
5. Fu FH, Bennett CH, Lattermann C, Ma CB. Current trends in anterior cruciate ligament reconstruction. Part 1: Biology and biomechanics of reconstruction. Am J Sports Med. 1999;27(6):821-30.
6. Fu FH, Bennett CH, Ma CB, Menetrey J, Lattermann C. Current trends in anterior cruciate ligament reconstruction. Part II. Operative procedures and clinical correlations. Am J Sports Med. 2000;28(1):124-30.
7. Risberg MA, Holm I. The long-term effect of 2 postoperative rehabilitation programs after anterior cruciate ligament reconstruction: a randomized controlled clinical trial with 2 years of follow-up. Am J Sports Med. 2009;37(10):1958-66.
8. Galatz LM, Rothermich SY, Zaegel M, Silva MJ, Havlioglu N, Thomopoulos S. Delayed repair of tendon to bone injuries leads to decreased biomechanical properties and bone loss. J Orthop Res. 2005;23(6):1441-7.
9. Lui PP, Lee YW, Mok TY, Cheuk YC, Chan KM. Alendronate reduced peri-tunnel bone loss and enhanced tendon graft to bone tunnel healing in anterior cruciate ligament reconstruction. European cells & materials. 2013;25:78-96.
10. Aspenberg P. Don't administer NSAID after bone surgery! Lakartidningen. 2002;99(22):2554.
11. Aspenberg P. Drugs and fracture repair. Acta Orthop. 2005;76(6):741-8.
12. Su B, O'Connor JP. NSAID therapy effects on healing of bone, tendon, and the enthesis. J Appl Physiol (1985). 2013;115(6):892-9.
13. Barry S. Non-steroidal anti-inflammatory drugs inhibit bone healing: a review. Vet Comp Orthop Traumatol. 2010;23(6):385-92.
14. Lisowska B, Kosson D, Domaracka K. Positives and negatives of nonsteroidal anti-inflammatory drugs in bone healing: the effects of these drugs on bone repair. Drug Des Devel Ther. 2018;12:1809-14.
15. Aspenberg P. Bisphosphonates and implants: an overview. Acta Orthop. 2009;80(1):119-23.
16. Wang JH. Mechanobiology of tendon. J Biomech. 2006;39(9):1563-82.
17. Thomopoulos S, Genin GM, Galatz LM. The development and morphogenesis of the tendon-to-bone insertion - what development can teach us about healing. J Musculoskelet Neuronal Interact. 2010;10(1):35-45.
18. Benjamin M, Kumai T, Milz S, Boszczyk BM, Boszczyk AA, Ralphs JR. The skeletal attachment of tendons--tendon "entheses". Comp Biochem Physiol A Mol Integr Physiol. 2002;133(4):931-45.

19. Woo SL-Y MJ, Butler D. . Ligament, tendon and joint capsule insertion to bone. Injury and repair of the musculoskeletal soft tissues. 1988:133–66.
20. Beaulieu ML, Carey GE, Schlecht SH, Wojtys EM, Ashton-Miller JA. On the heterogeneity of the femoral enthesis of the human ACL: microscopic anatomy and clinical implications. J Exp Orthop. 2016;3(1):14.
21. Majidinia M, Sadeghpour A, Yousefi B. The roles of signaling pathways in bone repair and regeneration. J Cell Physiol. 2018;233(4):2937-48.
22. Marsell R, Einhorn TA. The biology of fracture healing. Injury. 2011;42(6):551-5.
23. Walters G, Pountos I, Giannoudis PV. The cytokines and micro-environment of fracture haematoma: Current evidence. J Tissue Eng Regen Med. 2017.
24. Lin HN, Cottrell J, O'Connor JP. Variation in lipid mediator and cytokine levels during mouse femur fracture healing. J Orthop Res. 2016;34(11):1883-93.
25. Liu S, Liu Y, Jiang L, Li Z, Lee S, Liu C, et al. Recombinant human BMP-2 accelerates the migration of bone marrow mesenchymal stem cells via the CDC42/PAK1/LIMK1 pathway in vitro and in vivo. Biomater Sci. 2018;7(1):362-72.
26. Einhorn TA. The science of fracture healing. J Orthop Trauma. 2005;19(10 Suppl):S4-6.
27. McDonald MM, Dulai S, Godfrey C, Amanat N, Sztynda T, Little DG. Bolus or weekly zoledronic acid administration does not delay endochondral fracture repair but weekly dosing enhances delays in hard callus remodeling. Bone. 2008;43(4):653-62.
28. Schindeler A, McDonald MM, Bokko P, Little DG. Bone remodeling during fracture repair: The cellular picture. Semin Cell Dev Biol. 2008;19(5):459-66.
29. Colnot C, Thompson Z, Miclau T, Werb Z, Helms JA. Altered fracture repair in the absence of MMP9. Development. 2003;130(17):4123-33.
30. Bastian OW, Kuijer A, Koenderman L, Stellato RK, van Solinge WW, Leenen LP, et al. Impaired bone healing in multitrauma patients is associated with altered leukocyte kinetics after major trauma. J Inflamm Res. 2016;9:69-78.
31. Stewart SK. Fracture Non-Union: A Review of Clinical Challenges and Future Research Needs. Malays Orthop J. 2019;13(2):1-10.
32. Giannoudis PV, Einhorn TA, Marsh D. Fracture healing: the diamond concept. Injury. 2007;38 Suppl 4:S3-6.
33. Andrzejowski P, Giannoudis PV. The 'diamond concept' for long bone non-union management. J Orthop Traumatol. 2019;20(1):21.
34. Bernhardsson M, Aspenberg P. Osteoblast precursors and inflammatory cells arrive simultaneously to sites of a trabecular-bone injury. Acta Orthop. 2018;89(4):457-61.
35. Kon T, Cho TJ, Aizawa T, Yamazaki M, Nooh N, Graves D, et al. Expression of osteoprotegerin, receptor activator of NF-kappaB ligand (osteoprotegerin ligand) and related proinflammatory cytokines during fracture healing. J Bone Miner Res. 2001;16(6):1004-14.
36. Aspenberg P, Sandberg O. Distal radial fractures heal by direct woven bone formation. Acta Orthop. 2013;84(3):297-300.
37. Sandberg OH, Aspenberg P. Inter-trabecular bone formation: a specific mechanism for healing of cancellous bone. Acta Orthop. 2016;87(5):459-65.
38. Leung KS, Qin L, Fu LK, Chan CW. A comparative study of bone to bone repair and bone to tendon healing in patella-patellar tendon complex in rabbits. Clin Biomech (Bristol, Avon). 2002;17(8):594-602.

39. Rodeo SA, Arnoczky SP, Torzilli PA, Hidaka C, Warren RF. Tendon-healing in a bone tunnel. A biomechanical and histological study in the dog. J Bone Joint Surg Am. 1993;75(12):1795-803.
40. Newsham-West R, Nicholson H, Walton M, Milburn P. Long-term morphology of a healing bone-tendon interface: a histological observation in the sheep model. J Anat. 2007;210(3):318-27.
41. Janssen RP, van der Wijk J, Fiedler A, Schmidt T, Sala HA, Scheffler SU. Remodelling of human hamstring autografts after anterior cruciate ligament reconstruction. Knee Surg Sports Traumatol Arthrosc. 2011;19(8):1299-306.
42. Molloy T, Wang Y, Murrell G. The roles of growth factors in tendon and ligament healing. Sports Med. 2003;33(5):381-94.
43. Oguma H, Murakami G, Takahashi-Iwanaga H, Aoki M, Ishii S. Early anchoring collagen fibers at the bone-tendon interface are conducted by woven bone formation: light microscope and scanning electron microscope observation using a canine model. J Orthop Res. 2001;19(5):873-80.
44. Hibino N, Hamada Y, Sairyo K, Yukata K, Sano T, Yasui N. Callus formation during healing of the repaired tendon-bone junction. A rat experimental model. J Bone Joint Surg Br. 2007;89(11):1539-44.
45. Sauerschnig M, Stolberg-Stolberg J, Schmidt C, Wienerroither V, Plecko M, Schlichting K, et al. Effect of COX-2 inhibition on tendon-to-bone healing and PGE2 concentration after anterior cruciate ligament reconstruction. Eur J Med Res. 2018;23(1):1.
46. Rodeo SA, Suzuki K, Deng XH, Wozney J, Warren RF. Use of recombinant human bone morphogenetic protein-2 to enhance tendon healing in a bone tunnel. Am J Sports Med. 1999;27(4):476-88.
47. Hoher J, Moller HD, Fu FH. Bone tunnel enlargement after anterior cruciate ligament reconstruction: fact or fiction? Knee Surg Sports Traumatol Arthrosc. 1998;6(4):231-40.
48. Clatworthy MG, Annear P, Bulow JU, Bartlett RJ. Tunnel widening in anterior cruciate ligament reconstruction: a prospective evaluation of hamstring and patella tendon grafts. Knee Surg Sports Traumatol Arthrosc. 1999;7(3):138-45.
49. Aga C, Wilson KJ, Johansen S, Dornan G, La Prade RF, Engebretsen L. Tunnel widening in single- versus double-bundle anterior cruciate ligament reconstructed knees. Knee Surg Sports Traumatol Arthrosc. 2017;25(4):1316-27.
50. Fahey M, Indelicato PA. Bone tunnel enlargement after anterior cruciate ligament replacement. The American journal of sports medicine. 1994;22(3):410-4.
51. Fink C, Zapp M, Benedetto KP, Hackl W, Hoser C, Rieger M. Tibial tunnel enlargement following anterior cruciate ligament reconstruction with patellar tendon autograft. Arthroscopy. 2001;17(2):138-43.
52. Russell RG, Croucher PI, Rogers MJ. Bisphosphonates: pharmacology, mechanisms of action and clinical uses. Osteoporos Int. 1999;9 Suppl 2:S66-80.
53. Reid IR, Brown JP, Burckhardt P, Horowitz Z, Richardson P, Trechsel U, et al. Intravenous zoledronic acid in postmenopausal women with low bone mineral density. N Engl J Med. 2002;346(9):653-61.
54. Lampropoulou-Adamidou K, Dontas I, Stathopoulos IP, Khaldi L, Lelovas P, Vlamis J, et al. Chondroprotective effect of high-dose zoledronic acid: An experimental study in a rabbit model of osteoarthritis. J Orthop Res. 2014;32(12):1646-51.
55. Corrado A, Santoro N, Cantatore FP. Extra-skeletal effects of bisphosphonates. Joint Bone Spine. 2007;74(1):32-8.

56. Giuliani N, Pedrazzoni M, Negri G, Passeri G, Impicciatore M, Girasole G. Bisphosphonates stimulate formation of osteoblast precursors and mineralized nodules in murine and human bone marrow cultures in vitro and promote early osteoblastogenesis in young and aged mice in vivo. Bone. 1998;22(5):455-61.
57. Im GI, Qureshi SA, Kenney J, Rubash HE, Shanbhag AS. Osteoblast proliferation and maturation by bisphosphonates. Biomaterials. 2004;25(18):4105-15.
58. Fan M, Jiang WX, Wang AY, Wang Y, Peng J, Zhang L, et al. Effect and mechanism of zoledronate on prevention of collapse in osteonecrosis of the femoral head. Zhongguo Yi Xue Ke Xue Yuan Xue Bao. 2012;34(4):330-6.
59. Lee YK, Ha YC, Cho YJ, Suh KT, Kim SY, Won YY, et al. Does Zoledronate Prevent Femoral Head Collapse from Osteonecrosis? A Prospective, Randomized, Open-Label, Multicenter Study. J Bone Joint Surg Am. 2015;97(14):1142-8.
60. Eriksen EF. Treatment of bone marrow lesions (bone marrow edema). Bonekey Rep. 2015;4:755.
61. Andersson T, Agholme F, Aspenberg P, Tengvall P. Surface immobilized zoledronate improves screw fixation in rat bone: a new method for the coating of metal implants. J Mater Sci Mater Med. 2010;21(11):3029-37.
62. Harding AK, A WD, Geijer M, Toksvig-Larsen S, Tagil M. A single bisphosphonate infusion does not accelerate fracture healing in high tibial osteotomies. Acta Orthop. 2011;82(4):465-70.
63. Russell RG, Watts NB, Ebetino FH, Rogers MJ. Mechanisms of action of bisphosphonates: similarities and differences and their potential influence on clinical efficacy. Osteoporos Int. 2008;19(6):733-59.
64. Madsen JE, Berg-Larsen T, Kirkeby OJ, Falch JA, Nordsletten L. No adverse effects of clodronate on fracture healing in rats. Acta Orthop Scand. 1998;69(5):532-6.
65. Little DG, McDonald M, Bransford R, Godfrey CB, Amanat N. Manipulation of the anabolic and catabolic responses with OP-1 and zoledronic acid in a rat critical defect model. J Bone Miner Res. 2005;20(11):2044-52.
66. Amanat N, McDonald M, Godfrey C, Bilston L, Little D. Optimal timing of a single dose of zoledronic acid to increase strength in rat fracture repair. J Bone Miner Res. 2007;22(6):867-76.
67. Bosemark P, Isaksson H, McDonald MM, Little DG, Tagil M. Augmentation of autologous bone graft by a combination of bone morphogenic protein and bisphosphonate increased both callus volume and strength. Acta Orthop. 2013;84(1):106-11.
68. Turker M, Aslan A, Cirpar M, Kochai A, Tulmac OB, Balci M. Histological and biomechanical effects of zoledronate on fracture healing in an osteoporotic rat tibia model. Joint Diseases & Related Surgery. 2016;27(1):9-15.
69. Amanat N, Brown R, Bilston LE, Little DG. A single systemic dose of pamidronate improves bone mineral content and accelerates restoration of strength in a rat model of fracture repair. J Orthop Res. 2005;23(5):1029-34.
70. Xue D LF, Chen G, Yan S, Pan Z. Do bisphosphonates affect bone healing? A meta-analysis of randomized controlled trials. J Orthop Surg Res. 2014:9:45.
71. Thomopoulos S, Matsuzaki H, Zaegel M, Gelberman RH, Silva MJ. Alendronate prevents bone loss and improves tendon-to-bone repair strength in a canine model. J Orthop Res. 2007;25(4):473-9.

72. Rodeo SA, Kawamura S, Ma CB, Deng XH, Sussman PS, Hays P, et al. The effect of osteoclastic activity on tendon-to-bone healing: an experimental study in rabbits. J Bone Joint Surg Am. 2007;89(10):2250-9.
73. Tripathi KD. Essentials of medical pharmacology. Seventh edition. ed. New Delhi: Jaypee Brothers Medical Publishers (P), Ltd.; 2013. xvi, 1002 pages p.
74. Black DM, Delmas PD, Eastell R, Reid IR, Boonen S, Cauley JA, et al. Once-yearly zoledronic acid for treatment of postmenopausal osteoporosis. N Engl J Med. 2007;356(18):1809-22.
75. Lyles KW, Colon-Emeric CS, Magaziner JS, Adachi JD, Pieper CF, Mautalen C, et al. Zoledronic Acid in Reducing Clinical Fracture and Mortality after Hip Fracture. N Engl J Med. 2007;357:nihpa40967.
76. Eriksen EF, Lyles KW, Colon-Emeric CS, Pieper CF, Magaziner JS, Adachi JD, et al. Antifracture efficacy and reduction of mortality in relation to timing of the first dose of zoledronic acid after hip fracture. J Bone Miner Res. 2009;24(7):1308-13.
77. Colon-Emeric C, Nordsletten L, Olson S, Major N, Boonen S, Haentjens P, et al. Association between timing of zoledronic acid infusion and hip fracture healing. Osteoporos Int. 2011;22(8):2329-36.
78. Boonen S, Reginster JY, Kaufman JM, Lippuner K, Zanchetta J, Langdahl B, et al. Fracture risk and zoledronic acid therapy in men with osteoporosis. N Engl J Med. 2012;367(18):1714-23.
79. Chaudhary M TA, Sehgal R. Evaluation of Toxicity Profile of Zoledronic Acid in Wistar Rat: A Sub-chronic Toxicity Study. The Internet Journal of Toxicology. 2008;6(2).
80. Reid IR, Gamble GD, Mesenbrink P, Lakatos P, Black DM. Characterization of and risk factors for the acute-phase response after zoledronic acid. J Clin Endocrinol Metab. 2010;95(9):4380-7.
81. Brown JP. Antiresorptives: Safety Concerns-Clinical Perspective. Toxicol Pathol. 2017;45(7):859-63.
82. Grbic JT, Black DM, Lyles KW, Reid DM, Orwoll E, McClung M, et al. The incidence of osteonecrosis of the jaw in patients receiving 5 milligrams of zoledronic acid: data from the health outcomes and reduced incidence with zoledronic acid once yearly clinical trials program. J Am Dent Assoc. 2010;141(11):1365-70.
83. Khosla S, Burr D, Cauley J, Dempster DW, Ebeling PR, Felsenberg D, et al. Bisphosphonate-associated osteonecrosis of the jaw: report of a task force of the American Society for Bone and Mineral Research. J Bone Miner Res. 2007;22(10):1479-91.
84. Shane E, Burr D, Ebeling PR, Abrahamsen B, Adler RA, Brown TD, et al. Atypical subtrochanteric and diaphyseal femoral fractures: report of a task force of the American Society for Bone and Mineral Research. J Bone Miner Res. 2010;25(11):2267-94.
85. Schilcher J, Koeppen V, Aspenberg P, Michaelsson K. Risk of atypical femoral fracture during and after bisphosphonate use. Acta Orthop. 2015;86(1):100-7.
86. Bone HG, Dempster DW, Eisman JA, Greenspan SL, McClung MR, Nakamura T, et al. Odanacatib for the treatment of postmenopausal osteoporosis: development history and design and participant characteristics of LOFT, the Long-Term Odanacatib Fracture Trial. Osteoporos Int. 2015;26(2):699-712.
87. Drake MT, Clarke BL, Oursler MJ, Khosla S. Cathepsin K Inhibitors for Osteoporosis: Biology, Potential Clinical Utility, and Lessons Learned. Endocr Rev. 2017;38(4):325-50.
88. Khosla S, Oursler MJ, Monroe DG. Estrogen and the skeleton. Trends Endocrinol Metab. 2012;23(11):576-81.

89. Beral V, Million Women Study C. Breast cancer and hormone-replacement therapy in the Million Women Study. Lancet. 2003;362(9382):419-27.
90. Rossouw JE, Anderson GL, Prentice RL, LaCroix AZ, Kooperberg C, Stefanick ML, et al. Risks and benefits of estrogen plus progestin in healthy postmenopausal women: principal results From the Women's Health Initiative randomized controlled trial. JAMA. 2002;288(3):321-33.
91. de Villiers TJ, Gass ML, Haines CJ, Hall JE, Lobo RA, Pierroz DD, et al. Global Consensus Statement on menopausal hormone therapy. Maturitas. 2013;74(4):391-2.
92. Agnusdei D, Iori N. Raloxifene: results from the MORE study. J Musculoskelet Neuronal Interact. 2000;1(2):127-32.
93. Downs RW, Jr., Bell NH, Ettinger MP, Walsh BW, Favus MJ, Mako B, et al. Comparison of alendronate and intranasal calcitonin for treatment of osteoporosis in postmenopausal women. J Clin Endocrinol Metab. 2000;85(5):1783-8.
94. Formoso G, Perrone E, Maltoni S, Balduzzi S, Wilkinson J, Basevi V, et al. Short-term and long-term effects of tibolone in postmenopausal women. Cochrane Database Syst Rev. 2016;10:CD008536.
95. Brown JP, Prince RL, Deal C, Recker RR, Kiel DP, de Gregorio LH, et al. Comparison of the Effect of Denosumab and Alendronate on Bone Mineral Density and Biochemical Markers of Bone Turnover in Postmenopausal Women With Low Bone Mass: A Randomized, Blinded, Phase 3 Trial. J Bone Miner Res. 2009:1-34.
96. Miller PD, Pannacciulli N, Brown JP, Czerwinski E, Nedergaard BS, Bolognese MA, et al. Denosumab or Zoledronic Acid in Postmenopausal Women With Osteoporosis Previously Treated With Oral Bisphosphonates. J Clin Endocrinol Metab. 2016;101(8):3163-70.
97. Cummings SR, San Martin J, McClung MR, Siris ES, Eastell R, Reid IR, et al. Denosumab for prevention of fractures in postmenopausal women with osteoporosis. N Engl J Med. 2009;361(8):756-65.
98. AmgenInc. Prolia®(denosumab) Full prescribing information medication guide.; 2013 Sept 10.
99. Smith MR, Saad F, Egerdie B, Szwedowski M, Tammela TL, Ke C, et al. Effects of denosumab on bone mineral density in men receiving androgen deprivation therapy for prostate cancer. J Urol. 2009;182(6):2670-5.
100. Gerstenfeld LC, Sacks DJ, Pelis M, Mason ZD, Graves DT, Barrero M, et al. Comparison of effects of the bisphosphonate alendronate versus the RANKL inhibitor denosumab on murine fracture healing. J Bone Miner Res. 2009;24(2):196-208.
101. Kostenuik PJ, Nguyen HQ, McCabe J, Warmington KS, Kurahara C, Sun N, et al. Denosumab, a fully human monoclonal antibody to RANKL, inhibits bone resorption and increases BMD in knock-in mice that express chimeric (murine/human) RANKL. J Bone Miner Res. 2009;24(2):182-95.
102. Nalamachu S, Wortmann R. Role of indomethacin in acute pain and inflammation management: a review of the literature. Postgrad Med. 2014;126(4):92-7.
103. Majeed MH, Sherazi SAA, Bacon D, Bajwa ZH. Pharmacological Treatment of Pain in Osteoarthritis: A Descriptive Review. Curr Rheumatol Rep. 2018;20(12):88.
104. Bian YY, Wang LC, Qian WW, Lin J, Jin J, Peng HM, et al. Role of Parecoxib Sodium in the Multimodal Analgesia after Total Knee Arthroplasty: A Randomized Double-blinded Controlled Trial. Orthop Surg. 2018;10(4):321-7.
105. Pitchon DN, Dayan AC, Schwenk ES, Baratta JL, Viscusi ER. Updates on Multimodal Analgesia for Orthopedic Surgery. Anesthesiol Clin. 2018;36(3):361-73.

106. Needleman P, Turk J, Jakschik BA, Morrison AR, Lefkowith JB. Arachidonic acid metabolism. Annu Rev Biochem. 1986;55:69-102.
107. Dekel S, Lenthall G, Francis MJ. Release of prostaglandins from bone and muscle after tibial fracture. An experimental study in rabbits. J Bone Joint Surg Br. 1981;63-B(2):185-9.
108. Dubois RN, Abramson SB, Crofford L, Gupta RA, Simon LS, Van De Putte LB, et al. Cyclooxygenase in biology and disease. FASEB J. 1998;12(12):1063-73.
109. Seibert K, Zhang Y, Leahy K, Hauser S, Masferrer J, Perkins W, et al. Pharmacological and biochemical demonstration of the role of cyclooxygenase 2 in inflammation and pain. Proc Natl Acad Sci U S A. 1994;91(25):12013-7.
110. Zhang X, Schwarz EM, Young DA, Puzas JE, Rosier RN, O'Keefe RJ. Cyclooxygenase-2 regulates mesenchymal cell differentiation into the osteoblast lineage and is critically involved in bone repair. J Clin Invest. 2002;109(11):1405-15.
111. Simon AM, Manigrasso MB, O'Connor JP. Cyclo-oxygenase 2 function is essential for bone fracture healing. J Bone Miner Res. 2002;17(6):963-76.
112. Li M, Ke HZ, Qi H, Healy DR, Li Y, Crawford DT, et al. A novel, non-prostanoid EP2 receptor-selective prostaglandin E2 agonist stimulates local bone formation and enhances fracture healing. J Bone Miner Res. 2003;18(11):2033-42.
113. Bo J, Sudmann E, Marton PF. Effect of indomethacin on fracture healing in rats. Acta Orthop Scand. 1976;47(6):588-99.
114. Lindholm TS, Tornkvist H. Inhibitory effect on bone formation and calcification exerted by the anti-inflammatory drug ibuprofen. An experimental study on adult rat with fracture. Scand J Rheumatol. 1981;10(1):38-42.
115. Simon AM, O'Connor JP. Dose and time-dependent effects of cyclooxygenase-2 inhibition on fracture-healing. J Bone Joint Surg Am. 2007;89(3):500-11.
116. Yoon DS, Yoo JH, Kim YH, Paik S, Han CD, Lee JW. The effects of COX-2 inhibitor during osteogenic differentiation of bone marrow-derived human mesenchymal stem cells. Stem Cells Dev. 2010;19(10):1523-33.
117. Murnaghan M, Li G, Marsh DR. Nonsteroidal anti-inflammatory drug-induced fracture nonunion: an inhibition of angiogenesis? J Bone Joint Surg Am. 2006;88 Suppl 3:140-7.
118. Nagano A, Arioka M, Takahashi-Yanaga F, Matsuzaki E, Sasaguri T. Celecoxib inhibits osteoblast maturation by suppressing the expression of Wnt target genes. J Pharmacol Sci. 2017;133(1):18-24.
119. Sandberg O, Aspenberg P. Different effects of indomethacin on healing of shaft and metaphyseal fractures. Acta Orthop. 2015;86(2):243-7.
120. Meunier A, Aspenberg P. Parecoxib impairs early metaphyseal bone healing in rats. Arch Orthop Trauma Surg. 2006;126(7):433-6.
121. Dimmen S, Engebretsen L, Nordsletten L, Madsen JE. Negative effects of parecoxib and indomethacin on tendon healing: an experimental study in rats. Knee Surg Sports Traumatol Arthrosc. 2009;17(7):835-9.
122. Virchenko O, Skoglund B, Aspenberg P. Parecoxib impairs early tendon repair but improves later remodeling. Am J Sports Med. 2004;32(7):1743-7.
123. Cohen DB, Kawamura S, Ehteshami JR, Rodeo SA. Indomethacin and celecoxib impair rotator cuff tendon-to-bone healing. Am J Sports Med. 2006;34(3):362-9.
124. Dimmen S, Nordsletten L, Engebretsen L, Steen H, Madsen JE. The effect of parecoxib and indometacin on tendon-to-bone healing in a bone tunnel: an experimental study in rats. J Bone Joint Surg Br. 2009;91(2):259-63.

125. Soreide E, Granan LP, Hjorthaug GA, Espehaug B, Dimmen S, Nordsletten L. The Effect of Limited Perioperative Nonsteroidal Anti-inflammatory Drugs on Patients Undergoing Anterior Cruciate Ligament Reconstruction. Am J Sports Med. 2016.
126. Constantinescu DS, Campbell MP, Moatshe G, Vap AR. Effects of Perioperative Nonsteroidal Anti-inflammatory Drug Administration on Soft Tissue Healing: A Systematic Review of Clinical Outcomes After Sports Medicine Orthopaedic Surgery Procedures. Orthop J Sports Med. 2019;7(4):2325967119838873.
127. Duchman KR, Lemmex DB, Patel SH, Ledbetter L, Garrigues GE, Riboh JC. The Effect of Non-Steroidal Anti-Inflammatory Drugs on Tendon-to-Bone Healing: A Systematic Review with Subgroup Meta-Analysis. Iowa Orthop J. 2019;39(1):107-19.
128. Nussmeier NA, Whelton AA, Brown MT, Langford RM, Hoeft A, Parlow JL, et al. Complications of the COX-2 inhibitors parecoxib and valdecoxib after cardiac surgery. N Engl J Med. 2005;352(11):1081-91.
129. Diaz-Borjon E, Torres-Gomez A, Essex MN, Salomon P, Li C, Cheung R, et al. Parecoxib Provides Analgesic and Opioid-Sparing Effects Following Major Orthopedic Surgery: A Subset Analysis of a Randomized, Placebo-Controlled Clinical Trial. Pain Ther. 2017;6(1):61-72.
130. Schug SA, Parsons B, Li C, Xia F. The safety profile of parecoxib for the treatment of postoperative pain: a pooled analysis of 28 randomized, double-blind, placebo-controlled clinical trials and a review of over 10 years of postauthorization data. J Pain Res. 2017;10:2451-9.
131. Sengupta P. The Laboratory Rat: Relating Its Age With Human's. Int J Prev Med. 2013;2,6:624-30.
132. Ekeland A, Engesaeter LB, Langeland N. Torsional properties of rat femora. Eur Surg Res. 1984;16 Suppl 2:28-33.
133. Hebel R. Anatomy of the laboratory rat. Stromberg MW, editor. Baltimore: Williams & Wilkins; 1976.
134. Goh JC, Mech AM, Lee EH, Ang EJ, Bayon P, Pho RW. Biomechanical study on the load-bearing characteristics of the fibula and the effects of fibular resection. Clin Orthop Relat Res. 1992(279):223-8.
135. Ahmed Y, Khalaf MA, Khalil FJapa. Absence of Typical Haversian System from the Compact Bone of Some Reptile and Bird Species. 2017.
136. Hillier ML, Bell LS. Differentiating human bone from animal bone: a review of histological methods. J Forensic Sci. 2007;52(2):249-63.
137. Vignery A, Baron R. Dynamic histomorphometry of alveolar bone remodeling in the adult rat. Anat Rec. 1980;196(2):191-200.
138. Mills LA, Simpson AH. In vivo models of bone repair. J Bone Joint Surg Br. 2012;94(7):865-74.
139. Ekeland A, Engesaeter LB, Langeland N. Mechanical properties of fractured and intact rat femora evaluated by bending, torsional and tensile tests. Acta Orthop Scand. 1981;52(6):605-13.
140. Halpin RA, Geer LA, Zhang KE, Marks TM, Dean DC, Jones AN, et al. The absorption, distribution, metabolism and excretion of rofecoxib, a potent and selective cyclooxygenase-2 inhibitor, in rats and dogs. Drug Metab Dispos. 2000;28(10):1244-54.
141. Paulson SK, Zhang JY, Breau AP, Hribar JD, Liu NW, Jessen SM, et al. Pharmacokinetics, tissue distribution, metabolism, and excretion of celecoxib in rats. Drug metabolism and disposition: the biological fate of chemicals. 2000;28(5):514-21.

142. Dimmen S, Nordsletten L, Madsen JE. Parecoxib and indomethacin delay early fracture healing: a study in rats. Clin Orthop. 2009;467(8):1992-9.
143. Lin JH, Chen IW, deLuna FA. On the absorption of alendronate in rats. J Pharm Sci. 1994;83(12):1741-6.
144. Huang Q, Riviere JE. The application of allometric scaling principles to predict pharmacokinetic parameters across species. Expert opinion on drug metabolism & toxicology. 2014;10(9):1241-53.
145. West GB, Brown JH, Enquist BJ. A general model for the origin of allometric scaling laws in biology. Science. 1997;276(5309):122-6.
146. Schneider K, Oltmanns J, Hassauer M. Allometric principles for interspecies extrapolation in toxicological risk assessment--empirical investigations. Regul Toxicol Pharmacol. 2004;39(3):334-47.
147. Utvag SE, Fuskevag OM, Shegarfi H, Reikeras O. Short-term treatment with COX-2 inhibitors does not impair fracture healing. J Invest Surg. 2010;23(5):257-61.
148. Sigurdsen UE, Reikeras O, Utvag SE. External fixation compared to intramedullary nailing of tibial fractures in the rat. Acta Orthop. 2009;80(3):375-9.
149. Park SH, O'Connor K, Sung R, McKellop H, Sarmiento A. Comparison of healing process in open osteotomy model and closed fracture model. J Orthop Trauma. 1999;13(2):114-20.
150. Melhus G, Solberg LB, Dimmen S, Madsen JE, Nordsletten L, Reinholt FP. Experimental osteoporosis induced by ovariectomy and vitamin D deficiency does not markedly affect fracture healing in rats. Acta Orthop. 2007;78(3):393-403.
151. Nordsletten L, Madsen JE, Almaas R, Rootwelt T, Halse J, Konttinen YT, et al. The neuronal regulation of fracture healing. Effects of sciatic nerve resection in rat tibia. Acta Orthop Scand. 1994;65(3):299-304.
152. Engesaeter LB, Ekeland A, Langeland N. Methods for testing the mechanical properties of the rat femur. Acta Orthop Scand. 1978;49(6):512-8.
153. Soreide E, Denbeigh JM, Lewallen EA, Samsonraj RM, Berglund LJ, Dudakovic A, et al. Fibrin glue mediated delivery of bone anabolic reagents to enhance healing of tendon to bone. J Cell Biochem. 2018;119(7):5715-24.
154. Dimmen S, Nordsletten L, Engebretsen L, Steen H, Madsen JE. Negative effect of parecoxib on bone mineral during fracture healing in rats. Acta Orthop. 2008;79(3):438-44.
155. Histing T, Garcia P, Holstein JH, Klein M, Matthys R, Nuetzi R, et al. Small animal bone healing models: Standards, tips, and pitfalls results of a consensus meeting. Bone. 2011;49(4):591-9.
156. Dempster DW, Compston JE, Drezner MK, Glorieux FH, Kanis JA, Malluche H, et al. Standardized nomenclature, symbols, and units for bone histomorphometry: a 2012 update of the report of the ASBMR Histomorphometry Nomenclature Committee. J Bone Miner Res. 2013;28(1):2-17.
157. Gyger M, Berdoy M, Dontas I, Kolf-Clauw M, Santos AI, Sjoquist M. FELASA accreditation of education and training courses in laboratory animal science according to the Directive 2010/63/EU. Lab Anim. 2018:23677218788105.
158. Silva MJ, Boyer MI, Ditsios K, Burns ME, Harwood FL, Amiel D, et al. The insertion site of the canine flexor digitorum profundus tendon heals slowly following injury and suture repair. J Orthop Res. 2002;20(3):447-53.

159. Silva MJ, Thomopoulos S, Kusano N, Zaegel MA, Harwood FL, Matsuzaki H, et al. Early healing of flexor tendon insertion site injuries: Tunnel repair is mechanically and histologically inferior to surface repair in a canine model. J Orthop Res. 2006;24(5):990-1000.
160. Tsukada H, Ishibashi Y, Tsuda E, Kusumi T, Kohno T, Toh S. The actual tendon-bone interface strength in a rabbit model. Arthroscopy. 2010;26(3):366-74.
161. Bunker DL, Ilie V, Ilie V, Nicklin S. Tendon to bone healing and its implications for surgery. Muscles, ligaments and tendons journal. 2014;4(3):343-50.
162. Lazarides AL, Eward WC, Green K, Cardona DM, Brigman BE, Taylor DC. Histological Evaluation of Tendon-Bone Healing of an Anterior Cruciate Ligament Hamstring Graft in a 14-Year-Old Boy. Am J Sports Med. 2015;43(8):1935-40.
163. Robert H, Es-Sayeh J. The role of periosteal flap in the prevention of femoral widening in anterior cruciate ligament reconstruction using hamstring tendons. Knee Surg Sports Traumatol Arthrosc. 2004;12(1):30-5.
164. Sun R, Chen BC, Zhang XY, Wang F, Shao DC, Wang XF, et al. [Anterior cruciate ligament reconstruction using periosteum wrapped autologous hamstring tendons: clinical research]. Zhonghua Yi Xue Za Zhi. 2010;90(3):182-6.
165. Takigami J, Hashimoto Y, Yamasaki S, Terai S, Nakamura H. Direct bone-to-bone integration between recombinant human bone morphogenetic protein-2-injected tendon graft and tunnel wall in an anterior cruciate ligament reconstruction model. Int Orthop. 2015;39(7):1441-7.
166. Saccomanno MF, Sircana G, Cazzato G, Donati F, Randelli P, Milano G. Prognostic factors influencing the outcome of rotator cuff repair: a systematic review. Knee Surg Sports Traumatol Arthrosc. 2016;24(12):3809-19.
167. Chen X, Giambini H, Ben-Abraham E, An KN, Nassr A, Zhao C. Effect of Bone Mineral Density on Rotator Cuff Tear: An Osteoporotic Rabbit Model. PLoS One. 2015;10(10):e0139384.
168. Chung SW, Oh JH, Gong HS, Kim JY, Kim SH. Factors affecting rotator cuff healing after arthroscopic repair: osteoporosis as one of the independent risk factors. Am J Sports Med. 2011;39(10):2099-107.
169. Lui PP, Cheng YY, Yung SH, Hung AS, Chan KM. A randomized controlled trial comparing bone mineral density changes of three different ACL reconstruction techniques. The Knee. 2012;19(6):779-85.
170. Agholme F, Isaksson H, Li X, Ke HZ, Aspenberg P. Anti-sclerostin antibody and mechanical loading appear to influence metaphyseal bone independently in rats. Acta Orthop. 2011;82(5):628-32.
171. Bergenstock M, Min W, Simon AM, Sabatino C, O'Connor JP. A comparison between the effects of acetaminophen and celecoxib on bone fracture healing in rats. J Orthop Trauma. 2005;19(10):717-23.
172. Bissinger O, Kreutzer K, Gotz C, Hapfelmeier A, Pautke C, Vogt S, et al. A biomechanical, micro-computertomographic and histological analysis of the influence of diclofenac and prednisolone on fracture healing in vivo. BMC Musculoskelet Disord. 2016;17(1):383.
173. Goodman S, Ma T, Trindade M, Ikenoue T, Matsuura I, Wong N, et al. COX-2 selective NSAID decreases bone ingrowth in vivo. J Orthop Res. 2002;20(6):1164-9.
174. Gerstenfeld LC, Al-Ghawas M, Alkhiary YM, Cullinane DM, Krall EA, Fitch JL, et al. Selective and nonselective cyclooxygenase-2 inhibitors and experimental fracture-healing. Reversibility of effects after short-term treatment. J Bone Joint Surg Am. 2007;89(1):114-25.

175. Akritopoulos P, Papaioannidou P, Hatzokos I, Haritanti A, Iosifidou E, Kotoula M, et al. Parecoxib has non-significant long-term effects on bone healing in rats when administered for a short period after fracture. Arch Orthop Trauma Surg. 2009;129(10):1427-32.
176. Fader L, Whitaker J, Lopez M, Vivace B, Parra M, Carlson J, et al. Tibia fractures and NSAIDs. Does it make a difference? A multicenter retrospective study. Injury. 2018;49(12):2290-4.
177. Burd TA, Hughes MS, Anglen JO. Heterotopic ossification prophylaxis with indomethacin increases the risk of long-bone nonunion. J Bone Joint Surg Br. 2003;85(5):700-5.
178. Sagi HC, Jordan CJ, Barei DP, Serrano-Riera R, Steverson B. Indomethacin Prophylaxis for Heterotopic Ossification after Acetabular Fracture Surgery Increases the Risk for Non-Union of the Posterior Wall. J Orthop Trauma. 2014.
179. Aliuskevicius M, Ostgaard SE, Rasmussen S. No influence of ibuprofen on bone healing after Colles' fracture - A randomized controlled clinical trial. Injury. 2019;50(7):1309-17.
180. Wheatley BM, Nappo KE, Christensen DL, Holman AM, Brooks DI, Potter BK. Effect of NSAIDs on Bone Healing Rates: A Meta-analysis. J Am Acad Orthop Surg. 2019;27(7):e330-e6.
181. Kouroupis D. Mesenchymal Stem Cell Applications for Ligament Repair after Joint Trauma. Journal of Clinical & Experimental Pathology. 2014;04(04).
182. Borgeat A, Ofner C, Saporito A, Farshad M, Aguirre J. The effect of nonsteroidal anti-inflammatory drugs on bone healing in humans: A qualitative, systematic review. J Clin Anesth. 2018;49:92-100.
183. Richards CJ, Graf KW, Jr., Mashru RP. The Effect of Opioids, Alcohol, and Nonsteroidal Anti-inflammatory Drugs on Fracture Union. Orthop Clin North Am. 2017;48(4):433-43.
184. Chen TH, Weber FE, Malina-Altzinger J, Ghayor C. Epigenetic drugs as new therapy for tumor necrosis factor-alpha-compromised bone healing. Bone. 2019;127:49-58.
185. Roberts SJ, Ke HZ. Anabolic Strategies to Augment Bone Fracture Healing. Curr Osteoporos Rep. 2018;16(3):289-98.
186. Goldhahn J, Scheele WH, Mitlak BH, Abadie E, Aspenberg P, Augat P, et al. Clinical evaluation of medicinal products for acceleration of fracture healing in patients with osteoporosis. Bone. 2008;43(2):343-7.

II

Negative effect of zoledronic acid on tendon-to-bone healing

In vivo study of biomechanics and bone remodeling in a rat model

Geir Aasmund HJORTHAUG [1–4], Endre SØREIDE [1–3], Lars NORDSLETTEN [1–3], Jan Erik MADSEN [1–3], Finn P REINHOLT [5], Sanyalak NIRATISAIRAK [2,6], and Sigbjørn DIMMEN [2,3,7]

[1] Division of Orthopedic Surgery, Oslo University Hospital (OUS), Norway; [2] Institute of Clinical Medicine, Faculty of Medicine, University of Oslo (UIO); [3] Experimental Orthopedic Research, Institute for Surgical Research, OUS; [4] Department of Orthopedic Surgery, Martina Hansen's Hospital; [5] Department of Pathology, OUS; [6] Biomechanics Laboratory, Division of Orthopedic Surgery, OUS; [7] Department of Orthopedic Surgery, Lovisenberg Diaconal Hospital, Norway
Correspondence: geir.hjorthaug@me.com
Submitted 2017-09-08. Accepted 2018-01-18.

Background and purpose — Outcome after ligament reconstruction or tendon repair depends on secure tendon-to-bone healing. Increased osteoclastic activity resulting in local bone loss may contribute to delayed healing of the tendon–bone interface. The objective of this study was to evaluate the effect of the bisphosphonate zoledronic acid (ZA) on tendon-to-bone healing.

Methods — Wistar rats (n = 92) had their right Achilles tendon cut proximally, pulled through a bone tunnel in the distal tibia and sutured anteriorly. After 1 week animals were randomized to receive a single dose of ZA (0.1 mg/kg IV) or control. Healing was evaluated at 3 and 6 weeks by mechanical testing, dual-energy X-ray absorptiometry and histology including immunohistochemical staining of osteoclasts.

Results — ZA treatment resulted in 19% (95% CI 5–33%) lower pullout strength and 43% (95% CI 14–72%) lower stiffness of the tendon–bone interface, compared with control (2-way ANOVA; p = 0.009, p = 0.007). Administration of ZA did not affect bone mineral density (BMD) or bone mineral content (BMC). Histological analyses did not reveal differences in callus formation or osteoclasts between the study groups.

Interpretation — ZA reduced pullout strength and stiffness of the tendon–bone interface. The study does not provide support for ZA as adjuvant treatment in tendon-to-bone healing.

Tendons and ligaments attach to bone through a transitional fibrocartilage tissue, the enthesis. This transitional tissue is complex in composition and organization and is not regenerated during healing of injuries or surgical repair. Tendon and ligament injuries often require surgical repair or reconstruction to regain function, and a favorable outcome depends on solid tendon-to-bone healing (Harryman et al. 1991, Gulotta and Rodeo 2007, Ekdahl et al. 2008). The osteointegration of the graft is the weak link in early tendon-to-bone tunnel healing. In a randomized controlled trial, transient decrease in local bone mineral density (BMD) was observed in the knee region of patients undergoing anterior cruciate ligament (ACL) reconstruction (Lui et al. 2012). Bone loss has also been observed in experimental tendon–bone repair studies and is probably due to increased ostoclastic activity (Galatz et al. 2005, Rodeo et al. 2007). Furthermore, a negative correlation between local bone loss and strength of the tendon–bone interface has been reported (Silva et al. 2002). Bone surfaces with high osteoclastic activity and peri-tunnel bone loss may therefore become a less suitable scaffold for healing of the tendon graft. Thus, prevention of early bone loss could enhance tendon-to-bone healing and improve clinical outcomes.

Bisphosphonates (BPs) are rapidly incorporated into the crystal structure of apatite bone matrix (Cole et al. 2016) and bind to the bone present at the time of administration (Amanat et al. 2007). The main effect of BPs is inhibition of osteoclasts, resulting in increased BMD (Russell et al. 2008). Several experimental studies have reported that BP treatment may enhance fracture healing (Li et al. 2001, Amanat et al. 2005) and implant fixation (Andersson et al. 2010). Only a limited number of studies have assessed the effect of BPs using tendon-to-bone models, but improved healing has been reported for alendronate (Thomopoulos et al. 2007, Lui et al. 2013). Zoledronic acid (ZA) is the most potent BP available (Russell et al. 2008) and, to our knowledge, the effect of ZA on tendon-to-bone tunnel healing has not been tested.

DOI 10.1080/17453674.2018.1440189

We hypothesized that ZA treatment would improve the mechanical properties at 3 and 6 weeks of tendon-to-bone tunnel healing in rats by reducing the local bone loss.

Materials and methods

Animals

Female Wistar rats (n = 92) (Taconic Europe, Lille Skensved, Denmark), skeletally mature, mean weight of 238 g (SD 9), were included in the study. The animals were acclimatized for 2 weeks before the surgical procedure, and were kept 2 per wire-topped plastic cage in an accredited animal facility with controlled temperature (21°C ± 1), humidity (55% ± 10), ventilation and 12 hours light/dark cycles. They were allowed free access to water and standard laboratory rodent nutrition. Analgesics were given according to protocol (Hjorthaug et al. 2015). Anesthesia was induced and maintained by intraperitoneal (IP) injection of ZRF cocktail. The induction dose was 1.6 mL/kg; a volume of 0.4 mL. Antibiotics were not used.

Surgical procedure

The skin on the medial side of the right Achilles tendon was incised with a 10 mm longitudinal incision. The Achilles tendon was released proximally from the calf muscle while the calcaneal insertion distally was left intact. A drill hole was made in the distal tibia in a dorsoventral direction, 3 mm proximal to the ankle joint. Predrilling was done with a 1.0 mm drill bit followed by drilling with a 1.5 mm drill bit at 3,200 rpm. A holding suture was added to the released tendon in a Kessler suture fashion using a 2-string monofilament nonabsorbable suture. The sutures were guided through the tunnel from posterior to anterior and the tendon gently passed through the tunnel and sutured to the anterior soft tissue with the ankle joint in a 90° flexed position. The skin incision was closed using resorbable sutures and sealed with spray dressing. No restriction on weight bearing was applied postoperatively.

Groups

7 days postoperatively, single animals were allocated to either treatment (ZA group) or control group by computerized randomization. Under general anesthesia, induced by a low dose of ZRF cocktail (0.1 mL) IP and maintained by isoflurane (1.5–2.5%) inhalation anesthesia, the animals in the treatment group received a single ZA dose (0.1 mg/kg, total volume 0.5 mL) by IV infusion (Aclasta, Novartis, Frimley, UK) in the tail vein (Amanat et al. 2007). Control animals received an injection of saline in the same volume and route. The personnel giving the infusions were blinded to groups, as were observers before all further analyses. The animals were killed after 3 or 6 weeks.

Mechanical assessment

Animals allocated to mechanical assessments were killed by pentobarbital overdose. The right hind leg was disarticulated through the knee, and the fibula, talus, foot, and soft tissue including the long tendons were removed. The anterior suture was removed. The tibia, calcaneus, and tendon graft were carefully preserved and the specimens were tested and analyzed as described (Hjorthaug et al. 2015) in a material testing machine (Model 858 Mini Bionix with MTS FlexTest digital controller, MTS Systems Corporation, Eden Prairie, Minnesota, USA) in a custom-made jig, designed to firmly hold the tibia and calcaneus without applying pressure to the tendon insertion site. No pre-tensioning was done. A 250N load cell was pulled upwards at a constant speed of 0.1 mm/s. The sampling frequency was 20 Hz over 120 s. All specimens were pulled to complete failure. Data were analyzed for pullout strength, stiffness, energy, and elongation.

Histological evaluation

Tissues of 5 animals from each study group at each time point were fixed in vivo by vascular perfusion of 0.1 M phosphate-buffered 2% paraformaldehyde during deep anesthesia. The right leg containing the tendon-bone-interface was stripped of the skin only. The 3rd tail vertebra was debrided of all soft tissues. Specimens were immersed in the same fixative as above for 2 days, and decalcified in 7% EDTA in a 0.1 M phosphate buffer containing 0.5% paraformaldehyde. The specimens containing the tendon-bone-interface were embedded in paraffin and serial sectioned with 5 µm section thickness from anterior to posterior.

Light microscopy

For semiquantitative bone morphometric analyses of the bone–tendon interface, 1 representative section centrally in the coronal plane was analyzed. Digital images were analyzed using AnalySIS V (Olympus Soft Imaging Solutions GmbH, Münster, Germany). A circle of 1.6 mm in diameter was superimposed to the tunnel profile, the chosen diameter being 0.1 mm larger than the used drill bit to compensate for any elliptical shaped appearance of the bone tunnel due to manual drilling and the manual sectioning along the axis of the tunnel. Mineralized tissue formation inside the bone tunnel was measured. The bone–tendon ratio inside the tunnel was calculated by point counting using a square test grid (Figure 1).

Histochemistry

To identify and estimate the number of osteoclast profiles in the paraffin sections, a standard protocol for the osteoclast marker tartrate-resistant acid phosphatase (TRAP) was used as suggested by the provider of a commercially available kit (Acid Phosphatase Leukocyte, TRAP, 387A-1KT lot SLBB7136, Sigma Aldrich). The regions of interest (ROI) were the bone tunnel, the ipsilateral calcaneus and the 3rd tail vertebra. The analyses were performed both on unstained and on sections stained with hematoxylin as nuclear stain. The TRAP staining was graded as strong, weak, or none, and osteoclast profiles

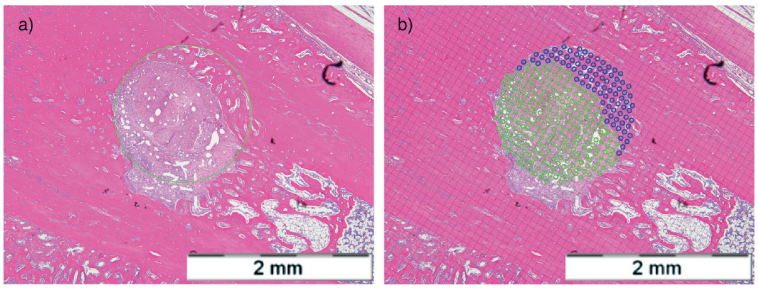

Figure 1. Medium power magnification (x10) light microscopy of a H&E stained histological section in a specimen from the 3 weeks ZA group from the middle of the bone tunnel showing (a) the superimposed circle of 1.6 mm and (b) the grid used to calculate the ratio of bone and tendon inside the tunnel. Scale bars = 2 mm.

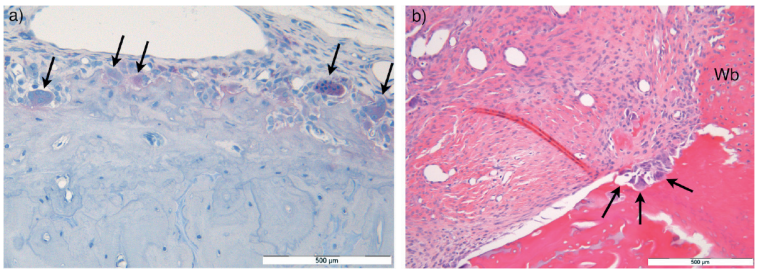

Figure 2. (a) High-power magnification (x40) light microscopy of section of the calcaneus from a specimen in the ZA group after 3 weeks subjected to TRAP enzyme histochemistry hematoxylin nuclear staining. Arrows indicate counted osteoclasts. (b) High-power magnification (x40) light microscopy of H&E stained section of the tendon–bone interface from a specimen in the control group after 6 weeks with bone resorption lacunae (arrows) in the tunnel wall containing osteoclasts. There is adjacent new woven bone (Wb) formation. Scale bars = 500 µm.

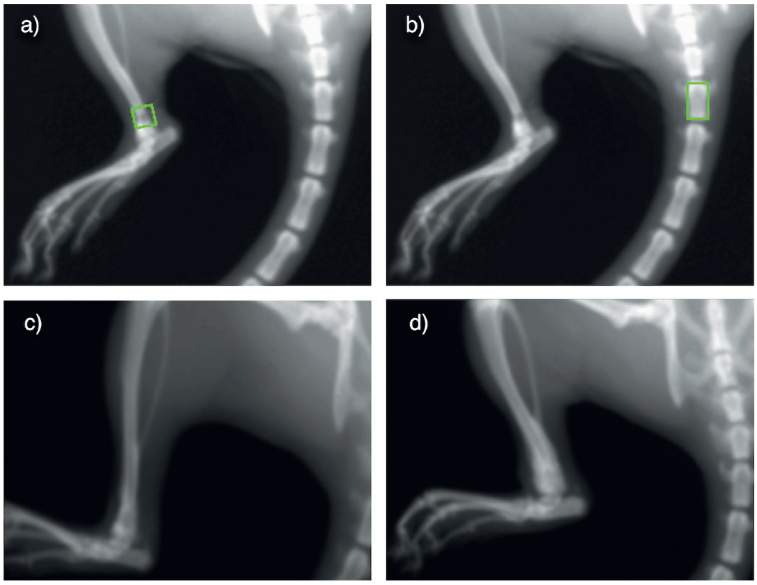

Figure 3. Upper panel: A specimen at baseline, showing the region of interest used for BMD and BMC measurements over the bone tunnel (a) and 3rd tail vertebra (b). Lower panel: X-rays of two 6-weeks specimens demonstrating bone formation around the bone tunnel in a specimen from the control group (c) and the ZA group (d). Radiographs were obtained from Lunar PIXImus.

were counted. Osteoclasts were defined as TRAP-positive cells containing more than 1 nucleus (Figure 2). Tissue from a previous study was used as positive control (Solberg et al. 2015).

Bone mineral measurement and radiographic evaluation

Under anesthesia at each time point in all animals, BMD and bone mineral content (BMC) were measured over the bone tunnel using DEXA (Lunar PIXImus, software v. 2.10, Lunar, Madison, WI, USA). The ROI consisted of 19 x 19 pixels (≈ 4 x 4 mm) that was aligned along the axis of the bone tunnel and placed flush with the anterior bone cortex. To assess systemic bone mineral effects, we used a secondary ROI, 19 x 33 pixels (≈ 4 x 7 mm), that was aligned to the 3rd tail vertebra (Figure 3). Radiographs were reviewed to reveal any complications.

Statistics

The number of animals was based on previous studies, and estimated based on our main outcome (Dimmen et al. 2009, Hjorthaug et al. 2015). An a priori power calculation for the sample size was not performed. The main outcome was pullout strength. Other outcomes were stiffness, energy absorption, elongation, and differences in BMD and BMC from baseline. 2 independent observers analyzed these 6 variables, and the mean values were calculated and used for the statistical analyses. Normality of the distribution was evaluated using histograms with normality curves. Variances were tested by Levenes' test, and in case of detected heterogeneity, comparisons for group mean differences with 95% confidence intervals (CI) were calculated on log-transformed data of all above outcomes except elongation. Differences between the groups were tested by 2-way Analysis of Variance (ANOVA), with time and treatment as fixed factors. If no interaction effects were found, analysis of the main effects for time and treatment was performed. Pairwise comparisons were run where effect estimates were expressed as a percentage of the mean of the corresponding group and the 95% confidence intervals (CI) and p-values were Bonferroni-adjusted to correct for multiple comparisons. The alpha level was set to 0.05. Results for semiquantitative data from histology are given as medians and ranges, and the groups were compared using the non-parametric Mann–Whitney test for independent samples, without correction of the p-values. Statistical analyses were performed using IBM SPSS® Statistics for Macintosh v. 23.0 (IBM Inc., Chicago, Illinois, USA).

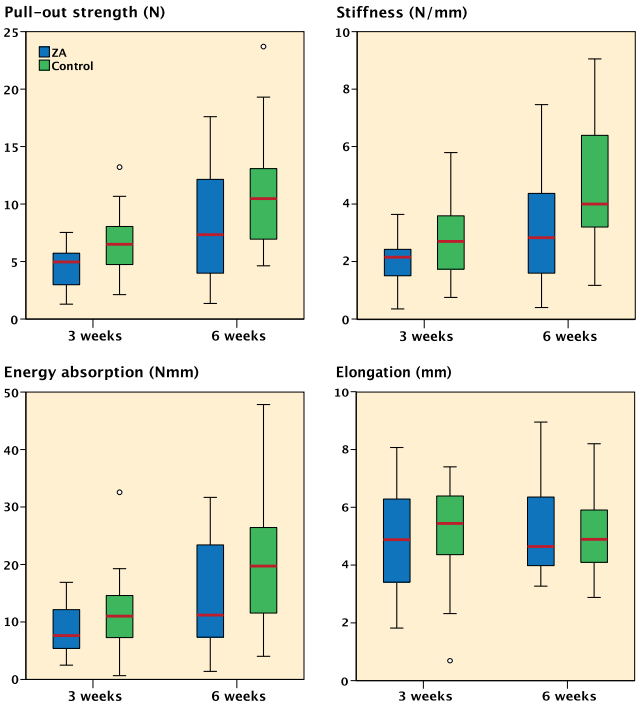

Figure 4. Clustered boxplots of data from mechanical testing of the tendon–bone interface. Except for elongation, all variables increased with time. There was a negative effect of ZA treatment in pullout strength and stiffness, but no significant differences in energy or elongation.

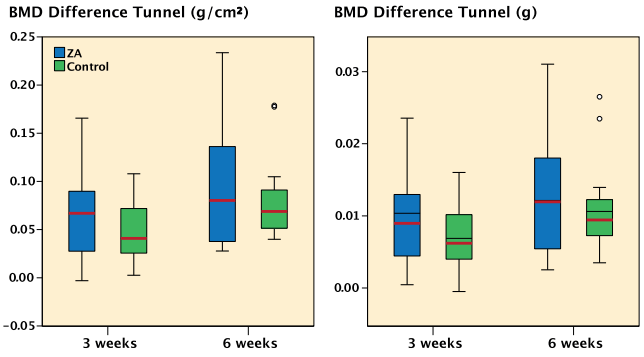

Figure 5. Clustered boxplots of data from DEXA measurements of the ROI over the bone tunnel: BMD and BMC difference from baseline.

Ethics, funding, and potential conflicts of interest

The experimental protocol was reviewed and approved by the Norwegian Animal Research Authority (2014, ID 5839), and the study conducted according to guidelines provided by Norecopa. The study was funded by internal hospital research grants. One author declares the following potential conflict of interest or source of funding: GAH received a minor research grant from Smith & Nephew in 2012.

Results

Animal inclusion

The body weight of all animals increased during the study period by mean 13.9 g (SD 6.4) and 25.3 g (SD 8.5), at 3 weeks and at 6 weeks respectively. 7 animals died perioperatively and 2 animals were killed due to wound complications during the first week. 83 animals were randomized to study groups. 2 animals died in the second anesthesia prior to injections 1 week postoperatively. Thus, 81 animals were available for final analysis including DEXA measurements. Of the 81 animals, 20 were selected for histology and 61 for mechanical tests. No fractures were observed clinically or on radiographs.

Mechanical assessment

The tendons of all specimens were completely pulled out, and they all ruptured at the tendon–bone tunnel interface. No fractures occurred during testing. Overall, mean pullout strength was 5.7 N (SD 2.7) at 3 weeks and 9.4 N (SD 5.2) at 6 weeks. Interaction effects of "time" or "treatment" were not found in any of the mechanical variables (2-way ANOVA), therefore main effects were calculated. Pullout strength increased from 3 to 6 weeks by 22% (CI 9–40%) (p = 0.002) in ZA-treated animals and controls. Stiffness and energy increased similarly by 40% (CI 12–70%) (p = 0.007) and 18% (CI 4–35%) (p = 0.02), respectively. Elongation did not increase with time (p = 0.7).

The main effect of ZA treatment was a reduction of pullout strength compared with control by 19% (CI 5–33%) (p = 0.009) at 3 and 6 weeks. ZA treatment reduced stiffness by 43% (CI 14–72%) (p = 0.004). No statistically significant differences for treatment between the groups were observed in energy (p = 0.1) or elongation (p = 0.9) (Figure 4).

Bone mineral measurements

Baseline BMD over the bone tunnels of the 81 included animals was mean 179 mg/cm2 (SD 24). Interaction effects between time and treatment were not found in any of the bone mineral variables, therefore main effects were calculated. BMD difference from baseline increased from 3 to 6 weeks by 15 % (CI 3–27%) (p = 0.01). However, administration of ZA did not affect BMD (9%) (CI –4% to 21%) (p = 0.2) or BMC (p = 0.9) (Figure 5). No systemic differences in bone mineral, as measured over the 3rd tail vertebra for time or treatment, were detected.

Histological findings

1 specimen (6 weeks control group) was excluded due to technical problems with decalcification, leaving 19 specimens for histological evaluation. All bone tunnels were located in the metaphysis, no tunnels extended into the ankle joint, no fractures were observed and heat necrosis was not pronounced. A moderate amount of periosteal callus was observed around the tibia at both 3 and 6 weeks. New woven bone formation appeared also in the diaphyseal bone marrow canal and inside

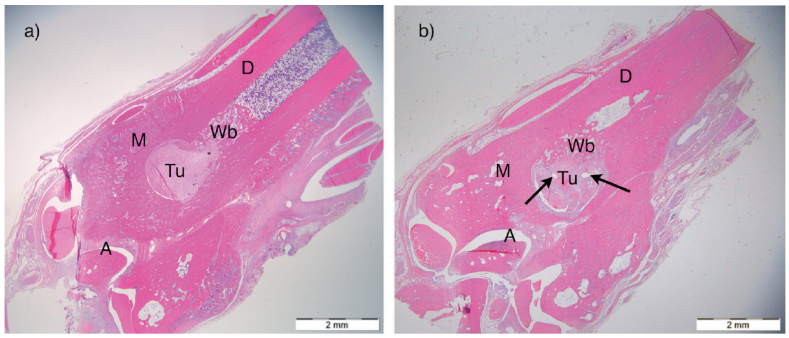

Figure 6. Low-power magnification (x4) light microscopy of H&E stained sections of distal leg showing anatomy and changes over time. The location of the bone tunnel (Tu) containing tendon graft was aimed 3 mm above the ankle joint in the transition between the tibia diaphysis (D) and metaphysis (M). The ankle joint (A) was visible in most sections. (a) 3-weeks ZA group: sharp tunnel edges. Callus/Wb. (b) 6-weeks control-group: Callus/Wb mature. The arrows point at large capillaries inside the tendon graft. Scale bars = 2 mm.

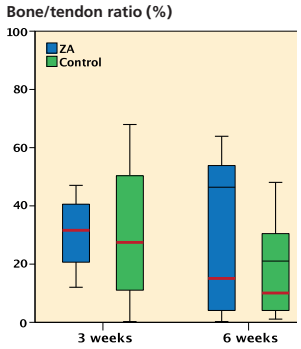

Figure 7. Clustered box-plots showing the bone–tendon ratio in the tunnel as measured by histomorphometry. No statistically significant effect of ZA treatment was observed at 3 weeks (p = 0.9, n = 8) or 6 weeks (p = 0.7, n = 9). Comparison of median values by independent samples Mann–Whitney test.

Total number of TRAP-positive osteoclast counts (median, range) in distal tibia containing the bone tunnel and the calcaneus of the ipsilateral leg. Comparison of median values by independent samples Mann–Whitney test. 1 outlier ([a]) of the 3-week controls was excluded from the above analyses due to a very high number of osteoclasts (> 200) in the calcaneus

	Distal tibia	Calcaneus
3 weeks		
Control [a] (n = 4)	Not measured	2 (1–4)
Zoledronic acid (n = 5)	Not measured	5 (4–15)
p-value		0.1
6 weeks		
Control (n = 4)	6 (5–23)	4 (1–4)
Zoledronic acid (n = 5)	17 (0–45)	6 (0–23)
p-value	1.0	1.0

the tunnel, sometimes replacing the tendon graft. The 6 weeks specimens demonstrated increased vascularity of the tendon graft in addition to more mature new bone formation (Figure 6). The inner surfaces of the bone tunnels were more irregular in the 6 weeks specimens. No evident tunnel widening or peri-tunnel bone loss was seen. Bone resorption lacunae were seen in both groups (see Figure 2). However, the ZA specimens were not histologically distinguishable from the control group in the H&E sections. The bone morphometric evaluation of new bone formation in the bone tunnels demonstrated no statistically significant differences between the groups in bone–tendon ratio at 3 or 6 weeks (Figure 7).

At 6 weeks, we noted both weak and strong TRAP-stained osteoclasts in the sections containing the bone tunnels. However, we could not detect differences between the ZA group and the controls, either regarding the number (Table) or the histologic distribution of osteoclasts. In the sections of 3rd tail vertebra, TRAP-positive osteoclasts were hardly present in any group.

Discussion

Our study demonstrated an unfavorable effect of a single dose of ZA on pullout strength and stiffness of the tendon–bone interface. We were not able to detect any differences in bone remodeling by DEXA, or histology with specific osteoclast staining and bone morphometric evaluation of mineralized tissue inside the bone tunnels, but the sample size of specimens evaluated by histology was small.

The early phase of tendon to bone healing is associated with regional bone loss and decreased mechanical strength, especially if a bone-tunnel technique is used, as described in a canine model of toe flexor injury and repair (Silva et al. 2006). In a subsequent study, the same group was able to prevent the regional bone loss and improve tendon-to-bone repair strength at 3 weeks by administration of the BP alendronate (Thomopoulos et al. 2007). In a study in rats, alendronate was reported to reduce peri-tunnel bone loss as measured by CT (Lui et al. 2013). This prevention of local bone loss correlated with increased mechanical strength, but no differences in stiffness were observed. We used an unrestricted model and preserved the fibrous and callus tissue surrounding the tendon to increase external validity. The suture was removed prior to mechanical testing, to ensure that we assessed the healing and not the fixation and/or healing. We did not confirm the positive BP effects reported in these two studies (Thomopoulos et al. 2007, Lui et al. 2013).

ZA treatment increased the native supraspinatus tendon failure stress and improved bone density at the rotator cuff footprint in ovariectomized rats after 12 weeks (Cadet et al. 2010), but may not be directly comparable to the tendon-to-bone tunnel healing in our study.

We chose the ZA dose, route, and delayed administration based on a study of fracture healing in rats (Amanat et al. 2007). They argued that delayed administration of the anti-catabolic ZA would allow bone formation to establish, and

increase the net difference between anabolism and catabolism by an increased uptake of ZA in the forming callus. Delayed administration of ZA has been used also in clinical bone-healing studies for the same reasons (Harding et al. 2010, 2011). However, the optimal dose and timing of ZA treatment in the presence of a fracture is not firmly established, and for tendon–bone healing it has not been much investigated.

There are some limitations to our model. The distal location for the bone tunnel on the tibia may provide limited healing potential with a reduced availability of marrow-derived mesenchymal stem cells due to the higher fat content of the marrow in the ankle region compared with the knee region. Nevertheless, the model may be relevant also for tendon transfers in foot/ankle surgery.

No clinical studies of BPs on tendon-to-bone healing exist. BMD was found to be one of the independent factors predicting tendon-to-bone healing in rotator cuff surgery (Chung et al. 2011), and local bone loss in the humeral head probably leads to a further decrease in cuff tendon insertion strength (Chen et al. 2015). Thus, the rationale for using bone resorption inhibitors as adjuvant treatment in tendon-to-bone healing remains plausible.

BPs in studies of fracture healing produce a larger callus and improved early mechanical fracture properties (Turker et al. 2016). In the early fracture-healing phase, a larger callus may explain an increased ability to withstand load. In the tendon-to-bone tunnel interface, the anatomical space for callus volume formation is limited. We were not able to observe delayed bone remodeling or prevention of local bone loss in the ZA-treated animals. If osteoclasts were inhibited by ZA a possible effect could be delayed transition from woven bone to lamellar bone, resulting in reduced tendon-to-bone healing.

In summary, our study of early tendon-to-bone tunnel healing in rats demonstrated that a single dose of ZA reduced pull-out strength and stiffness of the tendon–bone interface. Local bone loss was not evident, and no difference in BMD between ZA-treated animals and controls at 3 or 6 weeks was noted. Our study does not provide evidence supporting the use of ZA as adjuvant treatment in tendon-to-bone healing.

The authors would like to thank the Department of Comparative Medicine, Oslo University Hospital, Rikshospitalet for providing excellent animal facilities and enthusiastic personnel at our disposal. Senior Engineer Linda T. Dorg is acknowledged for excellent help with the histological work.

GAH, ES, LN, JEM, FPR, and SD were responsible for the design of the study. GAH performed surgery, DEXA measurements, mechanical testing, histological analyses, independent DEXA analyses, statistical calculations, and wrote the draft manuscript. ES performed surgery, DEXA measurements, and independent DEXA analyses. JEM and SD performed surgery and DEXA measurements. FPR supervised histological analyses. SN performed independent mechanical analyses. All authors approved the final version of the manuscript.

Amanat N, Brown R, Bilston L E, Little D G. A single systemic dose of pamidronate improves bone mineral content and accelerates restoration of strength in a rat model of fracture repair. J Orthop Res 2005; 23(5): 1029-34.

Amanat N, McDonald M, Godfrey C, Bilston L, Little D. Optimal timing of a single dose of zoledronic acid to increase strength in rat fracture repair. J Bone Miner Res 2007; 22(6): 867-76.

Andersson T, Agholme F, Aspenberg P, Tengvall P. Surface immobilized zoledronate improves screw fixation in rat bone: a new method for the coating of metal implants. J Mater Sci Mater Med 2010; 21(11): 3029-37.

Cadet E R, Vorys G C, Rahman R, Park S H, Gardner T R, Lee F Y, Levine W N, Bigliani L U, Ahmad C S. Improving bone density at the rotator cuff footprint increases supraspinatus tendon failure stress in a rat model. J Orthop Res 2010; 28(3): 308-14.

Chen X, Giambini H, Ben-Abraham E, An K N, Nassr A, Zhao C. Effect of bone mineral density on rotator cuff tear: an osteoporotic rabbit model. PLoS One 2015; 10(10): e0139384.

Chung S W, Oh J H, Gong H S, Kim J Y, Kim S H. Factors affecting rotator cuff healing after arthroscopic repair: osteoporosis as one of the independent risk factors. Am J Sports Med 2011; 39(10): 2099-107.

Cole L E, Vargo-Gogola T, Roeder R K. Targeted delivery to bone and mineral deposits using bisphosphonate ligands. Adv Drug Deliv Rev 2016; 99(Pt A): 12-27.

Dimmen S, Nordsletten L, Engebretsen L, Steen H, Madsen J E. The effect of parecoxib and indomethacin on tendon-to-bone healing in a bone tunnel: an experimental study in rats. J Bone Joint Surg Br 2009; 91(2): 259-63.

Ekdahl M, Wang J H, Ronga M, Fu F H. Graft healing in anterior cruciate ligament reconstruction. Knee Surg Sports Traumatol Arthrosc 2008; 16(10): 935-47.

Galatz L M, Rothermich S Y, Zaegel M, Silva M J, Havlioglu N, Thomopoulos S. Delayed repair of tendon to bone injuries leads to decreased biomechanical properties and bone loss. J Orthop Res 2005; 23(6): 1441-7.

Gulotta L V, Rodeo S A. Biology of autograft and allograft healing in anterior cruciate ligament reconstruction. Clin Sports Med 2007; 26(4): 509-24.

Harding A K, W-Dahl A, Geijer M, Toksvig-Larsen S, Tagil M. A single bisphosphonate infusion does not accelerate fracture healing in high tibial osteotomies. Acta Orthop 2011; 82(4): 465-70.

Harding A K, Toksvig-Larsen S, Tagil M, W-Dahl A. A single dose zoledronic acid enhances pin fixation in high tibial osteotomy using the hemicallotasis technique: a double-blind placebo controlled randomized study in 46 patients. Bone 2010; 46(3): 649-54.

Harryman D T, 2nd, Mack L A, Wang K Y, Jackins S E, Richardson M L, Matsen F A, 3rd. Repairs of the rotator cuff: correlation of functional results with integrity of the cuff. J Bone Joint Surg Am 1991; 73(7): 982-9.

Hjorthaug G A, Madsen J E, Nordsletten L, Reinholt F P, Steen H, Dimmen S. Tendon to bone tunnel healing: a study on the time-dependent changes in biomechanics, bone remodeling, and histology in a rat model. J Orthop Res 2015; 33(2): 216-23.

Li C, Mori S, Li J, Kaji Y, Akiyama T, Kawanishi J, Norimatsu H. Long-term effect of incadronate disodium (YM-175) on fracture healing of femoral shaft in growing rats. J Bone Miner Res 2001; 16(3): 429-36.

Lui P P, Cheng Y Y, Yung S H, Hung A S, Chan K M. A randomized controlled trial comparing bone mineral density changes of three different ACL reconstruction techniques. The Knee 2012; 19(6): 779-85.

Lui P P, Lee Y W, Mok T Y, Cheuk Y C, Chan K M. Alendronate reduced peri-tunnel bone loss and enhanced tendon graft to bone tunnel healing in anterior cruciate ligament reconstruction. Eur Cell Mater 2013; 25: 78-96.

Rodeo S A, Kawamura S, Ma C B, Deng X H, Sussman P S, Hays P, Ying L. The effect of osteoclastic activity on tendon-to-bone healing: an experimental study in rabbits. J Bone Joint Surg Am 2007; 89(10): 2250-9.

Russell R G, Watts N B, Ebetino F H, Rogers M J. Mechanisms of action of bisphosphonates: similarities and differences and their potential influence on clinical efficacy. Osteoporos Int 2008; 19(6): 733-59.

Silva M J, Boyer M I, Ditsios K, Burns M E, Harwood F L, Amiel D, Gelberman R H. The insertion site of the canine flexor digitorum profundus tendon heals slowly following injury and suture repair. J Orthop Res 2002; 20(3): 447-53.

Silva MJ, Thomopoulos S, Kusano N, Zaegel MA, Harwood FL, Matsuzaki H, Havlioglu N, Dovan TT, Amiel D, Gelberman RH. Early healing of flexor tendon insertion site injuries: tunnel repair is mechanically and histologically inferior to surface repair in a canine model. J Orthop Res 2006; 24(5): 990-1000.

Solberg L B, Stang E, Brorson SH, Andersson G, Reinholt F P. Tartrate-resistant acid phosphatase (TRAP) co-localizes with receptor activator of NF-KB ligand (RANKL) and osteoprotegerin (OPG) in lysosomal-associated membrane protein 1 (LAMP1)-positive vesicles in rat osteoblasts and osteocytes. Histochem Cell Biol 2015; 143(2): 195-207.

Thomopoulos S, Matsuzaki H, Zaegel M, Gelberman R H, Silva M J. Alendronate prevents bone loss and improves tendon-to-bone repair strength in a canine model. J Orthop Res 2007; 25(4): 473-9.

Turker M, Aslan A, Cirpar M, Kochai A, Tulmac O B, Balci M. Histological and biomechanical effects of zoledronate on fracture healing in an osteoporotic rat tibia model. Eklem Hastalik Cerrahisi 2016; 27(1): 9-15.

III

BJR

BONE BIOLOGY

Short-term perioperative parecoxib is not detrimental to shaft fracture healing in a rat model

G. A. Hjorthaug, E. Søreide, L. Nordsletten, J. E. Madsen, F. P. Reinholt, S. Niratisairak, S. Dimmen

Oslo University Hospital, Oslo, Norway

Objectives

Experimental studies indicate that non-steroidal anti-inflammatory drugs (NSAIDs) may have negative effects on fracture healing. This study aimed to assess the effect of immediate and delayed short-term administration of clinically relevant parecoxib doses and timing on fracture healing using an established animal fracture model.

Methods

A standardized closed tibia shaft fracture was induced and stabilized by reamed intramedullary nailing in 66 Wistar rats. A 'parecoxib immediate' (Pi) group received parecoxib (3.2 mg/kg bodyweight twice per day) on days 0, 1, and 2. A 'parecoxib delayed' (Pd) group received the same dose of parecoxib on days 3, 4, and 5. A control group received saline only. Fracture healing was evaluated by biomechanical tests, histomorphometry, and dual-energy x-ray absorptiometry (DXA) at four weeks.

Results

For ultimate bending moment, the median ratio between fractured and non-fractured tibia was 0.61 (interquartile range (IQR) 0.45 to 0.82) in the Pi group, 0.44 (IQR 0.42 to 0.52) in the Pd group, and 0.50 (IQR 0.41 to 0.75) in the control group ($n = 44$; $p = 0.068$). There were no differences between the groups for stiffness, energy, deflection, callus diameter, DXA measurements ($n = 64$), histomorphometrically osteoid/bone ratio, or callus area ($n = 20$).

Conclusion

This study demonstrates no negative effect of immediate or delayed short-term administration of parecoxib on diaphyseal fracture healing in rats.

Cite this article: *Bone Joint Res* 2019;8:472–480.

Keywords: Fracture healing, Cyclooxygenase inhibitors, Biomechanical, Histology, Rats

Article focus

- Cyclooxygenase (COX) inhibitors are used against pain following fractures and surgery, but several animal studies suggest a negative effect on bone healing.
- A previous study from our group utilizing the same model showed that parecoxib for seven days (medium term) impaired fracture healing.
- Is short-term perioperative administration of parecoxib unfavourable for fracture healing?

Key messages

- Three days of immediate or delayed parecoxib administration did not compromise diaphyseal fracture healing in rats.
- The effect of parecoxib on fracture healing seems to be time-dependent.

Strengths and limitations

- We used a standardized fracture model and clinically relevant dose and duration of parecoxib.
- Results from animal studies may not be directly translatable to humans.

Introduction

Sufficient pain control following fracture surgery is important in order to facilitate early mobilization, limit the risk of postoperative complications, and promote fracture healing. In trauma patients with fractures, non-steroidal anti-inflammatory drugs (NSAIDs)

Correspondence should be sent to G. A. Hjorthaug; email: geir.hjorthaug@me.com

doi: 10.1302/2046-3758.810.BJR-2018-0341.R1

Bone Joint Res 2019;8:472–480.

are commonly used due to their analgesic, anti-inflammatory, and antipyretic effects. NSAIDs inhibit cyclooxygenase (COX), a key enzyme essential for upregulating cell signalling prostaglandins, which is crucial for musculoskeletal tissue healing. However, there are concerns about the negative impact of COX inhibitors on bone metabolism.[1-4] Previous experimental studies indicate that both selective and non-selective COX-2 inhibitors can have a negative effect on fracture healing.[5-8] The effects of COX-2 inhibitors on bone metabolism and fracture healing are yet to be fully understood, although COX-2 has been shown to be essential for both induction of osteoblastogenesis[9] and for fracture healing.[10]

Due to the putative adverse effect of COX inhibitors on fracture healing, there are safety concerns attached to the use of COX inhibitors in pain management following fracture surgery. To our knowledge, studies assessing time- and dose-dependent effects of COX inhibitors on musculoskeletal healing are sparse. Parecoxib, a potent, effective analgesic, anti-inflammatory, and opioid-sparing drug without platelet inhibition, is used clinically for pain management in orthopaedic surgery.[11] Previously, we have found that seven days of treatment with parecoxib delayed fracture healing in a rat model.[8] The aim of the current study was to investigate the effect of immediate and delayed short-term treatment (three days) with clinically relevant parecoxib doses on fracture healing in an established closed tibia shaft fracture model in rats.

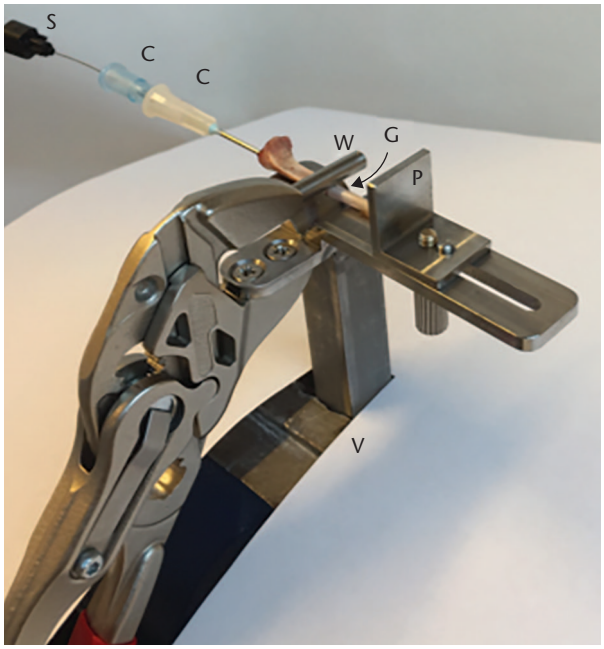

Fig. 1

Three-point loading fracture forceps secured in a vice (V). Photo from the pilot study using bone without soft tissue, showing the components of the nail: the stylus (S); and the two cannulas (C). *In vivo*, the heel was pressed against an adjustable plate (P) in order to obtain a standardized midshaft fracture as the wedge (W) pressed the leg into the groove (G) when the forceps was clamped.

Materials and Methods

Replacement, refinement, and reduction were all taken into serious consideration when planning the study. Humane endpoints were defined in order to ensure animal welfare throughout the study.

Animals. Wistar rats (n = 66) (Taconic Europe, Lille Skensved, Denmark), skeletally mature with a mean weight of 288 g (265 to 330), were included in the study. Due to an increased metabolism of COX inhibitors in male compared with female rats,[12,13] our previous studies utilizing the same model were conducted in female rats only.[7,8] Female rats were chosen for the current study to ensure internal quality control.

The animals were kept in pairs, each pair in a wire-topped plastic cage in an accredited animal facility in a controlled environment (mean temperature 21°C (SD 1°C), humidity 55% (SD 10%), ventilation air volume exchanged 20 times per hour, alternating 12-hour light and dark cycles). They were allowed free access to water and standard laboratory rodent nutrition (MR3, SD'S, Essex, United Kingdom, with 1.24% total calcium, 0.83% phosphorus, and 2948 IU/kg vitamin D3). Following ten days of acclimatization, all animals underwent the surgical procedure with general anaesthesia induced and maintained by Hypnorm (fluanisone 5 mg/ml and fentanyl citrate 0.1575 mg/ml; Jansen Pharmaceutica BV, Beerse, Belgium) and Dormicum (midazolam 2.5 mg/ml; Hoffmann La Roche, Basel, Switzerland) diluted in an equal amount of sterile water. The dose of this working solution was 0.2 ml/100 g body weight administered subcutaneously for anaesthesia. Antibiotics were not used. Inhalation anaesthesia (1% to 2.5% isoflurane; Isocare vet, Animalcare, York, United Kingdom) was used for the dual-energy x-ray absorptiometry (DXA) at two weeks. To ensure sufficient postoperative pain control, a subcutaneous dose of 0.05 mg/kg Buprenorphine (0.3 mg/ml) (Temgesic; Schering–Plough, Kenilworth, New Jersey) was administered postoperatively in all animals, and then every 12 hours for the first two days. Animal behaviour, appearance, movement, body weight, and wound status were registered throughout the study period in a predefined form with scores, defining thresholds for extra administration of buprenorphine and humane endpoints.

Surgical procedure. A 3 mm skin incision was made laterally on the right thigh 15 mm proximal to the knee to prevent conflict between the nail and wound. The skin was retracted distally to expose the patellar tendon. The nail consisted of two cannulas (23G 0.6 × 60 mm Sterican; Braun GmbH, Kronberg, Germany; 19G 1.1 × 40 mm Microlance 3; BD, Madrid, Spain), in addition to a spinal needle stylet (22G 0.7 × 90 mm Yale Spinal; BD). This was introduced to the medullary canal of the tibia medial to the patellar tendon. The canal was reamed using the

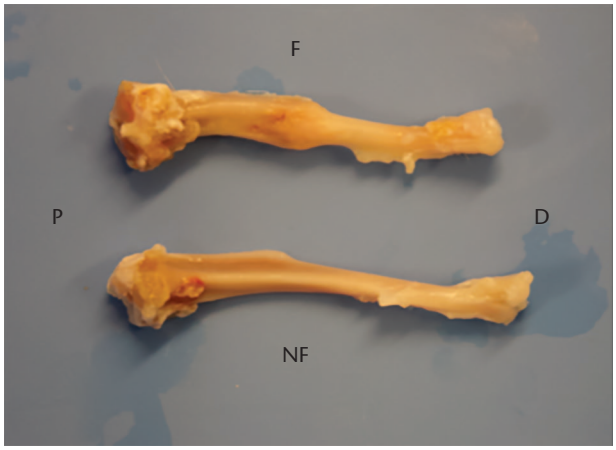

Fig. 2a

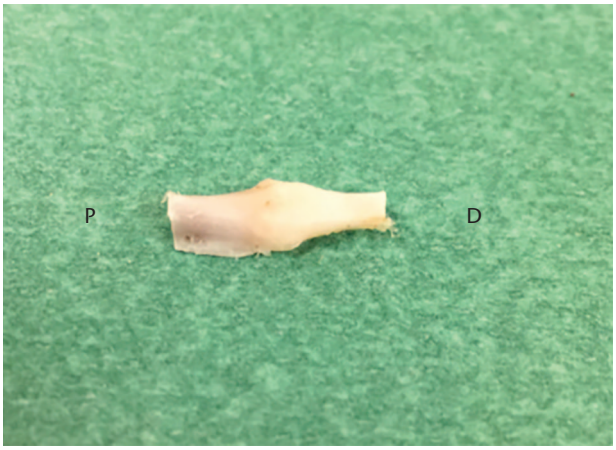

Fig. 2b

Lateral-view photographs of tibia *ex vivo* at four weeks of healing. Orientation is proximal (P) to distal (D). a) Fractured (F) and non-fractured (NF) tibia from a specimen ('parecoxib immediate' (Pi) group) prepared for biomechanical tests. b) Segment of middle tibia containing callus in a specimen (control group) fixed for histological analysis.

cannulas as they were advanced toward the distal tibia. The two cannulas were withdrawn to the proximal tibia after sufficient reaming of the canal. A standardized closed midshaft tibia fracture was created with the stylet remaining inside the full length of the medullary canal as a guidewire. This enabled technically easy fracture reduction as the two cannulas were reintroduced over the fracture site. Finally, the nail was cut flush with the tibial plateau before the skin was closed with absorbable sutures. Unrestricted weight-bearing was allowed for all rats.

The custom-made three-point fracture-inducing forceps were a modified version of previously described forceps.[14] The modified forceps' ability to induce a closed standardized midshaft tibial fracture, with minimal soft-tissue damage, was assessed in a pilot study on cadaveric rat tibiae with and without soft tissue prior to this experiment (Fig. 1).

Study groups. Single animals were allocated by computerized randomization into two parecoxib intervention groups or a control group (i.e. 22 animals in each group). The study staff was blinded to the group and outcome allocation.

All animals received injections (parecoxib or saline, volume 0.04 ml intramuscular) twice a day for six days perioperatively; a total of 12 injections. The daily dose of parecoxib (Dynastat; Pfizer, Puurs, Belgium) was estimated to be 6.4 mg/kg body weight, using allometric scaling based on the basic calorific demand, which is increased by a factor of four in rats compared with humans.[15-17] The 'parecoxib immediate' (Pi) group received the first dose of parecoxib 30 minutes preoperatively, then on days 0 to 2 postoperatively, and then saline injections on days 3 to 5. The 'parecoxib delayed' (Pd) group received saline injections on days 0 to 2, then parecoxib injections on days 3 to 5. The control (C) group received saline injections on days 0 to 5, and no COX inhibitors. All animals were killed at four weeks.

Biomechanical testing. Animals that were allocated to biomechanical tests were killed by a pentobarbital overdose (Pentobarbital-Natrium vet, 100 mg/ml; Norsk Medicinaldepot, Oslo, Norway) under general anaesthesia. The harvested tissue was preserved in Ringer Acetat (Fresenius Kabi, Oslo, Norway) at –20°C until testing. Following thawing, both tibiae were dissected free of soft tissue, and the fibulas were removed. The anteroposterior (AP) and mediolateral (ML) diameters of callus formation in the right tibiae were measured using a sliding caliper with an accuracy of ± 0.01 mm. The nail was carefully removed and fracture union was evaluated macroscopically (Fig. 2a). The tibiae were loaded in a three-point ventral cantilever bending test to failure,[8,18] using a hydraulic material testing machine (Model 858 Mini Bionix with MTS FlexTest digital controller; MTS Systems Corporation, Eden Prairie, Minnesota). A preload of 0.5 N was applied prior to the start of the test to remove any lag from the setup. With a 250 N load cell, speed set to 2.67 mm per second, yielding a tibia bending rate of 7.2° per second, with the fulcrum placed over the fracture callus, data were collected at 20 Hz. The non-fractured left tibia was fractured at the same level in the same manner. This allowed for the collection of data on force, time, and deflection, which were exported to Origin (Origin v. 8.6 for Windows; OriginLab Corporation, Northampton, Massachusetts) for final analysis of ultimate bending moment, stiffness, energy absorption, and deflection.

Histological evaluation. Tissues of animals allocated to histological evaluation were fixed *in vivo* by vascular perfusion of 0.1 M phosphate-buffered 2% paraformaldehyde during deep anaesthesia. Following removal of the nail, fibula, and soft tissues, a 15 mm tibial shaft segment containing the fracture with callus was harvested using an oscillating saw (Fig. 2b). These segments were fixed overnight in the same fixative as mentioned above, dehydrated in series of ethanol, incubated, and embedded in

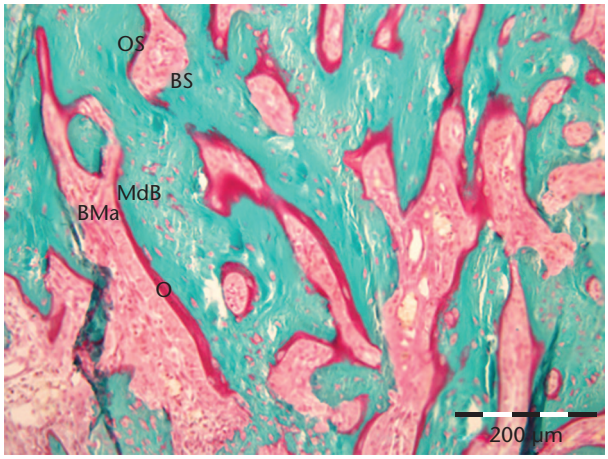

Fig. 3a

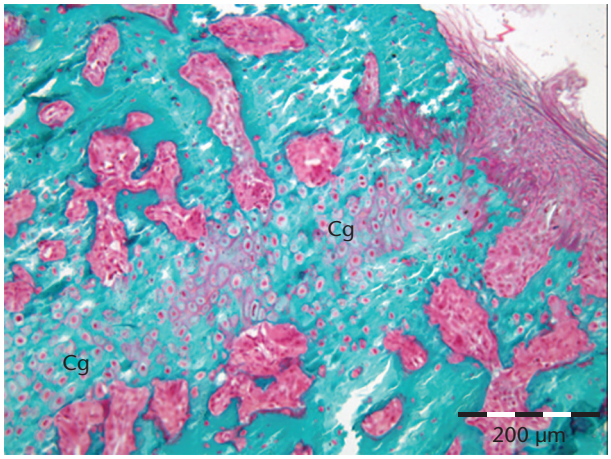

Fig. 3b

High-power magnification light microscopy of tibial fracture calluses. Masson–Goldner trichrome staining of mineralized tissue provides good differentiation between osteoid (O, purple) and mineralized bone matrix (MdB, green). Non-mineralized bone marrow (BMa, red) is distributed between the mineralized bone trabeculae. a) Woven bone formation (control group) with mainly osteoid trabecular surfaces (OS) and a few bone surfaces (BS). b) An immature region within the callus-containing cartilage (Cg) and partly mineralized matrix with ongoing endochondral ossification. Scale bars = 200 µm.

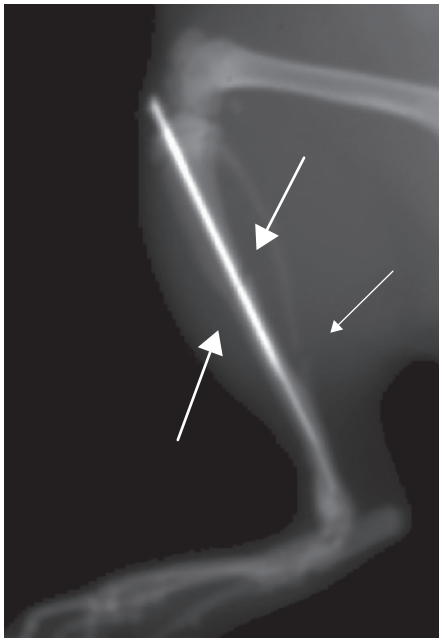

Fig. 4

Representative lateral radiograph at baseline showing a short oblique tibial fracture (large arrows) fixed with an intramedullary nail and concomitant fibular fracture (small arrow). Specimen from the control group.

plastic (K-plast; DiaTec Systems for Laboratory, Hallstadt, Germany), following a standard protocol. The undecalcified specimens were cut from anterior to posterior (thickness 5 µm). The central section containing the thickest callus was chosen as the region of interest (ROI).

Histomorphometry. Masson–Goldner's trichrome-stained sections were evaluated by light microscopy. Digital images were analyzed using AnalySIS V (Olympus Soft Imaging Solutions, Münster, Germany). The ROI was defined at 1.25 × magnification by outlining the perimeter of the callus, including any cortical fracture surface, but excluding original cortical or trabecular bone, periosteum, and bone marrow. This ROI was defined as total callus area. A virtual grid of lines (random angles, space 100 µm) was superimposed onto sections at 10 × magnification. Presence of osteoid surfaces or mineralized bone surfaces was noted. The osteoid surface per bone surface (OS/BS; %) were calculated as an indirect measure of bone formation (Fig. 3a). Presence of cartilage within the callus ROI was registered in each specimen (Fig. 3b). The nomenclature used is in accordance with the recommendations of the American Society for Bone and Mineral Research (ASBMR).[19]

Bone mineral measurement and radiological evaluation. Bone mineral density (BMD) and bone mineral content (BMC) were measured over the fracture site in all animals *in vivo* using DXA (Lunar PIXImus with software v. 2.10; Lunar, Madison, Wisconsin) immediately after surgery, and again at two and four weeks. The ROI (14 × 14 pixels) was aligned over the fracture and included the anterior cortical bone, the callus, and the nail. The BMD and BMC values were corrected for an independently measured value for the nail before final analysis. Radiographs were reviewed for fracture pattern and potential complications (Fig. 4).

Statistical analysis. An *a priori* power calculation for the sample size was not performed, but the number of animals was estimated based on previous studies.[7,8] The main outcome was the ultimate bending moment ratio between fractured and non-fractured tibia. Other outcomes were ratios of bending stiffness, energy absorption, deflection, callus AP and ML diameter, and time-dependent difference in BMD and BMC. Two independent observers (GAH and SN for biomechanical variables; GAH and ES for DXA variables) analyzed these outcomes, and the mean values were calculated and used for the statistical analyses. Normality of the distribution was evaluated using

Table I. Biomechanical results showing ratios between fractured and non-fractured tibia and callus diameters at four weeks

Group	Parecoxib immediate (n = 15)	Parecoxib delayed (n = 15)	Control (n =14)	p-value*
Median moment, ratio (IQR)	0.61 (0.45 to 0.82)	0.44 (0.42 to 0.52)	0.50 (0.41 to 0.75)	0.068
Median stiffness, ratio (IQR)	1.07 (0.85 to 1.46)	1.01 (0.89 to 1.13)	1.22 (0.75 to 1.37)	0.691
Median energy, ratio (IQR)	0.39 (0.21 to 0.5)	0.22 (0.17 to 0.3)	0.26 (0.19 to 0.39)	0.127
Median deflection, ratio (IQR)	0.69 (0.54 to 0.84)	0.55 (0.46 to 0.61)	0.54 (0.45 to 0.78)	0.083
Median AP diameter, mm (IQR)	4.5 (3.9 to 5.1)	5.1 (4.2 to 5.9)	4.4 (3.7 to 4.9)	0.082
Median ML diameter, mm (IQR)	3.1 (2.8 to 3.8)	3.5 (2.9 to 3.8)	3.2 (2.9 to 3.5)	0.590

*Kruskal–Wallis test
IQR, interquartile range; AP, anteroposterior; ML, mediolateral

Table II. Difference in bone mineral density (BMD) and bone mineral content (BMC) from baseline

Group	Parecoxib immediate (n = 22)	Parecoxib delayed (n = 22)	Control (n = 20)	p-value*
Mean BMD: 2 wks, mg/cm^2 (range)	101 (-32 to 282)	58 (-161 to 224)	75 (-56 to 182)	0.171
Mean BMC: 2 wks, mg (range)	7 (1 to 16)	4 (-9 to 17)	6 (1 to 13)	0.153
Mean BMD: 4 wks, mg/cm^2 (range)	152 (15 to 281)	106 (-69 to 341)	103 (-11 to 210)	0.106
Mean BMC: 4 wks, mg (range)	10 (1 to 20)	8 (-7 to 22)	7 (1 to 15)	0.257

*One-way analysis of variance (ANOVA) test

histograms with normality curves. Homogeneity of variance for the main outcome was proven by Levene's test ($p = 0.073$). Biomechanical and histomorphometrical data are presented as medians and interquartile ranges (IQRs), and groups are compared using the Kruskal–Wallis test. A non-parametric test was used due to limited sample size. The BMD and BMC differences are presented as mean and range, and the groups compared with one-way analysis of variance (ANOVA). The alpha level was set to 0.05. Statistical analyses were performed using IBM SPSS Statistics for Macintosh v. 24.0 (IBM, Armonk, New York).

Results

Animal inclusion. The body weight of all animals was measured every week throughout the study period. At four weeks, the mean increase in body weight from baseline was 13.4 g (-15 to 25), with no difference between the study groups ($p = 0.510$, one-way ANOVA). A closed midshaft fracture was successfully created in all animals (n = 66), and correct placement of the nail to stabilize the fracture was confirmed in radiographs postoperatively. Four animals had minor wound problems that were resolved without any further issues. No animals were excluded due to infection or penetration of the skin by the nail. Two animals (control group) died during anaesthesia, leaving a total of 64 animals available for final analyses. Next, 44 animals (14 or 15 from each of the three study groups) were assessed biomechanically. The remaining 20 animals (six or seven from each study group) were assessed histologically.

Biomechanical assessment. No nonunion was observed. A few degrees of external rotation were observed in most of the fractures. Overall, the median maximum bending moment of fractured tibiae was 18.9 Nm $\times 10^{-2}$ (IQR 14.9 to 22.4) compared with 35.1 Nm $\times 10^{-2}$ (IQR 30 to 38.9) in non-fractured tibiae. Ratios of fractured and non-fractured tibia in ultimate bending moment, stiffness, energy, and deflection showed no differences between the study groups (Table I). The macroscopically measured callus diameters were also equal between the groups.

Bone mineral measurements and radiology. Overall, mean BMD at baseline was 160 mg/cm^2 (3 to 267), 240 mg/cm^2 (67 to 357) at two weeks, and 280 mg/cm^2 (146 to 474) at four weeks. There were no differences between the groups in BMD or BMC from baseline to two or four weeks (Table II). The baseline radiographs showed that all fractures were simple transverse or short oblique fractures. Wedge fragments were observed in only 2/64 fractures (3%), and no comminuted fractures were observed. The fibula was fractured 2 mm to 5 mm proximal to the rat anatomical tibiofibular synostosis in 44/64 specimens (69%). Radiographs obtained at four weeks demonstrated fracture healing by callus formation in all animals. Nail migration was not observed in any of the specimens.

Histological findings. Light microscopy confirmed the radiological evaluation of fracture patterns. All fractures were healed, as defined by a mineralized callus with woven bone formation bridging the cortical fracture gap at two sides (Fig. 5). Two fractures (Pi and Pd groups) had a bridging callus on the compression side and fibrous tissue in the fracture gap of the tension side. A bridging callus was observed on both sides in the coronal sections in 18/20 fractures (90%). Hyaline cartilage with vascular invasion suggested that early endochondral ossification was still taking place (Fig. 3b). It was observed in the calluses of nine fractures and evenly distributed among the groups (Table III). The remaining 11 had more mature calluses, consisting mainly of woven bone with both non-mineralized (osteoid) and mineralized bone matrix (Fig. 6). The OS/BS (%), as measured by

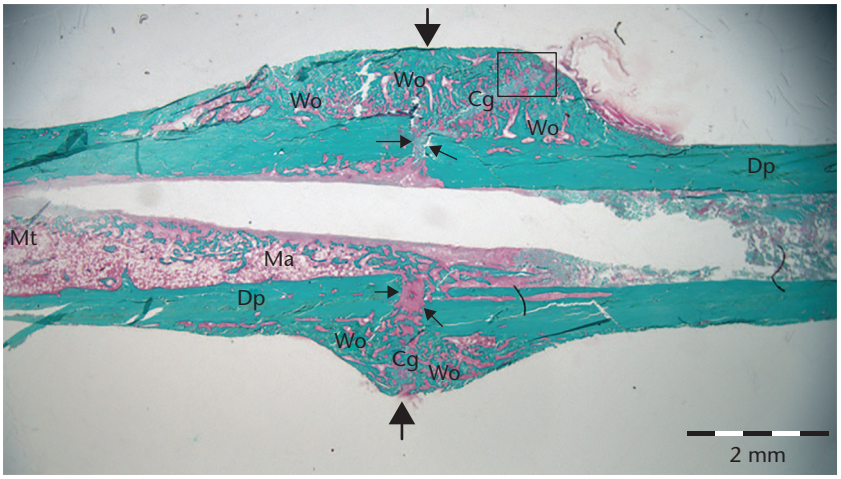

Fig. 5

Low-power magnification light microscopy of Masson–Goldner trichrome-stained coronal section of diaphyseal (Dp) tibial fracture (between large arrows) at four weeks ('parecoxib immediate' (Pi) group), showing bridging callus formation on both sides. Callus consists of woven bone (Wo) and immature cartilage (Cg). The metaphyseal (Mt) region in the section is localized proximally. Small arrows indicate the original cortical fracture gap. The medullary canal contains displaced bone marrow (Ma). The clear space represents the area of the extracted nail. The rectangle shows the area displayed at high magnification in Figure 3b. Scale bar = 2 mm.

Table III. Histomorphometric measurements of osteoid surfaces per bone surface (OS/BS; %), total callus area, and presence of immature cartilaginous zones

Group	Parecoxib immediate (n = 7)	Parecoxib delayed (n = 7)	Control (n = 6)	p-value*
Median OS/BS, % (IQR)	*38* (30 to 47)	*48* (39 to 53)	*49* (44 to 52)	0.092
Median callus area, mm^2 (IQR)	13.5 (11.7 to 18.7)	11.3 (8.3 to 14.5)	11.6 (7.5 to 19.8)	0.282
Cartilaginous zones, n	3	4	2	0.697

*Kruskal–Wallis test
IQR, interquartile range

histomorphometry, was equally distributed between the groups, and no difference in total callus area was noted (Table III).

Discussion

This study shows that immediate or delayed short-term treatment with parecoxib did not compromise closed tibia shaft fracture healing at four weeks. The parecoxib dose used in rat studies varies. We used a relatively high daily dose of 6.4 mg/kg body weight, as suggested by Virchenko et al,[20] to prevent the risk of type II experimental error. In previous studies, utilizing the same model, we found that seven days of parecoxib treatment delayed early fracture healing. Even with a daily parecoxib dose as low as 1 mg/kg body weight, bending moment, stiffness, and BMD were significantly reduced at three weeks.[7,8] In the current study, immediate or delayed three-day treatment with parecoxib did not negatively affect the biomechanical properties, callus maturation, or bone formation at four weeks, despite using a 2.7-fold larger dosage in this study than in our previous studies. In light of the previous findings of a negative impact with the seven-day parecoxib treatment, the fact that the current study showed no effect at three days of treatment may provide useful additional information. Thus, our collective findings could be indicative of a time-dependent effect of parecoxib on fracture healing. The COX-2 messenger RNA (mRNA) level remained elevated for two weeks after femoral fracture in a rat study by Gerstenfeld et al.[21] In a mouse study, the COX-2 mRNA level peaked four days following a muscle injury, but the maximum COX-2 protein concentration was observed as early as day 1.[22] Delayed short-term perioperative administration of COX inhibitors may be a plausible strategy to avoid interference with fracture healing, but a three-day delay of a three-day treatment period did not compromise fracture healing in our study. However, due to interspecies differences in fracture healing and drug metabolism, the translational potential is uncertain and should be taken into consideration when interpreting our findings.

The tibial shaft fracture model in rats is well established and has recently been further developed by our group. As opposed to osteotomy models, the closed fracture model may have an advantage in validity. Moreover, the model allowed reaming of the medullary canal, similar fracture patterns, reliable reduction, and fixation of the fracture. Refinements, compared with our previous fracture studies, included blinding of the study staff, randomized allocation of animals to limit any bias, and two independent observers analyzing biomechanical and

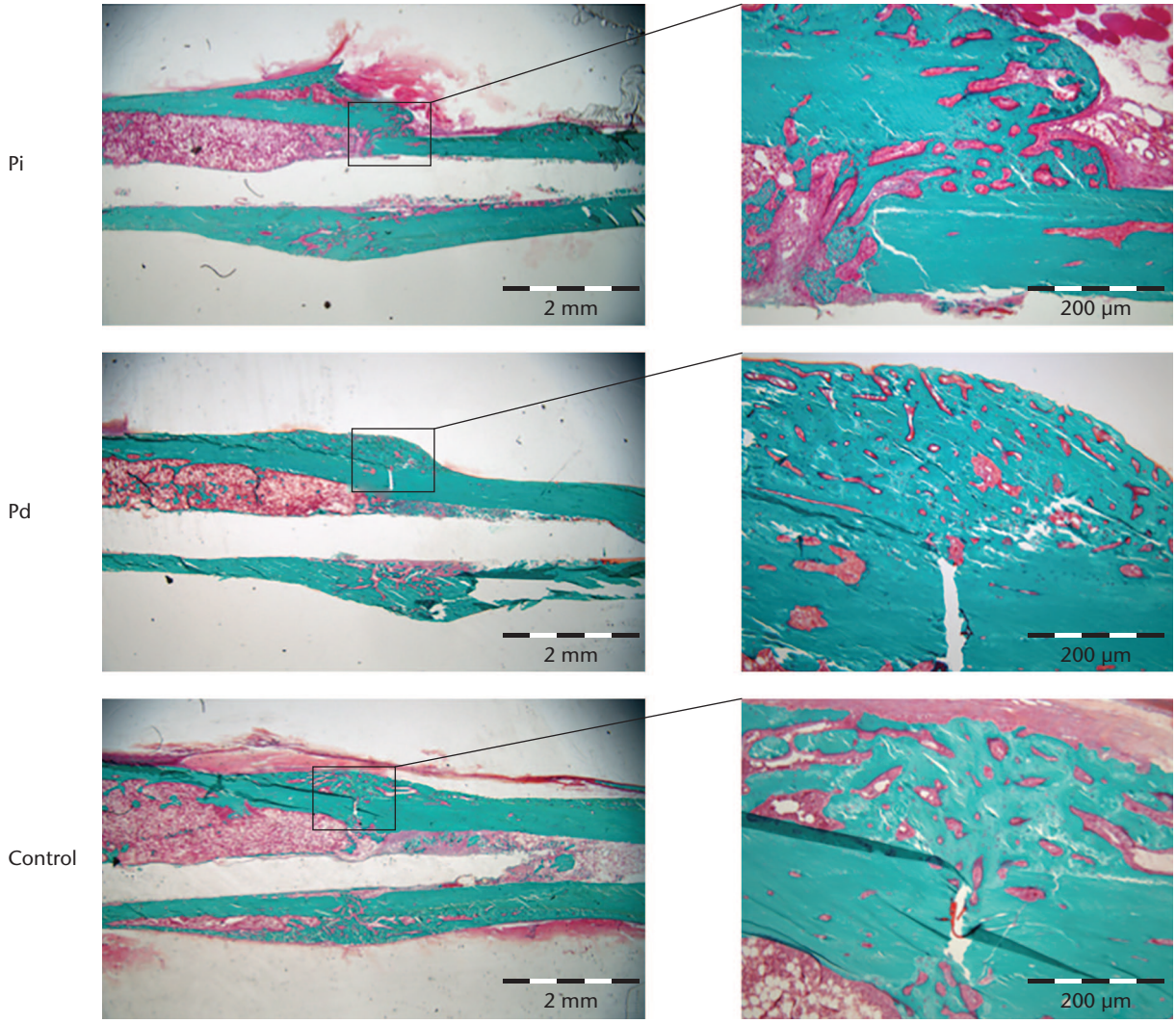

Fig. 6

Low-power (left panels) and high-power (right panels) magnification light microscopy of representative Masson–Goldner trichrome-stained sections of tibial fractures from the three study groups. Qualitatively, no differences between the study groups were observed. Scale bars = 2 mm (left panels) and 200 µm (right panels).

bone mineral data. We also included fracture evaluation by histology.

Limitations of the three-point cantilever bending test and the BMD measurement that included the nail have been discussed in detail previously.[8] In addition, the method of fracture induction with a concomitant fibular fracture and fracture fixation without blocking of rotation could explain the observed tendency of fracture healing in external rotation in most specimens. However, all fractures healed without any further complications, and a normal pattern of secondary bone healing was observed by histology. Therefore, we believe the nail provided sufficient stability to evaluate the aim of this study. However, the results may not be directly translated to a clinical setting, where the instability from the concomitant fibular fracture is compensated for by interlocking of the tibial nail.

Delayed shaft fracture union is reported in several animal studies with COX-2 inhibitors, including rofecoxib,[23] celecoxib,[5] and parecoxib.[24] COX-2 inhibition may adversely affect healing, particularly in the early phase following the fracture.[6,25] However, if the duration of treatment is short, the negative biological effect seems to be reversible,[24] which could explain the findings in the present study.

The negative effect of COX inhibition on fracture healing seems well documented in experimental studies.[26] However, these negative effects have been hard to reproduce in clinical trials, as they depend on dose, drug metabolism, timing and duration of treatment, soft-tissue damage, and fracture pattern. Indomethacin (non-selective COX inhibitor) greatly impaired healing of diaphyseal fractures, but had only minimal effect on metaphyseal fractures in mice.[27] Animal studies often

utilize cortical fracture models while patients more often have corticocancellous fractures. Differences in fracture location and stability may therefore explain some of the discrepancies between experimental studies and clinical experience. In addition, other regulatory pathways, including transforming growth factor beta and Wnt, and epigenetic regulators are involved in bone metabolism and fracture healing, which further complicates the overall understanding.[28,29] Also, a variety of patient-related confounding factors are likely to influence bone healing.

The number of clinical studies of COX inhibitors in humans is limited. Long-term (six weeks) treatment with indomethacin to prevent heterotopic ossification in trauma patients with acetabular fractures revealed an increased risk for development of nonunion in concomitant long bone fractures.[30] Giannoudis et al[31] also reported an association between COX inhibitors and increased risk of nonunion in femoral fractures in a retrospective study. The correlation between COX inhibitors and nonunion was especially strong when COX inhibitors were used for longer than four weeks. In addition, medium-term use (one week) of COX inhibitors was associated with a prolonged time to union in this study. A systematic review concluded that short-duration COX inhibitor administration is safe concerning bone healing,[32] while another stated that COX-2 inhibitors should be considered a potential risk factor for fracture healing, and should therefore be avoided in patients at risk of delayed fracture healing.[33] The current understanding of the overall effect of COX inhibitors on bone healing remains limited[34] and lacks the clinical evidence to support strong recommendations.[35]

In conclusion, this study demonstrated no negative effect of immediate or delayed three-day treatment with parecoxib on diaphyseal fracture healing in rats.

References

1. **Aspenberg P.** Don't administer NSAID after bone surgery! *Lakartidningen* 2002;99:2554. (Article in Swedish)
2. **Aspenberg P.** Drugs and fracture repair. *Acta Orthop* 2005;76:741-748.
3. **Su B, O'Connor JP.** NSAID therapy effects on healing of bone, tendon, and the enthesis. *J Appl Physiol (1985)* 2013;115:892-899.
4. **Barry S.** Non-steroidal anti-inflammatory drugs inhibit bone healing: a review. *Vet Comp Orthop Traumatol* 2010;23:385-392.
5. **Bergenstock M, Min W, Simon AM, Sabatino C, O'Connor JP.** A comparison between the effects of acetaminophen and celecoxib on bone fracture healing in rats. *J Orthop Trauma* 2005;19:717-723.
6. **Simon AM, O'Connor JP.** Dose and time-dependent effects of cyclooxygenase-2 inhibition on fracture-healing. *J Bone Joint Surg [Am]* 2007;89-A:500-511.
7. **Dimmen S, Nordsletten L, Engebretsen L, Steen H, Madsen JE.** Negative effect of parecoxib on bone mineral during fracture healing in rats. *Acta Orthop* 2008;79:438-444.
8. **Dimmen S, Nordsletten L, Madsen JE.** Parecoxib and indomethacin delay early fracture healing: a study in rats. *Clin Orthop Relat Res* 2009;467:1992-1999.
9. **Zhang X, Schwarz EM, Young DA, et al.** Cyclooxygenase-2 regulates mesenchymal cell differentiation into the osteoblast lineage and is critically involved in bone repair. *J Clin Invest* 2002;109:1405-1415.
10. **Simon AM, Manigrasso MB, O'Connor JP.** Cyclo-oxygenase 2 function is essential for bone fracture healing. *J Bone Miner Res* 2002;17:963-976.
11. **Diaz-Borjon E, Torres-Gomez A, Essex MN, et al.** Parecoxib provides analgesic and opioid-sparing effects following major orthopedic surgery: a subset analysis of a randomized, placebo-controlled clinical trial. *Pain Ther* 2017;6:61-72.
12. **Halpin RA, Geer LA, Zhang KE, et al.** The absorption, distribution, metabolism and excretion of rofecoxib, a potent and selective cyclooxygenase-2 inhibitor, in rats and dogs. *Drug Metab Dispos* 2000;28:1244-1254.
13. **Paulson SK, Zhang JY, Breau AP, et al.** Pharmacokinetics, tissue distribution, metabolism, and excretion of celecoxib in rats. *Drug Metab Dispos* 2000;28:514-521.
14. **Ekeland A, Engesaeter LB, Langeland N.** Mechanical properties of fractured and intact rat femora evaluated by bending, torsional and tensile tests. *Acta Orthop Scand* 1981;52:605-613.
15. **West GB, Brown JH, Enquist BJ.** A general model for the origin of allometric scaling laws in biology. *Science* 1997;276:122-126.
16. **Schneider K, Oltmanns J, Hassauer M.** Allometric principles for interspecies extrapolation in toxicological risk assessment—empirical investigations. *Regul Toxicol Pharmacol* 2004;39:334-347.
17. **Huang Q, Riviere JE.** The application of allometric scaling principles to predict pharmacokinetic parameters across species. *Expert Opin Drug Metab Toxicol* 2014;10:1241-1253.
18. **Engesaeter LB, Ekeland A, Langeland N.** Methods for testing the mechanical properties of the rat femur. *Acta Orthop Scand* 1978;49:512-518.
19. **Dempster DW, Compston JE, Drezner MK, et al.** Standardized nomenclature, symbols, and units for bone histomorphometry: a 2012 update of the report of the ASBMR Histomorphometry Nomenclature Committee. *J Bone Miner Res* 2013;28:2-17.
20. **Virchenko O, Skoglund B, Aspenberg P.** Parecoxib impairs early tendon repair but improves later remodeling. *Am J Sports Med* 2004;32:1743-1747.
21. **Gerstenfeld LC, Thiede M, Seibert K, et al.** Differential inhibition of fracture healing by non-selective and cyclooxygenase-2 selective non-steroidal anti-inflammatory drugs. *J Orthop Res* 2003;21:670-675.
22. **Bondesen BA, Mills ST, Kegley KM, Pavlath GK.** The COX-2 pathway is essential during early stages of skeletal muscle regeneration. *Am J Physiol Cell Physiol* 2004;287:C475-C483.
23. **Goodman S, Ma T, Trindade M, et al.** COX-2 selective NSAID decreases bone ingrowth in vivo. *J Orthop Res* 2002;20:1164-1169.
24. **Gerstenfeld LC, Al-Ghawas M, Alkhiary YM, et al.** Selective and nonselective cyclooxygenase-2 inhibitors and experimental fracture-healing. Reversibility of effects after short-term treatment. *J Bone Joint Surg [Am]* 2007;89-A:114-125.
25. **Meunier A, Aspenberg P.** Parecoxib impairs early metaphyseal bone healing in rats. *Arch Orthop Trauma Surg* 2006;126:433-436.
26. **Cottrell J, O'Connor JP.** Effect of non-steroidal anti-inflammatory drugs on bone healing. *Pharmaceuticals (Basel)* 2010;3:1668-1693.
27. **Sandberg O, Aspenberg P.** Different effects of indomethacin on healing of shaft and metaphyseal fractures. *Acta Orthop* 2015;86:243-247.
28. **Walters G, Pountos I, Giannoudis PV.** The cytokines and micro-environment of fracture haematoma: current evidence. *J Tissue Eng Regen Med* 2018;12:e1662-e1677.
29. **Morcos MW, Al-Jallad H, Li J, et al.** PHOSPHO1 is essential for normal bone fracture healing: an animal study. *Bone Joint Res* 2018;7:397-405.
30. **Burd TA, Hughes MS, Anglen JO.** Heterotopic ossification prophylaxis with indomethacin increases the risk of long-bone nonunion. *J Bone Joint Surg [Br]* 2003;85-B:700-705.
31. **Giannoudis PV, MacDonald DA, Matthews SJ, et al.** Nonunion of the femoral diaphysis. The influence of reaming and non-steroidal anti-inflammatory drugs. *J Bone Joint Surg [Br]* 2000;82-B:655-658.
32. **Kurmis AP, Kurmis TP, O'Brien JX, Dalén T.** The effect of nonsteroidal anti-inflammatory drug administration on acute phase fracture-healing: a review. *J Bone Joint Surg [Am]* 2012;94-A:815-823.
33. **Geusens P, Emans PJ, de Jong JJ, van den Bergh J.** NSAIDs and fracture healing. *Curr Opin Rheumatol* 2013;25:524-531.
34. **Marquez-Lara A, Hutchinson ID, Nuñez F Jr, Smith TL, Miller AN.** Nonsteroidal anti-inflammatory drugs and bone-healing: a systematic review of research quality. *JBJS Rev* 2016;4:4.
35. **Richards CJ, Graf KW Jr, Mashru RP.** The effect of opioids, alcohol, and nonsteroidal anti-inflammatory drugs on fracture union. *Orthop Clin North Am* 2017;48:433-443.

Author information

- G. A. Hjorthaug, MD, Consultant Orthopedic Surgeon, Department of Orthopedic Surgery, Martina Hansens Hospital, Sandvika, Norway; Institute of Clinical Medicine, Faculty of Medicine, University of Oslo (UIO), Oslo, Norway; Experimental Orthopedic Research, Institute for Surgical Research, Oslo University Hospital (OUS), Oslo, Norway.

- E. Søreide, MD, Consultant Orthopedic Surgeon, Division of Orthopedic Surgery, OUS, Oslo, Norway; Institute of Clinical Medicine, Faculty of Medicine, UIO, Oslo, Norway; Experimental Orthopedic Research, Institute for Surgical Research, OUS, Oslo, Norway.
- L. Nordsletten, MD, PhD, Professor and Senior Consultant, Division of Orthopedic Surgery, OUS, Oslo, Norway; Institute of Clinical Medicine, Faculty of Medicine, UIO, Oslo, Norway; Experimental Orthopedic Research, Institute for Surgical Research, OUS, Oslo, Norway.
- J. E. Madsen, MD, PhD, Professor and Senior Consultant, Division of Orthopedic Surgery, OUS, Oslo, Norway; Institute of Clinical Medicine, Faculty of Medicine, UIO, Oslo, Norway; Experimental Orthopedic Research, Institute for Surgical Research, OUS, Oslo, Norway.
- F. P. Reinholt, MD, PhD, Professor, Department of Pathology, OUS, Oslo, Norway.
- S. Niratisairak, MS, PhD, Senior Engineer, Institute of Clinical Medicine, Faculty of Medicine, UIO, Oslo, Norway; Biomechanics Lab, Division of Orthopedic Surgery, OUS, Oslo, Norway.
- S. Dimmen, MD, PhD, Consultant Orthopedic Surgeon, Department of Orthopedic Surgery, Lovisenberg Diaconal Hospital, Oslo, Norway; Institute of Clinical Medicine, Faculty of Medicine, UIO, Oslo, Norway; Experimental Orthopedic Research, Institute for Surgical Research, OUS, Oslo, Norway.

Author contributions

- G. A. Hjorthaug: Designed the study, Performed the surgeries, DXA measurements, histological analyses, and statistical calculations, Carried out the independent DXA analyses and biomechanical testing, Wrote the manuscript.
- E. Søreide: Designed the study, Performed the surgeries and DXA measurements, Carried out the independent DXA analyses and biomechanical testing.
- L. Nordsletten: Designed the study.
- J. E. Madsen: Designed the study.
- F. P. Reinholt: Designed the study, Supervised the histological analyses.
- S. Niratisairak: Performed the independent biomechanical analyses, Assisted in performing the biomechanical calculations.
- S. Dimmen: Designed the study, Performed the surgeries.

Funding statement

- No benefits in any form have been received or will be received from a commercial party related directly or indirectly to the subject of this article.

Acknowledgements

- The authors would like to thank the Department of Comparative Medicine, Oslo University Hospital, Rikshospitalet, Oslo, Norway for providing excellent animal facilities and enthusiastic personnel at our disposal. Senior Engineer Linda T. Dorg (Department of Pathology, University of Oslo, Oslo, Norway) is acknowledged for excellent help with the histological work.

Ethical review statement

- The experimental protocol was reviewed and approved by The Norwegian Animal Research Authority (IRB: FOTS ID 8155).